



AFRL-RI-RS-TR-2011-034

**ROBUST CONNECTIVITY IN SENSORY AND AD HOC NETWORKS**

---

SYRACUSE UNIVERSITY

*FEBRUARY 2011*

FINAL TECHNICAL REPORT

*APPROVED FOR PUBLIC RELEASE; DISTRIBUTION UNLIMITED.*

STINFO COPY

**AIR FORCE RESEARCH LABORATORY  
INFORMATION DIRECTORATE**

## NOTICE AND SIGNATURE PAGE

Using Government drawings, specifications, or other data included in this document for any purpose other than Government procurement does not in any way obligate the U.S. Government. The fact that the Government formulated or supplied the drawings, specifications, or other data does not license the holder or any other person or corporation; or convey any rights or permission to manufacture, use, or sell any patented invention that may relate to them.

This report is the result of contracted fundamental research deemed exempt from public affairs security and policy review in accordance with SAF/AQR memorandum dated 10 Dec 08 and AFRL/CA policy clarification memorandum dated 16 Jan 09. This report is available to the general public, including foreign nationals. Copies may be obtained from the Defense Technical Information Center (DTIC) (<http://www.dtic.mil>).

AFRL-RI-RS-TR-2011-034 HAS BEEN REVIEWED AND IS APPROVED FOR PUBLICATION IN ACCORDANCE WITH ASSIGNED DISTRIBUTION STATEMENT.

FOR THE DIRECTOR:

/s/

MICHAEL J. GANS  
Work Unit Manager

/s/

WARREN H. DEBANY JR, Technical Advisor  
Information Grid Division  
Information Directorate

This report is published in the interest of scientific and technical information exchange, and its publication does not constitute the Government's approval or disapproval of its ideas or findings.

**REPORT DOCUMENTATION PAGE***Form Approved*  
**OMB No. 0704-0188**

Public reporting burden for this collection of information is estimated to average 1 hour per response, including the time for reviewing instructions, searching data sources, gathering and maintaining the data needed, and completing and reviewing the collection of information. Send comments regarding this burden estimate or any other aspect of this collection of information, including suggestions for reducing this burden to Washington Headquarters Service, Directorate for Information Operations and Reports, 1215 Jefferson Davis Highway, Suite 1204, Arlington, VA 22202-4302, and to the Office of Management and Budget, Paperwork Reduction Project (0704-0188) Washington, DC 20503.

**PLEASE DO NOT RETURN YOUR FORM TO THE ABOVE ADDRESS.**

<b>1. REPORT DATE (DD-MM-YYYY)</b> February 2011			<b>2. REPORT TYPE</b> Final Technical Report		<b>3. DATES COVERED (From - To)</b> March 2005 – September 2010	
<b>4. TITLE AND SUBTITLE</b>  ROBUST CONNECTIVITY IN SENSORY AND AD HOC NETWORKS					<b>5a. CONTRACT NUMBER</b> N/A	
					<b>5b. GRANT NUMBER</b> FA8750-05-2-0120	
					<b>5c. PROGRAM ELEMENT NUMBER</b> 62702F	
6. AUTHOR(S)  Biao Chen					<b>5d. PROJECT NUMBER</b> CITE	
					<b>5e. TASK NUMBER</b> CH	
					<b>5f. WORK UNIT NUMBER</b> EN	
<b>7. PERFORMING ORGANIZATION NAME(S) AND ADDRESS(ES)</b> Syracuse University Department of EECS 113 Bowne Hall Syracuse, NY 13244-0001					<b>8. PERFORMING ORGANIZATION REPORT NUMBER</b>	
<b>9. SPONSORING/MONITORING AGENCY NAME(S) AND ADDRESS(ES)</b> Air Force Research Laboratory/Information Directorate Rome Research Site/RIGF 525 Brooks Road Rome, NY 13441					<b>10. SPONSOR/MONITOR'S ACRONYM(S)</b> AFRL/RI	
					<b>11. SPONSORING/MONITORING AGENCY REPORT NUMBER</b> AFRL-RI-RS-TR-2011-034	
<b>12. DISTRIBUTION AVAILABILITY STATEMENT</b> Approved for Public Release; Distribution Unlimited. This report is the result of contracted fundamental research deemed exempt from public affairs security and policy review in accordance with SAF/AQR memorandum dated 10 Dec 08 and AFRL/CA policy clarification memorandum dated 16 Jan 09.						
<b>13. SUPPLEMENTARY NOTES</b>						
<b>14. ABSTRACT</b> The project consists of two major thrusts. The first thrust is on robust inference and connectivity for sensor and ad hoc networks involving decentralized sensor nodes with unreliable communication channels. The second thrust studies throughput issues for MIMO communications under different scenarios.						
<b>15. SUBJECT TERMS</b>  Sensors, Connectivity, Networks, Arrays, Channel Capacity						
<b>16. SECURITY CLASSIFICATION OF:</b>			<b>17. LIMITATION OF ABSTRACT</b>  UU	<b>18. NUMBER OF PAGES</b>  48	<b>19a. NAME OF RESPONSIBLE PERSON</b> MICHAEL J. GANS	
<b>a. REPORT</b> U	<b>b. ABSTRACT</b> U	<b>c. THIS PAGE</b> U			<b>19b. TELEPHONE NUMBER (Include area code)</b> N/A	

# Contents

<b>1 Executive Summary</b>	1
<b>2 Introduction</b>	3
2.1 Robust inference in sensor and ad hoc networks.....	3
2.2 Minimum error probability cooperative relay design.....	4
2.3 Throughput Optimality of Orthogonal Transmissions for MIMO Multiple Access Channels .....	4
2.4 MIMO Communications in Airborne Platforms.....	5
2.5 Summary of Other Contributions.....	5
2.6 Acknowledgment.....	5
<b>3 GUI System for Throughput Analysis of Free Space MIMO Systems</b>	6
3.1 Introduction.....	6
3.2 GUI Overview.....	7
3.2.1 Main Window.....	7
3.2.2 Jet Parameters Window.....	8
3.2.3 Channel Parameter Window.....	9
3.2.4 Plot & Animation Window.....	9
3.2.5 Other Options Window.....	10
3.2.6 Jet Parameters for Random Trajectories Window.....	10
3.3 Formulae.....	10
3.3.1 Channel Blind MIMO Rate.....	11
3.3.2 MIMO Rate 2 (Beamforming).....	12
3.3.3 MIMO Capacity (Waterfilling).....	12
3.3.4 Rayleigh Ergodic Capacity.....	12
3.3.5 SISO Rate.....	13
3.3.6 Channelized MIMO Rate.....	13
<b>4 Bibliography</b>	14
<b>5 Appendix</b>	16

# List of Figures

1. Main Window.....	7
2. 2 Plots.....	8
3. 4 Plots.....	9
4. Jet Parameters .....	10
5. Channel Parameters .....	11
6. Plots and Animation Parameters .....	11
7. Other Options .....	12
8. Jet Parameters For Random Trajectories.....	13

# 1 Executive Summary (ABSTRACT)

The project consists of two major thrusts.

**Robust inference for sensor networks** The first thrust is on robust inference and connectivity for sensor and ad hoc networks involving decentralized sensor nodes with unreliable communication channels. The effort spans FY05-FY07. We have investigated two major problems under this thrust:

1. Decentralized signal processing for statistical inference when the communication between the sensors and the fusion center is subject to channel outage. Major findings of the work were published in the following paper:

- Y. Lin, B. Chen, and B. Suter, "Robust binary quantizers for detection in sensor networks," IEEE Trans. Wireless Communications, vol. 6, pp.2172-2181, June 2007.

In the paper, the multiple description principle was adopted to provide robust inference performance at the fusion center in the event that only a subset of the sensors successfully send their output to the fusion center. It was found that proactively designing local sensor processing provides significant performance gain over the approach that all sensor outputs were presumed reliably available at the fusion center when channel outage occurs.

2. Cooperative relay that minimizes the error probability at the destination. Recognizing the equivalence between cooperative relay with finite alphabet sources and decentralized hypothesis testing, we have developed a new framework for relay processing design that aims to optimize the performance at the destination node in terms of error probability. Major findings of the work were published in the following paper:

- B. Liu, B. Chen, and R.S. Blum, "Minimum error probability cooperative relay design," IEEE Trans. Signal Processing, vol. 6, pp. 2172-2181, June 2007.

**Throughput study of multi-user and free space MIMO communications** The second thrust study throughput issues for MIMO communications under different scenarios. The first scenario is when multiple MIMO transmitters communication with a single MIMO receiver and we study

the sum-rate optimality of orthogonal transmission for such systems. Major findings of the work were published in

- X. Shang, B. Chen, and J. Matyjas, "Sum capacity optimality of orthogonal communications over vector Gaussian multiple access channels, *IEEE Trans. Wireless communications*, vol. 7, pp. 4304-4311, November 2008.

Sufficient conditions and necessary conditions, in terms of channel matrices and transmitter power constraints, for orthogonal transmissions to achieve the sum capacity of a vector Gaussian MAC were obtained. The obtained conditions provide a unified framework that helps explain many intuitive and known results as well as explore cases that have not been addressed. In the cases when these conditions are violated, the developed results enable us to quantify the suboptimality of orthogonal transmission when the sum capacity can only be achieved by overlay transmission. The second scenario concerns MIMO communication with airborne platforms, i.e., free space MIMO communication when there is a lack of scattering in the transmission medium. Our primary effort for this problem involves the development of a GUI software system that studies the theoretical throughput under realistic channel conditions in terms of antenna size/spacing, platform velocity, and power constraints. The developed software allows us to study throughput of MIMO peer-to-peer communications under various airborne network configuration. One of the major findings is that for most tested platform trajectories, the impact of interference is rather limited even when the receivers completely ignore the interference, i.e., treating interference as noise. The primary reason is that the spatial diversity as afforded by the large antenna aperture (instead of scattering for terrestrial channels) gives rise to the immunity of multi-user interference for concurrent transmissions.

The rest of the final report will primarily involve results related to the development of the GUI software. For the other three problems investigated under this effort, we have included the three archival papers cited above as Appendix for this final report as the results.

## 2 Introduction

The project consists of two thrusts: 1) robust inference in sensor and ad hoc networks; 2) throughput analysis of multiuser MIMO systems. This chapter provides a synopsis of the major contributions under this effort. Many of the research results have been reported in archival papers and have been widely disseminated to the research community. Thus we will briefly summarize those research results and leave the details to the archival papers which are attached as appendix of this report. Instead, we will describe in details on the development of the GUI system for throughput study of free space MIMO communications in the next chapter.

### 2.1 Robust inference in sensor and ad hoc networks

For the emerging wireless sensor networks (WSN), distributed signal processing design has to deal with various physical limitations imposed by severe resource constraints. For example, the power and bandwidth constraints, coupled with the interference and channel fading, may result in transmission loss due to channel outage [1]. In addition, low cost sensor nodes deployed in harsh environments may be subject to sensor failure, making them unavailable for sensing/ communication [2].

Our work studied robust signal processing techniques for inference-centric distributed sensor networks operating in the presence of possible sensor and/or communication failures. Motivated by the multiple description (MD) principle [3,4], we develop robust distributed quantization schemes for a decentralized detection system. Specifically, focusing on a two-sensor system, our design criterion mirrors that of MD principle: if one of the two transmissions fails, we can guarantee an acceptable performance, while enhanced performance can be achieved if both transmissions are successful. Different from the conventional MD problem is the distributed nature of the problem as well as the use of error probability as the performance measure. Two different optimization criteria are used in the distributed quantizer design, the first a constrained optimization problem, and the second using an erasure channel model. We demonstrate that these two formulations are intrinsically related to each other. Further, using a person-by-person optimization approach, we propose an iterative algorithm to find the optimal local quantization thresholds. A design example is provided to illustrate the validity of the iterative algorithm and the improved robustness compared to the classical distributed detection approach that disregards

the possible transmission losses.

Technical details can be found [5] which is attached in the appendix of this final report.

## 2.2 Minimum error probability cooperative relay design

In wireless networks, a severe limiting factor is multipath- induced channel fading. One of the most effective methods in mitigating fading is to exploit diversity [6]. Examples include spatial diversity when multiple antennas are used at the transceivers, multipath diversity in frequency-selective channels, and temporal diversity in time-selective fading channels through the use of coding/interleaving. More recently, a new diversity resource has attracted considerable attention, especially in the context of wireless ad hoc networks [7–9]. There, multiple nodes collaborate in transmitting their information, thus providing diversity by exploiting the independence of the fading channels of different users. This is generally referred to as the cooperative diversity, and the collection of cooperating nodes, including the source and the destination nodes, are referred to as a relay network.

Recognizing the connection between cooperative relay with finite alphabet sources and the distributed detection problem, our effort studies relay signaling design via channel aware distributed detection theory. Focusing on a wireless relay network composed of a single sourcedestination pair with relay nodes, we derive the necessary conditions for optimal relay signaling that minimizes the error probability at the destination node. The derived conditions are person-by-person optimal: each local relay rule is optimized by assuming fixed relay rules at all other relay nodes and fixed decoding rule at the destination node. An iterative algorithm is proposed for finding a set of relay signaling approaches that are simultaneously person-by-person optimal. Numerical examples indicate that the proposed scheme provides performance improvement over the two existing cooperative relay strategies, namely amplify-forward and decode-forward.

Technical details can be found in [10], also attached in the appendix of this final report.

## 2.3 Throughput Optimality of Orthogonal Transmissions for MIMO Multiple Access Channels

It is well known that, for a scalar Gaussian MAC, orthogonal transmissions, e.g., frequency division multiple access (FDMA) or time division multiple access (TDMA) under an average power constraint, can achieve the sum capacity [11]. As such, although FDMA and TDMA is suboptimal in terms of the entire capacity region, if only the system throughput is of concern, orthogonal transmissions are sufficient, resulting in a much simplified transceiver structure, i.e., no successive interference cancellation is needed. Similar result holds for a scalar Gaussian MAC with more than two users. With vector Gaussian MAC, the above claim - that orthogonal transmissions achieve the sum capacity - is not necessarily true. Indeed, it is observed that in most cases orthogonal transmissions fall well short of achieving the sum capacity of a vector Gaussian MAC [12].

The goal of this study is twofold. First, we establish sufficient and necessary conditions for orthog-

onal transmissions to be optimal in achievable sum rate for a vector Gaussian MAC. The established conditions, in terms of singular values and singular vectors of the channel matrices as well as the power constraints, provide a unified framework behind many intuitive and well known results. In addition, it allows us to examine cases that have not been explored before in terms of the (sub)optimality of orthogonal transmissions for vector Gaussian MAC. We show that the channel must have proportional singular values, well aligned singular vectors and appropriate power constraints in order for FDMA/TDMA to achieve the sum capacity. Secondly, using the established conditions, we attempt to provide quantitative measure for the performance degradation of orthogonal transmission when they are suboptimal.

Technical details can be found in [13], attached in the appendix of this final report.

## **2.4 MIMO Communications in Airborne Platforms**

Free space MIMO had not been a fruitful research area due to the belief that the lack of scattering prevents us from harvesting the potential throughput gains of MIMO communications. However, Dr. Gans, using realistic settings of airborne platforms, demonstrated that free space MIMO still yields considerable throughput gains that warrant a serious second look. Our effort is to develop a GUI simulation system that allows one to visualize the throughput comparison of various airborne communication scenarios. The GUI system will be described in details in the next chapter.

## **2.5 Summary of Other Contributions**

The award has provided (partial) financial support to several graduate students over the past years. Two of them, Drs. Ying Lin and Bin Liu, have since graduated and have taken academic appointments at US and overseas. This award was also instrumental in facilitating close collaboration between the PI and AFRL researchers. The PI has visited AFRL/Rome Research Site numerous times during the project period. Some of the research results presented in this report result from direct collaborations with AFRL researchers.

## **2.6 Acknowledgment**

The PI would like to express his sincere gratitude to many of the Air Force Research Lab (AFRL) collaborators that he has had the fortune to work with over the years, including Dr. Michael Gans, Dr. John Matyjas, and Dr. Bruce Suter. Such collaborations were not only fruitful in terms generating cutting edge research results, but have also helped the PI to keep informed of research problems that are relevant to the AF and DoD at large. The PI has benefited greatly by many discussions with Drs. Gans, Matyjas, and Suter, some of the during the regular coffee breaks at the lab. The PI is especially indebted to Dr. Gans, who graciously hosted the PI's summer visits in 2004 and 2005. Dr. Gans' technical expertise in diverse areas ranging from communication theory to antenna to hardware design, his valuable insight on many of the seemingly complex problems, and above all, the scientific rigor with which he conducts research have been a constant inspiration to the PI.

# 3 GUI System for Throughput Analysis of Free Space MIMO Systems

## 3.1 Introduction

Communication systems utilizing multiple antenna elements were shown to provide throughput improvement of several magnitudes compared with the single antenna systems [14]. The throughput gain is attained because of the spatial diversity which were typically believed to only exist in a rich scattering environment. As such there had been much doubt on the suitability and relevance of MIMO communications in airborne platforms where scatterers are hard to find.

However, using realistic aircraft platforms, it was demonstrated in [15] that free space MIMO communication may still harvest potentially significant throughput gains due to the existence of spatial diversity arising from the large aperture of transceiver antenna arrays. This work largely motivates the development of this simulation platform that attempt to validate the throughput potential of free space MIMO as well as to provide insights on the impact of the existence of multiple transceiver pairs to network throughput in the context of free space MIMO system.

The purpose of any simulation is to provide foresight on how an actual system might function when put to work. Our simulation software provides a comparison on the data rates that can be achieved by a Line of Sight (LOS) MIMO system using different transmission schemes. Here, by LOS MIMO systems we refer to airborne networks. This simulation software was developed in MATLAB version 7.0.0.19920 (R14).

The different transmission schemes that we consider can be broadly classified into two categories, viz., Channel Blind and Channel Aware. For the Channel Blind case we put equal power on all the antennas. In case of Channel Aware approach, we use Beamforming or Waterfilling. All these schemes are compared with the ergodic capacity that can be achieved under suitable channel conditions. Another feature of this simulation software is to provide a visualization of the trajectories that the airborne objects follow and the corresponding data rates.

## 3.2 GUI Overview

The simulation software GUI consists of one (1) Main (or parent) window and four (4) children windows. There are two primary purposes of the parent window. One, to invoke the children windows and set Jet parameters. Second, to display the plots in different configurations. Other purposes that the parent window serves are to invoke the Animation window and display Jet Parameters window. Jet Parameters window is used to set the trajectory, number of antennas, antenna configuration and speed of a Jet. Channel Parameters window is used to set the communication parameters viz., the carrier frequency & the bandwidth. Plot and Animation window is used for data rates and trajectory visualization.

For the given start and end co-ordinates of a Jet, it is assumed to move in a straight line such that its length is oriented along the line joining the co-ordinates. There is no rolling of the Jet about the line joining these co-ordinates.

### 3.2.1 Main Window

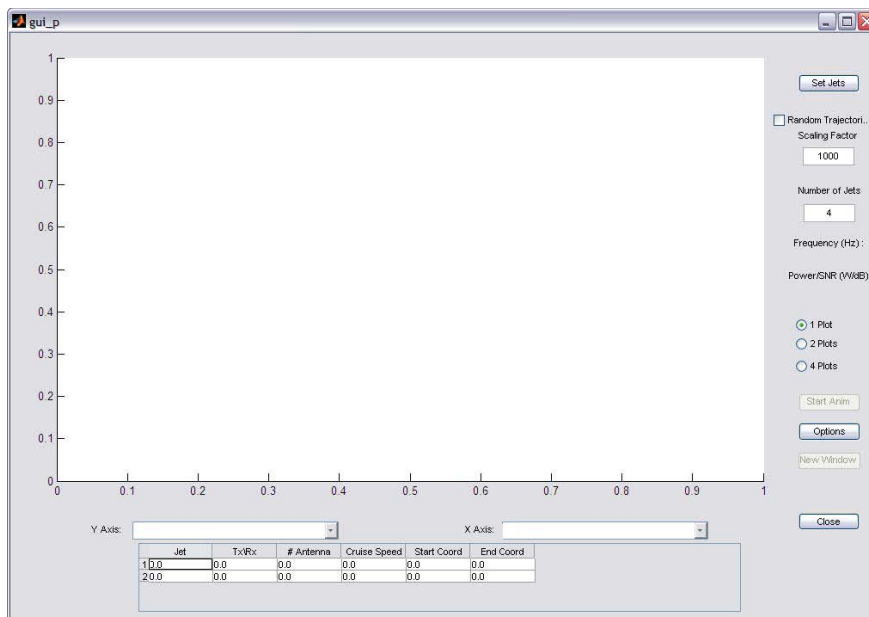


**Figure 1: Main Window**

This window is the main and first user interface that the simulation software provides the user when it is run. We start the simulation by setting the Number of Jets edit box and then pressing Set Jets button, which is situated above the edit box. This invokes Jet Parameters window and then consequently Channel Parameters window. After the user is done with inputting the required parameters, the application starts calculating the data points. These data points can be plotted in 3 different configurations on the window, i.e., 1 Plot, 2 Plots & 4 Plots.

By checking the Random Trajectories check box, the application will fill in randomly generated values in the start and end co-ordinates of the Jets. The start and end co-ordinates are generated from

a uniform distribution between 0 and 1. *Scaling Factor* is used to scale them up to the desired values.

The *Y Axis* and *X Axis* popup menu are used to select the data the corresponding axes should plot. The table below the popup menus gives the Jet parameters for the selected communication pair.

The *New Window* button is used to export the selected plot to a new axes window. This allows the user to access the features that are available in the axes window, which are not available on the Parent Window axes.

The *Start Animation* button invokes Plot and Animation window, which is used to display animation of the jets along with their corresponding data rates. The *New Window* and *Start Animation* buttons are disabled until the data points are available.

The different plot configurations are shown in figure 2 and figure 3:

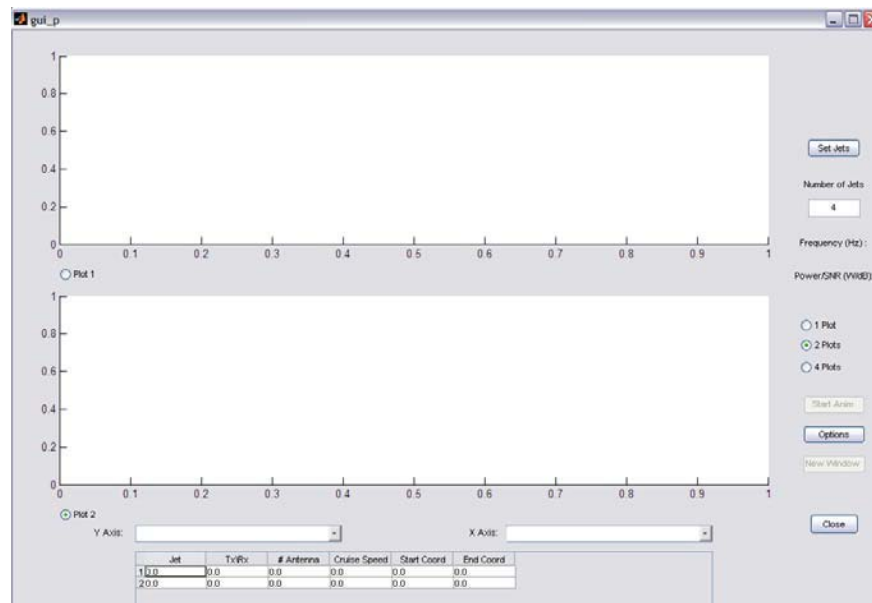


**Figure 2: 2 Plots**

### 3.2.2 Jet Parameters Window

The purpose of this window is to get Jet parameters from the user. When the window is invoked by *Set Jets* button on parent window, it passes the previously used jets parameters as input to this window. This prevents the user from re-entering the parameters, if no or very few changes are to be made. All the fields on the window are self-explanatory.

We enter the start and end co-ordinates for the jets in the corresponding fields. The *Cruise Speed* has to be set in km/hr. The antenna co-ordinates file contains the antenna co-ordinates. Once, all these parameters are entered, we need to tell the application which other jet this current jet intends to communicate. This can be done by checking the appropriate box on the right side of the window. Only one box can be checked at a time.

The number of windows that are opened sequentially depend on the value that is put in the *Number*

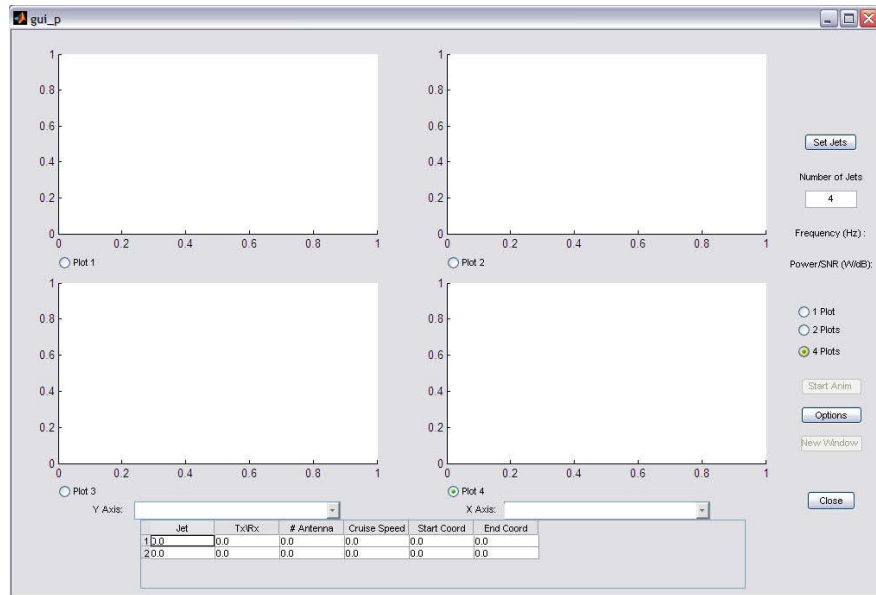


**Figure 3: 4 Plots**

of *Jets* edit box in the parent window. After all the parameters for all the jets are set Channel Parameters Window is invoked.

### 3.2.3 Channel Parameter Window

This window is used to get the communication parameters from the user. Communication can take place in two modes, viz. Fixed Power & Fixed SNR. This can be selected by checking the appropriate radio button. Similarly, the *Frequency* and *Bandwidth* has to be set by the user. These parameters apply to all the communicating pairs.

Similar to Jet Parameters window, the Main window passes previously stored channel parameters while invoking this window, so as to avoid re-entering them. After pressing the OK button, it returns a *JetsPairParam* object to the Parent Window and the main application starts calculating the data points.

### 3.2.4 Plot & Animation Window

This window is invoked when user presses *Start Animation* button on the Main window. The left axes on the window shows the trajectories of the Jets. Each solid blue circle indicates the Jet position. The Jet number and role it is playing in communication i.e. whether it is acting as transmitter or receiver (T & R respectively) are displayed above the Jet position. The solid line indicates communicating pair and the dashed line indicates interference from other transmitters.

The right axes shows the corresponding data rates that are achieved at that location.

The slider is used to control the position of the Jets in time domain. After pressing the play button, slider is moved periodically in forward direction, which changes the Jet positions, thereby giving the effect of animation.

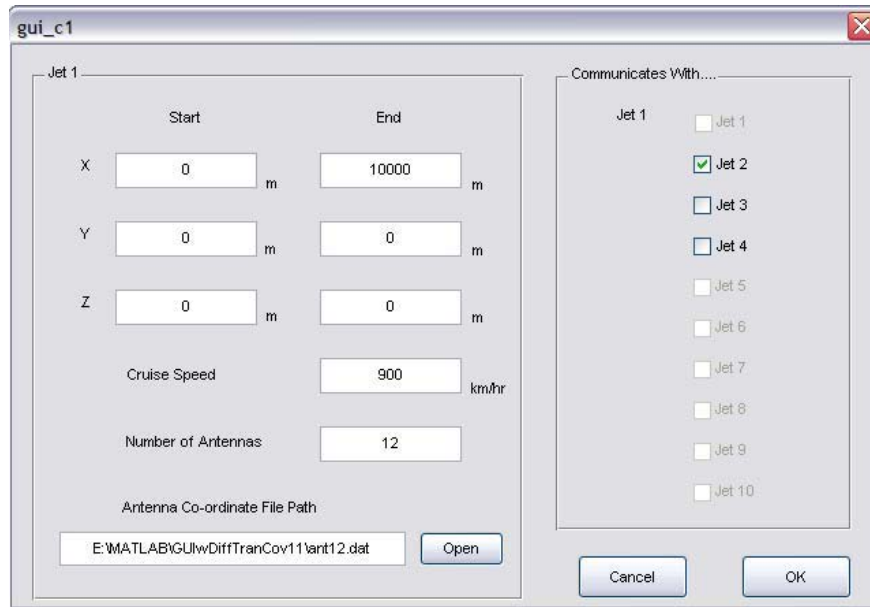


**Figure 4: Jet Parameters**

### 3.2.5 Other Options Window

This window can be opened by pressing the *Options* button on the Main window. Here, the *Resolution* edit box gives the number of data points that need to be calculated. The *Scatter Loss* gives the scaling parameter for the scatter matrix.

For our simulation purpose, we use two kinds of scatter matrices. One is the deterministic case. In this case, we set the scatter points on the jet surface and calculate the scatter matrix accordingly. Second is the random case. In this case, we consider each element of the matrix to be Complex Gaussian distributed with mean 0 and variance 1.

### 3.2.6 Jet Parameters for Random Trajectories Window

This window is invoked when the *Random Trajectories* check box is checked and the user presses *Set Jets* on the Main window. The *Cruise Speed*, *Number of Antennas* and the *Antennas File Path* are common to all the jets in this case.

## 3.3 Formulae

Let  $\mathbf{H}_{ij}$  be the channel matrix between receiver  $i$  and transmitter  $j$  as calculated in [15],  $\mathbf{K}_{jj}$  be the transmit covariance matrix,  $t$  be the number of transmit antennas and  $r$  be the number of receive antennas. We assume the noise to be complex Gaussian distributed with mean 0 and variance 1.

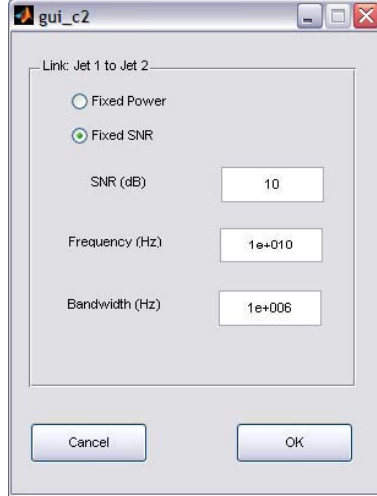


**Figure 5: Channel Parameters**

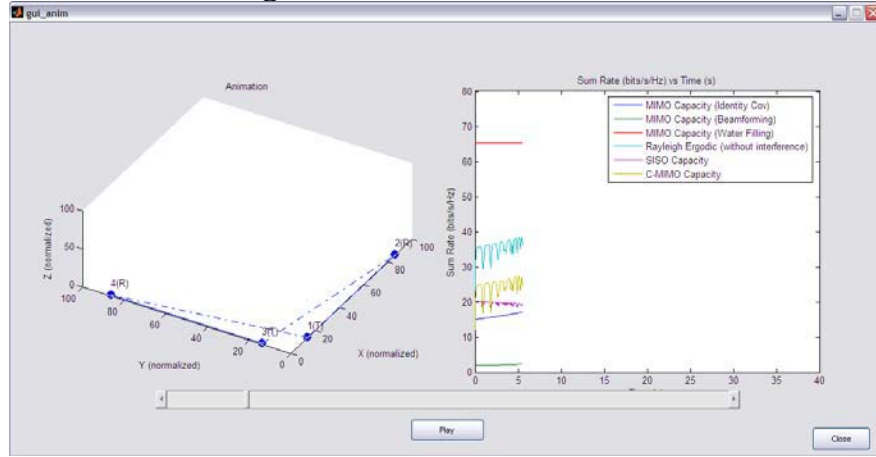


**Figure 6: Plots and Animation Parameters**

### 3.3.1 Channel Blind MIMO Rate

In this approach i.e. when the transmitter doesn't know the Channel State Information (CSI), the transmitter puts equal power on all the transmit antennas, such that the transmit covariance matrix is

$$\mathbf{K}_{ij} = \frac{P}{t} \mathbf{I}_t, \text{ where } P \text{ is the total power constraint on the transmitter and } \mathbf{I}_t \text{ is a } t \times t \text{ identity matrix.}$$

The rate at receiver  $i$ , treating interference as noise is given below,

$$R_i^{Non-CSI} = \log_2 \left| \mathbf{I} + \rho \mathbf{H}_{ii} \mathbf{K}_{ii} \mathbf{H}_{ii}^+ \left( \mathbf{I} + \sum_{l \neq i} \eta_{il} \mathbf{H}_{il} \mathbf{K}_{ll} \mathbf{H}_{il}^+ \right)^{-1} \right| \quad (1)$$

Here,  $\mathbf{H}_{ij}^+$  is the hermitian of  $\mathbf{H}_{ij}$  and  $\mathbf{I}$  is an identity matrix of size  $r \times r$ .

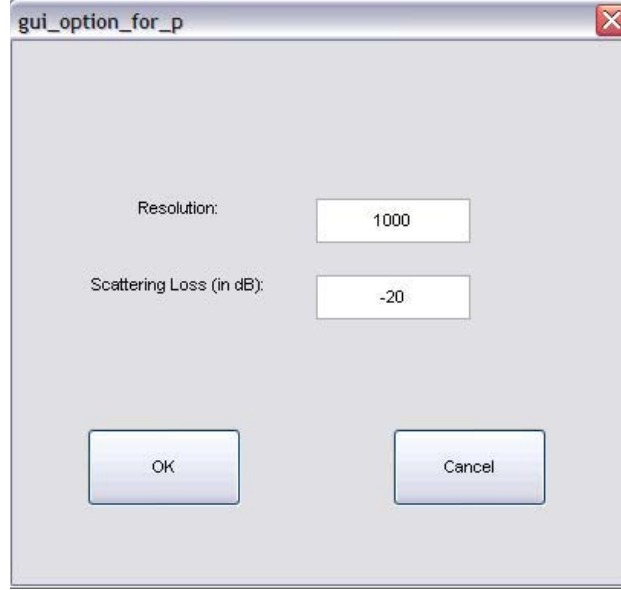


**Figure 7: Other Options**

### 3.3.2 MIMO Rate 2 (Beamforming)

This transmission scheme is used when the transmitter knows the Channel State Information such that it knows the right dominant eigenvector of the channel matrix by means of some feedback mechanism from the receiver. Let  $\mathbf{v}_i$  be the right dominant eigen vector of the channel matrix  $\mathbf{H}_{ii}$ . We set the channel covariance matrix  $\mathbf{K}_{ii}$  as

$$\mathbf{K}_{ii}^{\text{BF}} = \mathbf{v}_i \mathbf{v}_i^+ \quad (2)$$

We calculate the corresponding rate by plugging in this  $\mathbf{K}_{ii}^{\text{BF}}$  in the above capacity expression.

### 3.3.3 MIMO Capacity (Waterfilling)

We calculate the waterfilling matrix  $\mathbf{K}_{ii}^{\text{WF}}$  from the given channel matrix  $\mathbf{H}_{ii}$ , and plug it in (1). We can use this transmission scheme only when the transmitter has complete channel state information.

### 3.3.4 Rayleigh Ergodic Capacity

For this case we use the formula given in [15], which is as follows:

$$C^{\text{Ergodic}} = M \left\{ 2 \log_2 [1 + \rho + \sigma] - \frac{\sigma}{\rho \ln 2} \right\} \quad (3)$$

where,  $\sigma = 0.25(\sqrt{4\rho + 1} - 1)$ ,  $M$  is the number of antennas and  $\rho$  is the average SNR at each receiver antenna. We assume same number of antennas at the transmitter as well as receiver.

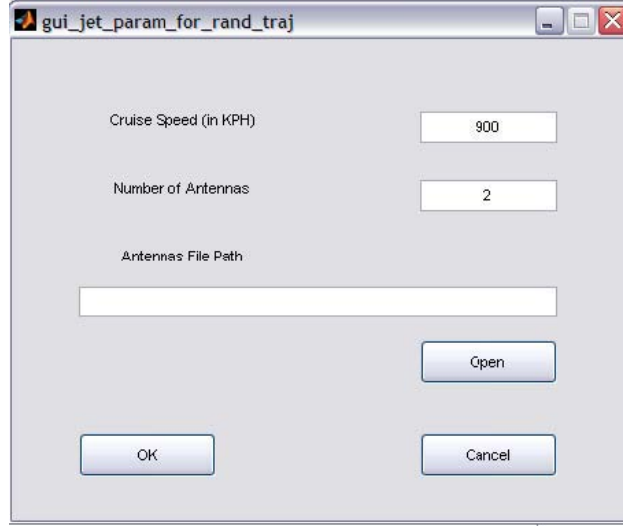


**Figure 8: Jet Parameters For Random Trajectories**

### 3.3.5 SISO Rate

This is the rate for a single input single output case,

$$R^{SISO} = \log_2 \left( 1 + \rho(1 + \eta)^{-1} \right) \quad (4)$$

where,  $\rho$  is the average SNR at the receiver antenna and  $\eta$  is the INR.

### 3.3.6 Channelized MIMO Rate

If there are  $M$  communicating pairs, assuming FDMA or TDMA the rate for each  $i^{th}$  link is given by

$$R_i^{Ch-MIMO} = \frac{1}{M} \log_2 \left| \mathbf{I} + \rho_i M \mathbf{H}_{ii} \mathbf{K}_{ii} \mathbf{H}_{ii}^+ \right| \quad (5)$$

## 4 Bibliography

- [1] B. Chen and P.K. Willett, "On the optimality of likelihood ratio test for local sensor decisions in the presence of non-ideal channels," *IEEE Trans. Inf. Theory*, vol. 51, pp. 693–699, Feb. 2005.
- [2] T. Wang, Y-S. Han, B. Chen, and P.K. Varshney, "A combined decision fusion and channel coding scheme for distributed fault-tolerant classification in wireless sensor networks," *IEEE Trans. Wireless Communications*, vol. 5, pp. 1695-1705, July 2006.
- [3] V. Vaishampayan, "Design of multiple description scalar quantizer," *IEEE Trans. on Inf. Theory*, vol. 39, pp. 821–834, May 1993.
- [4] V.K. Goyal, "Multiple description coding: compression meets the network," *IEEE Signal Processing Magazine*, vol. 19, pp. 74–93, Sep. 2002.
- [5] Y. Lin, B. Chen, and B. Suter, "Robust binary quantizers for detection in sensor networks," *IEEE Trans. Wireless Communications*, vol. 6, pp. 2172-2181, June 2007.
- [6] T. Rappaport, *Wireless Communications — Principles and Practices*, Prentice Hall, Upper Saddle River, NJ, 1996
- [7] A. Sendonaris, E. Erkip, and B. Aazhang, "User cooperation diversity: Part I System description," *IEEE Trans. Comm.*, vol. 51, pp. 1927–1938, Nov. 2003.
- [8] A. Sendonaris, E. Erkip, and B. Aazhang, "User cooperation diversity: Part I Implementation aspects and performance analysis," *IEEE Trans. Comm.*, vol. 51, pp. 1939–1948, Nov. 2003.
- [9] J.N. Laneman, D.N.C. Tse, and G.W. Wornell, "Cooperative diversity in wireless networks: Efficient protocols and outage behavior," *IEEE Trans. Inf. Theory*, vol. 50, pp. 3062–3080, Dec. 2004.
- [10] B. Liu, B. Chen, and R.S. Blum, "Minimum error probability cooperative relay design," *IEEE Trans. Signal Processing*, vol. 6, pp. 2172-2181, June 2007.
- [11] T.M. Cover and J.A. Thomas, *Elements of Information Theory*, Wiley, New York, 1991.
- [12] D. Tse and P. Viswanath, *Fundamentals of Wireless Communications*, Cambridge University Press, Cambridge, UK, 2005.

[13] X. Shang, B. Chen, and J. Matyjas, "Sum capacity optimality of orthogonal communications over vector Gaussian multiple access channels, IEEE Trans. Wireless communications, vol. 7, pp. 4304-4311, November 2008.

[14] G.J. Foschini and M.J. Gans, "On limits of wireless communications in a fading environment when using multiple antennas", Wireless Personal Communications, vol. 6, pp. 311-335, 1998.

[15] M.J. Gans, "Aircraft Free-Space MIMO Communications," Proc. 43rd Asilomar conference on Signals, systems and computers, Monterey, CA, October 2009.

# 5 Appendix

The appendix include three archival papers whose results were partly supported under this effort:

- Y. Lin, B. Chen, and B. Suter, "Robust binary quantizers for detection in sensor networks," IEEE Trans. Wireless Communications, vol. 6, pp. 2172-2181, June 2007.
- B. Liu, B. Chen, and R.S. Blum, "Minimum error probability cooperative relay design," IEEE Trans. Signal Processing, vol. 6, pp. 2172-2181, June 2007.
- X. Shang, B. Chen, and J. Matyjas, "Sum capacity optimality of orthogonal communications over vector Gaussian multiple access channels, IEEE Trans. Wireless communications, vol. 7, pp. 4304-4311, November 2008.

# Robust Binary Quantizers for Distributed Detection

Ying Lin, *Student Member, IEEE*, Biao Chen, *Senior Member, IEEE*, and Bruce Suter, *Senior Member, IEEE*

**Abstract**—We consider robust signal processing techniques for inference-centric distributed sensor networks operating in the presence of possible sensor and/or communication failures. Motivated by the multiple description (MD) principle, we develop robust *distributed* quantization schemes for a decentralized detection system. Specifically, focusing on a two-sensor system, our design criterion mirrors that of MD principle: if one of the two transmissions fails, we can guarantee an acceptable performance, while enhanced performance can be achieved if both transmissions are successful. Different from the conventional MD problem is the distributed nature of the problem as well as the use of error probability as the performance measure. Two different optimization criteria are used in the distributed quantizer design, the first a constrained optimization problem, and the second using an erasure channel model. We demonstrate that these two formulations are intrinsically related to each other. Further, using a person-by-person optimization approach, we propose an iterative algorithm to find the optimal local quantization thresholds. A design example is provided to illustrate the validity of the iterative algorithm and the improved robustness compared to the classical distributed detection approach that disregards the possible transmission losses.

**Index Terms**—Distributed detection, erasure channels, fading channels, sensor networks.

## I. INTRODUCTION

FOR the emerging wireless sensor networks (WSN), distributed signal processing design has to deal with various physical limitations imposed by severe resource constraints. For example, the power and bandwidth constraints, coupled with the interference and channel fading, may result in transmission loss due to channel outage. In addition, low-cost sensor nodes deployed in harsh environments may be subject to sensor failure, making them unavailable for sensing/communication.

A conventional approach to combat transmission loss is to exploit channel diversity through the use of multiple description (MD) design [1] such as the MD codes [2] or MD quantizers [3]. This MD idea is illustrated in Fig. 1(a) with two encoders and three decoders [2]. The encoders are so designed that in the case of loss of one of the two transmissions, the side decoders (Decoder 1 or Decoder 2) are guaranteed with certain acceptable performance; if both transmissions are successful, the central decoder output (corresponding to Decoder 0) will

Manuscript received October 14, 2005; revised April 21, 2006; accepted April 24, 2006. The associate editor coordinating the review of this paper and approving it for publication was J. Zhang. This work was supported in part by the National Science Foundation under grant ECS-0501534 and by the Air Force Research Laboratory under agreement FA8750-05-2-0120.

Y. Lin and B. Chen are with the Department of Electrical Engineering and Computer Science, Syracuse University, 335 Link Hall, Syracuse, NY 13244 USA (e-mail: ylin20@ecs.syr.edu; bichen@ecs.syr.edu).

B. Suter is with AFRL/IFGC, 525 Brooks Rd., Rome, NY 13442 USA (email: suterb@rl.af.mil).

Digital Object Identifier 10.1109/TWC.2007.05769.

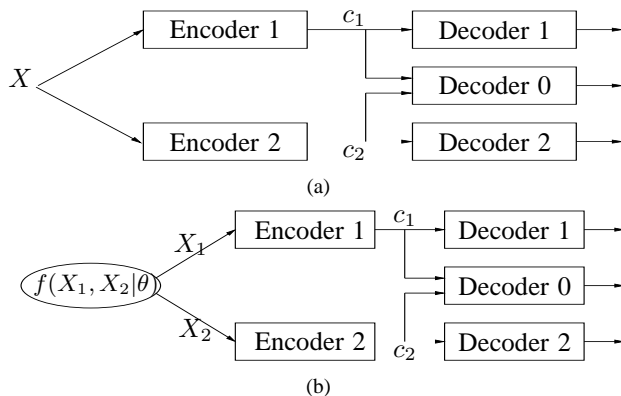


Fig. 1. Comparison between (a) conventional MD, and (b) distributed MD for sensor network applications. In (a), Encoders 1 and 2 have access to the same observation  $X$ . In (b), Encoder 1 encodes  $X_1$  without access to  $X_2$  while Encoder 2 encodes  $X_2$  without access to  $X_1$ .

have enhanced performance. As sensor failure can be dealt with in an identical fashion under the MD framework, we will no longer distinguish the two types of losses, one due to channel outage and the other due to sensor failure.

To carry over the MD principle to sensor network applications, care must be taken in considering the distinct features for distributed sensor networks. Two of the critical differences are listed below and are what motivate the current work.

- Distributed nature of WSN.

In the conventional MD framework, two encoders operate on a common source. In WSN, each encoder resides in a sensor and operates only on its own observations *without* access to the other sensor's observations. This is illustrated in Fig. 1.

- Inference-centric nature of WSN.

In WSN applications, all the sensor nodes are typically engaged in a collective inference task. The ultimate goal may be the evaluation of some underlying state instead of recovering the sensor observations. In reference to Fig. 1(b), the goal may be inferring about the unknown parameter  $\theta$  instead of recovering  $X_1$  and  $X_2$ . This is in comparison with the conventional MD problem where the goal is to recover the original source data. A direct consequence is that, instead of using the conventional distortion measures in the traditional MD quantizer design, other performance metrics that cater toward the inference task may be more relevant.

In this paper, we study how the MD principle can be adapted to inference-centric applications with distributed quantizer design. By focusing on a binary decentralized hypothesis testing problem (i.e.,  $\theta$  is binary in Fig. 1(b)), we investigate distributed binary quantizer design using the MD principle. We term this new framework distributed multiple descriptioQ

quantizer (DMDQ) design. The DMDQ approach achieve robust inference performance in the presence of channel outage or sensor failure as it strikes a better balance/tradeoff between the detection performance at the fusion center and that of local sensors.

The proposed scalar quantizer design is closely related to the classical distributed detection problem [4], [5] as it involves the design of multiple sensor decision rules that are coupled with each other. Major differences exist, and the most significant is that we no longer deal with a single objective function (minimum error probability at the fusion center). Instead, multiple design objectives need to be considered, each corresponding to the end-to-end inference performance for a particular channel outage or sensor failure state.

To explain the significance of the proposed approach, and in particular, to understand its improved robustness compared with the classical distributed detection design, consider the following simple example. Assume a binary hypothesis testing problem with a two-sensor parallel fusion system where each sensor employs a binary quantizer. The two hypotheses under test,  $H_0$  and  $H_1$ , are *a priori* equally likely. The local sensor observations at the two sensors,  $X_1$  and  $X_2$ , are conditionally independent and identically distributed ternary random variables with

$$\begin{cases} P(X_k = 0|H_0) = 0.95 \\ P(X_k = 1|H_0) = 0.05 \\ P(X_k = 2|H_0) = 0 \end{cases} \quad \begin{cases} P(X_k = 0|H_1) = 0.05 \\ P(X_k = 1|H_1) = 0.9 \\ P(X_k = 2|H_1) = 0.05 \end{cases}$$

for  $k = 1, 2$ . By the monotonicity of the likelihood ratio (LR) in the sensor observations (i.e., the local sensor LR values are monotone in  $X_k$ ), we need to consider only the two binary local decision rules at each sensor [6]:

$$\text{Rule A} \quad U_k = \begin{cases} 0 & X_k = 0 \\ 1 & X_k = 1 \text{ or } 2 \end{cases}$$

$$\text{Rule B} \quad U_k = \begin{cases} 0 & X_k = 0 \text{ or } 1 \\ 1 & X_k = 2 \end{cases}$$

Adopting the classical distributed detection approach, it is straightforward to show that the two sensors should employ different decision rules to achieve a minimum error probability of 0.04875 at the fusion center. Assume that, without loss of generality, sensor 1 uses Rule A while sensor 2 uses Rule B. If sensor 1's decision does not reach the fusion center, either due to a channel outage or a sensor failure, the actual minimum error probability by using the decision from sensor 2 alone becomes 0.475, which is a significant degradation from the case when both sensor outputs are available. This error probability essentially renders the detection system essentially useless as it is close to 0.5. A more robust design is to use decision rule Rule A at both sensors. In this case, both the fusion center and each local sensor have identical error probability 0.05 thus there is no degradation in the event of a lost transmission<sup>1</sup>. Compared with the classical distributed detection approach (whose error probability pair are 0.04875 and 0.475), the alternative approach provides a more robust performance in the presence of a transmission loss.

<sup>1</sup>This simple example also indicates that, depending on the local decision rules used and the observation distributions, having more sensors in the system may not always improve the overall performance.

The proposed DMDQ also provides an alternative approach to the channel aware design for a decentralized detection problem [7]–[9] in dealing with imperfect channels. The channel-aware quantization schemes require that the channel state information (CSI) be available to attain optimum performance. Acquiring CSI, however, may be too costly in systems with stringent resource constraints. It is, therefore, imperative to consider quantizer design that is robust to potential channel outages *without* the knowledge of CSI. The proposed DMDQ framework is an initial attempt toward robust and proactive signaling for distributed sensor networks in the absence of CSI.

The rest of the paper is organized as follows. In the next section, we describe the problem formulation and introduce the two-sensor fusion network with possible transmission losses. In Section III, we apply the Lagrangian method to solve the constrained minimization and to obtain necessary conditions for optimum binary quantizers in the form of LR test (LRT) thresholds. In Section IV, we impose the discrete memoryless erasure channel model and obtain the corresponding optimum local decision rules using the channel-aware quantizer design methodology described in [7], [8]. Numerical results are presented in Section V to demonstrate how the proposed quantizer design can be implemented and the improved robustness over the classical distributed detection approach. We conclude in Section VI.

## II. PROBLEM FORMULATION

Fig. 2 depicts a two-sensor parallel fusion network tasked with a hypothesis testing problem. Each sensor collects data that are generated according to one of the two hypotheses ( $H_0$  and  $H_1$ ) under test. We assume in the present work that the local observations  $X_1$  and  $X_2$  are conditionally independent given the underlying hypothesis, i.e., for  $i = 0, 1$ ,

$$f(X_1, X_2|H_i) = f(X_1|H_i)f(X_2|H_i).$$

It is easy to establish that with this conditional independence assumption, the LR pair of the local sensor observations

$$\left( L(X_1) = \frac{f(X_1|H_1)}{f(X_1|H_0)}, L(X_2) = \frac{f(X_2|H_1)}{f(X_2|H_0)} \right)$$

form a sufficient statistic for the detection problem.

Based on its local observation  $X_k$ , the  $k$ th local sensor implements a binary quantizer whose output  $U_k \in \{1, 0\}$ , for  $k = 1, 2$ , will be sent to the fusion center. The transmission, however, is subject to channel outage or sensor failure. When both transmissions are successful, Decoder 0 will perform as a fusion center and make a final decision on which hypothesis is true using both  $U_1$  and  $U_2$ . Otherwise, if only one of the two transmissions is successful, either Decoder 1 or Decoder 2 will make a final decision based on the successfully received  $U_k$ . In our current work, as  $U_k$  is binary, Decoders 1 and 2 will simply take  $U_1$  and  $U_2$  as their respective output, as illustrated in Fig. 2.

Adopting a Bayesian framework, we use error probability as the performance measure. Define  $P_{ek}$  the probability of error at Decoder  $k$ :

$$P_{ek} = \pi_0 P(U_k = 1|H_0) + \pi_1 P(U_k = 0|H_1), \quad k = 0, 1, 2 \quad (1)$$

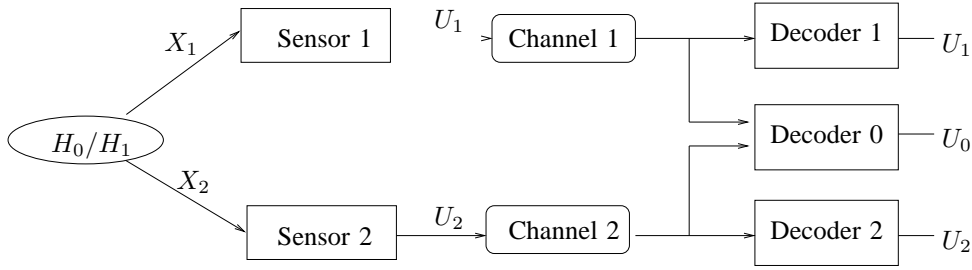


Fig. 2. A two-sensor parallel fusion network with possible transmission failures.

where  $\pi_j = P(H_j)$  is the prior probability for hypothesis  $H_j$ , and  $U_0$  denotes the decision output for Decoder 0. Thus  $P_{e0}$  corresponds to the error probability of the fusion center when both  $U_1$  and  $U_2$  are available while  $P_{e1}$  and  $P_{e2}$  are respectively the error probabilities at individual sensors. Classical distributed detection theory aim to minimize  $P_{e0}$  while our present work strives for a balance in performance between  $P_{e0}$  and  $P_{ek}$  for  $k = 1, 2$ .

Our approach is derived from the MD principle [1]: we aim to design sensor decision (quantization) rules such that if one of the two transmissions is lost, an acceptable performance (in terms of error probability) is guaranteed; if both transmissions are successful, a better performance can be achieved. Catering toward the hypothesis testing problem, we can succinctly summarize the design criterion using the following constrained minimization problem

$$\begin{aligned} \min \quad & P_{e0} \\ \text{subject to} \quad & P_{e1} \leq \varepsilon_1 \quad \text{and} \quad P_{e2} \leq \varepsilon_2. \end{aligned} \quad (2)$$

where  $\varepsilon_1$  and  $\varepsilon_2$  are the pre-specified error probabilities that are guaranteed if only  $U_1$  or  $U_2$  is successfully received. This design criterion is reminiscent of the MD scalar quantizer design [3] where a general distortion measure is used.

### III. NECESSARY CONDITIONS FOR OPTIMALITY AND A DESIGN ALGORITHM

The constrained optimization problem readily admits a Lagrangian formulation which is used to solve the minimization problem below. The Lagrangian function is given by

$$L(\tau_1, \tau_2, \lambda_1, \lambda_2) = P_{e0} + \lambda_1(P_{e1} - \varepsilon_1) + \lambda_2(P_{e2} - \varepsilon_2)$$

where  $\tau_k$  is the local sensor LRT threshold,  $\lambda_k$  is the Lagrangian multipliers, for  $k = 1, 2$ .

Using the Kuhn-Tucker theorem [10], the set of optimum solution of the constrained minimization problem must satisfy the following necessary conditions, for  $k = 1, 2$ ,

$$\frac{\partial P_{e0}}{\partial \tau_k} + \lambda_1 \frac{\partial P_{e1}}{\partial \tau_k} + \lambda_2 \frac{\partial P_{e2}}{\partial \tau_k} = 0 \quad (3)$$

$$\lambda_k \geq 0 \quad (4)$$

$$P_{ek} - \varepsilon_k \leq 0 \quad (5)$$

$$\lambda_k(P_{ek} - \varepsilon_k) = 0 \quad (6)$$

Given the above necessary conditions, the optimum solutions for the local decision rules are described in the following theorem.

*Theorem 1:* Assume that the two local observations,  $X_k$ 's, are conditionally independent. Further, if the fusion rule and the  $k$ th local sensor decision rule satisfy, for  $k = 1, 2$

$$\begin{cases} P(U_0 = 1|U_k = 1, U_{\bar{k}}) - P(U_0 = 1|U_k = 0, U_{\bar{k}}) \geq 0 \\ P(U_0 = 0|U_k = 0, U_{\bar{k}}) - P(U_0 = 0|U_k = 1, U_{\bar{k}}) \geq 0 \end{cases}$$

where  $\bar{k} \triangleq 3 - k$ , thus  $\bar{1} = 2$  and  $\bar{2} = 1$ . Then the optimum solution of the constrained minimization problem in Eq. (2) is given by the following LRT, for  $k = 1, 2$

$$P(U_k = 1|X_k) = \begin{cases} 1, & \text{if } \frac{p(X_k|H_1)}{p(X_k|H_0)} \geq \tau_k \\ 0, & \text{otherwise} \end{cases} \quad (7)$$

where  $\tau_k$ , the optimal LRT threshold for the  $k$ th local sensor, is determined as follows:

- When  $\lambda_k = 0$  (inactive constraint),

$$\tau_k = \frac{\pi_0 A_k}{\pi_1 B_k} \quad (8)$$

- When  $\lambda_k > 0$  (active constraint),  $\tau_k$  is obtained by solving

$$P_{ek} - \varepsilon_k = 0 \quad (9)$$

The associated  $\lambda_k$  can be obtained by

$$\lambda_k = \frac{\pi_0 A_k - \pi_1 B_k \tau_k}{\pi_1 \tau_k - \pi_0} \quad (10)$$

from which we get,

$$\tau_k = \frac{\pi_0(A_k + \lambda_k)}{\pi_1(B_k + \lambda_k)} \quad (11)$$

The quantities  $A_k$  and  $B_k$  in Eqs. (8-11) are defined respectively as

$$\begin{aligned} A_k &= \sum_{U_{\bar{k}}} P(U_{\bar{k}}|H_0) \\ &\quad [P(U_0 = 1|U_k = 1, U_{\bar{k}}) - P(U_0 = 1|U_k = 0, U_{\bar{k}})] \end{aligned} \quad (12)$$

$$\begin{aligned} B_k &= \sum_{U_{\bar{k}}} P(U_{\bar{k}}|H_1) \\ &\quad [P(U_0 = 0|U_k = 0, U_{\bar{k}}) - P(U_0 = 0|U_k = 1, U_{\bar{k}})] \end{aligned} \quad (13)$$

Theorem 1 is proved in Appendix I.

#### Remarks:

- Note that the forms of  $\tau_k$ ,  $A_k$ , and  $B_k$  indicate that the threshold for the  $k$ th sensor is a function of the decision rule at the other sensor. Thus, as expected, the optimal thresholds at sensor 1 and 2 are coupled with each other.

- In order for the constrained optimization to have feasible solutions,  $\epsilon_1$  and  $\epsilon_2$  can not be chosen to be too small. Specifically,  $\epsilon_k$  needs to be no smaller than the minimum achievable error probability at sensor  $k$ . More discussions about this can be found in Section V after we introduce an alternative design approach (Approach 3 in Section V).
- $P_{e0}$  is the achievable error probability using both  $U_1$  and  $U_2$ . On the other hand,  $P_{e1}$  and  $P_{e2}$  are respectively the error probabilities at local sensors, each associated with  $U_1$  or  $U_2$ . Thus  $P_{e0} \leq \min\{P_{e1}, P_{e2}\}$  where the inequality is due to the fact that one can simply ignore one of  $\{U_1, U_2\}$  and the error probability should thus be no worse than either  $P_{e1}$  or  $P_{e2}$ . Due to the constraints  $P_{e1} \leq \epsilon_1$  and  $P_{e2} \leq \epsilon_2$ , we have

$$P_{e0} \leq \min\{P_{e1}, P_{e2}\} \leq \min\{\epsilon_1, \epsilon_2\}$$

That is, the error probability achieved when both transmissions are successful is upper bounded by the error probability constraints at local sensors.

- If  $P_{e1} < \epsilon_1$  and  $P_{e2} < \epsilon_2$ , i.e.,  $\lambda_k = 0$  for  $k = 1, 2$ ,  $P_{e0}$  is the minimum error probability that can be achieved at the fusion center. The constrained optimization approach yields the same result as the unconstrained approach that minimizes the error probability at the fusion center. This happens when the constraints  $\epsilon_k$  are large enough.
- Eq. (11) is a unifying expression of the optimal local LR threshold for the two cases of  $\lambda_k > 0$  and  $\lambda_k = 0$ .
- The conditions described in Theorem 1 do not admit closed-form solutions. Simultaneously optimizing  $\tau_1$  and  $\tau_2$  is intractable due to the distributed nature - it typically involves some exhaustive search over a two dimension space for the  $(\tau_1, \tau_2)$  pair. However, the necessary conditions established in Theorem 1 allows us to adopt a person-by-person optimization (PBPO) approach where each threshold is optimized assuming fixed threshold at the other sensor. The PBPO approach has been widely used in optimizing decentralized systems, and in particular, in the classical distributed detection (see, e.g., [11], [12]) when joint optimization is typically intractable.
- Theorem 1 describes necessary conditions for the optimum LRT thresholds; thus multiple initializations are needed to find the globally optimum thresholds.

The following iterative algorithm describes this PBPO procedure.

#### Iterative Algorithm

- Step 1. Initialize  $\tau_k$ , for  $k = 1, 2$ .
- Step 2. Obtain the optimum fusion rule for fixed  $\tau_1$  and  $\tau_2$ .
- Step 3. For fixed fusion rule and  $\tau_2$ , calculate  $\tau_1$  using (8).
- Step 4. Check to see if  $\tau_1$  satisfies  $P_{e1} - \epsilon_1 \leq 0$ .
  - If yes, go to Step 5.
  - If no, calculate  $\tau_1$  using (9).
- Step 5. For fixed fusion rule and  $\tau_1$ , calculate  $\tau_2$  in a similar fashion.
- Step 6. Check convergence, i.e, if the obtained  $\tau_1$  and  $\tau_2$  are identical (up to a prescribed tolerance) to that from the previous iteration.

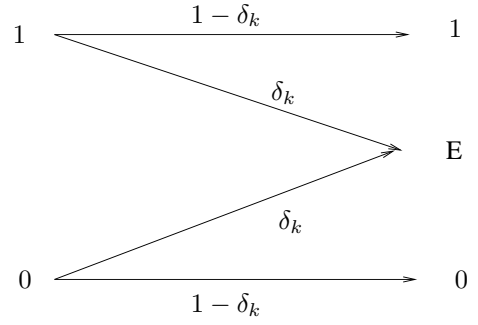


Fig. 3. A discrete memoryless erasure channel model for the channel between sensor  $k$  and the fusion center.

- If yes, stop.
- Otherwise, go to Step 2.

At each iteration,  $\tau_k$  is optimized for a given fusion rule and the other threshold  $\tau_{\bar{k}}$ , hence the error probability is monotone decreasing until a stationary point is reached.

#### IV. OPTIMAL LOCAL DECISION RULE DESIGN UNDER AN ERASURE CHANNEL MODEL

The constrained minimization approach provides a proactive design methodology that avoids severe performance degradation in the absence of CSI. We propose in this section an alternative approach by imposing a certain parametric model on the channel/sensor failures. This allows us to adopt existing channel aware approach [8] to design the local quantizers. Similar to [13], we model the potential transmission loss using *erasure* channels where the erasure accounts for possible sensor failures/channel outages. This channel model is illustrated in Fig. 3 where  $\delta_k = P(X_k = E|U_k)$  is the erasure probability corresponding to sensor  $k$ . Our alternative optimization criterion is to minimize the average error probability  $P_e$ , defined as

$$P_e = (1 - \delta_1)(1 - \delta_2)P_{e0} + \delta_2(1 - \delta_1)P_{e1} + \delta_1(1 - \delta_2)P_{e2} + \min\{\pi_0, \pi_1\}\delta_1\delta_2 \quad (14)$$

where the last term corresponds to the error probability when both transmissions are lost. This constant term has no effect on the quantizer design, hence can be dropped in the design problem.

The following theorem provides the solution for the sensor decision rules that minimize  $P_e$ .

*Theorem 2:* Assume that the two local observations,  $X_k$ 's, are conditionally independent and channels are independent discrete memoryless erasure channels. Further, if the fusion rule and the  $k$ th local sensor decision rule satisfy, for  $k = 1, 2$

$$\begin{cases} P(U_0 = 1|U_k = 1, U_{\bar{k}}) - P(U_0 = 1|U_k = 0, U_{\bar{k}}) \geq 0 \\ P(U_0 = 0|U_k = 0, U_{\bar{k}}) - P(U_0 = 0|U_k = 1, U_{\bar{k}}) \geq 0 \end{cases}$$

where  $\bar{k}$  is defined similar as in Theorem 1. Then the optimum local rule for the  $k$ th sensor amounts to the following LRT, for  $k = 1, 2$

$$P(U_k = 1|X_k) = \begin{cases} 1 & \text{if } \frac{p(X_k|H_1)}{p(X_k|H_0)} \geq \frac{\pi_0(A_k + \alpha_k)}{\pi_1(B_k + \alpha_k)} \\ 0 & \text{otherwise} \end{cases} \quad (15)$$

where

$$\alpha_1 = \frac{\delta_2}{1 - \delta_2} \text{ and } \alpha_2 = \frac{\delta_1}{1 - \delta_1}, \quad (16)$$

and  $A_k$  and  $B_k$  are defined in Eqs. (12) and (13).

A proof is given in Appendix II. Following the same spirit of the iterative algorithm in Section III, we can devise a similar procedure to find the optimal thresholds using Theorem 2.

Comparing Eqs. (11) and (15), we have some interesting observations that suggest intrinsic connections between the erasure channel model and the constrained minimization formulation. From Eq. (14), if we drop the last term and divide the average probability by  $(1 - \delta_1)(1 - \delta_2)$ , the new function to be minimized becomes

$$Q \triangleq P_{e0} + \alpha_1 P_{e1} + \alpha_2 P_{e2}.$$

with  $\alpha_1$  and  $\alpha_2$  defined as in Eq. (16). The design problem reduces to a problem of minimizing  $Q$  subject to  $\alpha_1 \geq 0$  and  $\alpha_2 \geq 0$ . Compare this with Eq. (3), we see that  $\alpha_k$  plays a similar role as the Lagrangian multiplier  $\lambda_k$ .

Further more, the first-order necessary conditions for minimizing  $Q$  are given by:

$$\frac{\partial P_{e0}}{\partial \tau_k} + \alpha_1 \frac{\partial P_{e1}}{\partial \tau_k} + \alpha_2 \frac{\partial P_{e2}}{\partial \tau_k} = 0 \quad (17)$$

$$\alpha_k \geq 0 \quad (18)$$

Comparing Eq. (17) and (18) to Eq. (3-6), we notice that these two formulations are similar except that the constrained optimization approach has more restrictive constraints (Eq. (5) and (6)). Next we elaborate when these two formulations will have identical optimal solutions.

Consider the first case: when  $\lambda_k = 0$ , i.e., the constraints  $P_{ek} \leq \epsilon_k$  are satisfied. In this case, set  $\alpha_k = \lambda_k = 0$ , and the two formulations have the same optimal thresholds. The case of  $\lambda_k > 0$  is more complicated. With  $\lambda_k > 0$ , we have  $P_{ek} = \epsilon_k$ ,  $k = 1, 2$ . Assume the erasure channel model yields  $L$  local minima, with the corresponding threshold pair  $(\tau_1^l, \tau_2^l)$ ,  $l = 1, 2, \dots, L$ . Denote by  $P_{ej}^l$ ,  $j = 0, 1, 2$ , the error probabilities associated with  $(\tau_1^l, \tau_2^l)$ . By virtue of the problem formulation, there must exist one  $(\tau_1^m, \tau_2^m)$  whose local error probabilities satisfy  $P_{ek}^m = \epsilon_k$ ,  $k = 1, 2$ . If

$$Q^m \triangleq P_{e0}^m + \alpha_1 \epsilon_1 + \alpha_2 \epsilon_2 \leq P_{e0}^j + \alpha_1 P_{e1}^j + \alpha_2 P_{e2}^j \triangleq Q^j \quad (19)$$

for  $j \neq m$ ,  $j = 1, 2, \dots, L$ . Then  $(\tau_1^m, \tau_2^m)$  is the optimal solution for both constrained minimization formulation and the erasure channel formulation. We will further illustrate these connections using some numerical examples in the next section.

## V. A NUMERICAL EXAMPLE

In this section, we use several numerical examples to highlight the robust performance of the proposed local quantizer design compared with the classical distributed detection approach. Consider the detection of a known signal in independent Gaussian noises using two sensors:

$$\begin{aligned} H_0 : & \quad X_k = n_k \\ H_1 : & \quad X_k = s + n_k \end{aligned}$$

where  $s$  is a known signal and  $n_k$  is zero mean Gaussian noise with variance  $\sigma^2$ , for  $k = 1, 2$ . Without loss of generality, we assume  $s = 1$  and  $\sigma^2 = 1$ . Each local sensor makes a binary decision using its observation  $X_k$  and a decision rule  $\gamma_k$ , i.e.,  $U_k = \gamma_k(X_k) \in \{1, 0\}$ . The transmission of  $U_k$ , however, is subject to channel losses. If both  $U_1$  and  $U_2$  are successfully received, Decoder 0 will implement the maximum *a posteriori* probability decoding (detection) rule, i.e.,

$$P(U_0 = 1|U_1, U_2) = \begin{cases} 1, & \text{if } \frac{P(U_1, U_2|H_1)}{P(U_1, U_2|H_0)} \geq \frac{\pi_0}{\pi_1} \\ 0, & \text{otherwise} \end{cases} \quad (20)$$

For simplicity, we consider a symmetric setting where we use identical error probability constraints (i.e.,  $\epsilon_1 = \epsilon_2$ ) for the constrained minimization approach, and identical erasure probabilities (i.e.,  $\delta_1 = \delta_2$ ) for the erasure channel model approach.

In addition to the proposed approaches, we also present results using alternative approaches to highlight the robustness of the proposed MD principle based framework. The complete list of approaches used in the simulations is as follows.

Approach 1 Constrained minimization described in Section III (Theorem 1).

Approach 2 Erasure channel model approach described in Section IV (Theorem 2).

Approach 3 Minimizing the local error probabilities  $P_{e1}$  and  $P_{e2}$ . We denote by  $P_{ek,3}$  ( $k = 1, 2$ ) the minimum achievable local error probabilities, and  $P_{e0,3}$  the corresponding error probability at Decoder 0, respectively. Note that  $P_{ek,3}$  provides the lower bound for the local error probability constraint  $\epsilon_k$ , i.e., one must have  $\epsilon_k \geq P_{ek,3}$  for the constrained minimization formulation to have a solution.

Approach 4 Minimizing the error probability at the fusion center. We denote by  $P_{e0,4}$  the minimum achievable error probability at Decoder 0, and  $P_{ek,4}$  ( $k = 1, 2$ ) the corresponding local error probabilities, respectively. *This approach corresponds to the classical distributed detection with a single objective function.* An interesting observation is that this approach can be considered as a special case of the erasure channel model with  $\delta_k = 0$ , for  $k = 1, 2$ . As such, one only need to minimize  $P_{e0}$  as both transmissions are always assumed successful.

Notice that Approaches 3 and 4 are conflicting with each other: one can show that optimizing  $P_{e0}$  and  $P_{ek}$  for  $k = 1, 2$  can not be simultaneously achieved [14]. Otherwise, the entire distributed MD framework will become trivial as one can simultaneously optimize the local error probability and that of Decoder 0 (the fusion center).

As we are considering a Gaussian problem, the obtained LRT thresholds at the sensors can be directly translated into thresholds for the original observations. Thus in the following presentation, we will use thresholds for the original observations, denoted by  $\eta_k$  for  $k = 1, 2$ .

The numerical results are summarized in Tables I-III as well as in Figs. 4-6. Specifically,

- Tables I and II enumerate respectively the parameters and the obtained thresholds and error probabilities of the two

TABLE I  
THRESHOLDS AND ERROR PROBABILITIES OBTAINED USING APPROACH 1

$\pi_0 = 0.6$					$\pi_0 = 0.8$				
$\epsilon_k$	$\eta_k$	$P_{ek}$	$P_{e0}$	$\lambda_k$	$\epsilon_k$	$\eta_k$	$P_{ek}$	$P_{e0}$	$\lambda_k$
0.33	0.2629	0.33	0.2574	0.0177	0.25	0.8474	0.2466	0.1686	0
0.32	0.3609	0.32	0.2591	0.1652	0.21	1.1737	0.21	0.1744	0.1788
0.31	1.2895	0.3047	0.2632	0.0001	0.2	2.0292	0.1866	0.1775	0.001
0.30	1.1812	0.30	0.2649	0.4023	0.19	2.0292	0.1866	0.1775	0.001

TABLE II  
THRESHOLDS AND ERROR PROBABILITIES OBTAINED USING APPROACH 2

$\pi_0 = 0.6$					$\pi_0 = 0.8$				
$\delta_k$	$\eta_k$	$P_{ek}$	$P_{e0}$	$\alpha_k$	$\delta_k$	$\eta_k$	$P_{ek}$	$P_{e0}$	$\alpha_k$
0.0174	0.2629	0.33	0.2574	0.0177	0.01	0.8667	0.2438	0.1686	0.0101
0.2869	1.1812	0.3	0.2649	0.4023	0.4	1.9757	0.1864	0.1777	0.8
0.5	1.0971	0.2973	0.2685	1.0	0.5	1.9616	0.1863	0.1778	1
0.7	1.018	0.2955	0.2738	2.3333	0.7	1.9324	0.1863	0.1780	2.3333
0.9	0.9417	0.2946	0.2807	9.0	0.9	1.902	0.1862	0.1784	9.0

TABLE III  
THRESHOLDS AND ERROR PROBABILITIES OBTAINED USING  
APPROACHES 3 AND 4

Approach 3	$\eta_k$	$P_{ek,3}$	$P_{e0,3}$
$\pi_0 = 0.6$	0.9059	0.2945	0.2846
$\pi_0 = 0.8$	1.8863	0.1862	0.1787
Approach 4	$\eta_k$	$P_{ek,4}$	$P_{e0,4}$
$\pi_0 = 0.6$	0.2495	0.3315	0.2574
$\pi_0 = 0.8$	0.8474	0.2466	0.1686

TABLE IV  
LOCAL MINIMA OBTAINED BY THE ERASURE CHANNEL MODEL  
APPROACH,  $\epsilon_k = 0.32$ ,  $\alpha_k = \lambda_k = 0.1652$

$\delta_k$	$\eta_k$	$P_{ek}$	$P_{e0}$	$Q$
0.1418	1.237	0.3023	0.2636	0.3635
0.1418	0.3609	0.32	0.2591	0.3648

proposed approaches (Approaches 1 and 2).

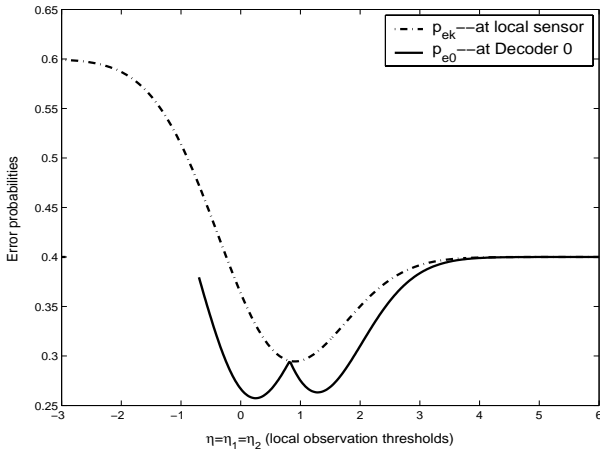
- Tables III gives the obtained thresholds and error probabilities of the two alternative approaches (Approaches 3 and 4).
- Figs. 4 and 5 give the analytically calculated error probabilities (both of the fusion center and local sensors) versus threshold plots with two different priors,  $\pi_0 = 0.6$  and  $\pi_0 = 0.8$ , respectively. In each plot, (b) is a zoom-in of (a) for better visualization.
- Fig. 6 is the error probability versus erasure probability plot.

Our observations from the numerical results are summarized below.

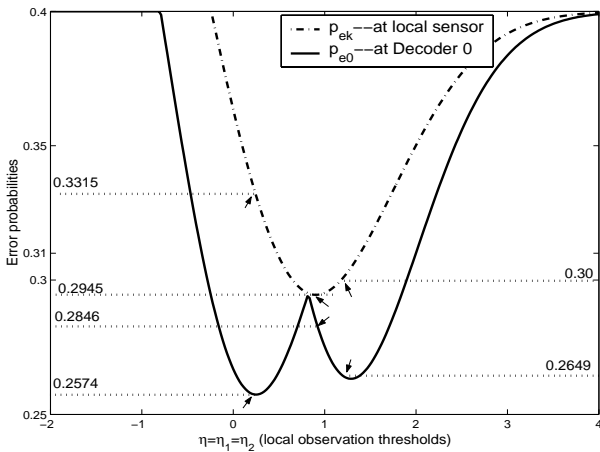
- For Approach 1, the iterative algorithm indeed yields thresholds that are solutions to the constrained optimization problem. For example, with  $\pi_0 = 0.6$  and error probability constraint  $\epsilon_k = 0.3$ , the threshold obtained using Approach 1 is  $\eta_k = 1.1812$  with corresponding error probabilities  $P_{e0} = 0.2649$  and  $P_{e1} = P_{e2} = 0.30$  (the left half of the last row of Table I). This is consistent with Fig. 4 (the corresponding values are marked on Fig. 4(b)). Similarly, with  $\pi_0 = 0.8$  and  $\epsilon_k = 0.2$ , the minimum achievable  $P_{e0} = 0.1775$  with the corresponding threshold  $\eta_k = 2.0311$  and local error probability  $P_{ek} = 0.1866$ . These values are marked on Fig. 5 and are consistent with those listed in Table I (right half of the last row).
- From Table I, it can be seen that, by comparing columns corresponding to  $P_{ek}$  and  $P_{e0}$ , smaller local sensor error

probabilities typically result in larger error probability at the fusion center. In general, having a generous constraint on local sensor error probabilities (large  $\epsilon_k$ ) imposes less restriction on the admissible threshold pairs, which typically gives rise to smaller  $P_{e0}$ . In the extreme case, for example, when  $\epsilon_k = 0.5$ , the obtained thresholds will always coincide with that of Approach 4.

- The classical distributed detection (Approach 4) that minimizes error probability at the fusion center suffers significant performance loss in the event of a lost transmission. This can be illustrated using Fig. 4(b) along with Table III. At  $\pi_0 = 0.6$ , Approach 4 yields a globally minimum error probability  $P_{e0} = 0.2574$  at the fusion center. However, if one of the transmission is lost, the error probability suffers a significant degradation to  $P_{ek} = 0.3315$  (marked on the dash-dotted curve). Clearly, the constrained optimization approach is much more robust (a degradation from  $P_{e0} = 0.2649$  to  $P_{ek} = 0.30$ ). This effect is even more pronounced for the case of  $\pi_0 = 0.8$ . Approach 4 yields a fusion center error probability  $P_{e0} = 0.1686$  (corresponding to the minimum point of the solid curve in Fig. 5(b)). However, if only one transmission reach the fusion center, the error probability becomes  $P_{ek} = 0.2466$  which essentially renders this system useless – as the prior probability is  $\pi_0 = 0.8$ , the error probability should be capped at 0.2. This seemingly pathological result is due to the fact that the threshold design at local sensors for the classical distributed detection *always* assumes successful transmissions from other collaborating sensors.
- Approach 3 which optimizes local sensor performance does not have significant improvement when both trans-



(a)



(b)

Fig. 4. Analytically calculated error probability versus threshold plot for  $\pi_0 = 0.6$ ; (b) is a zoom-in of (a).

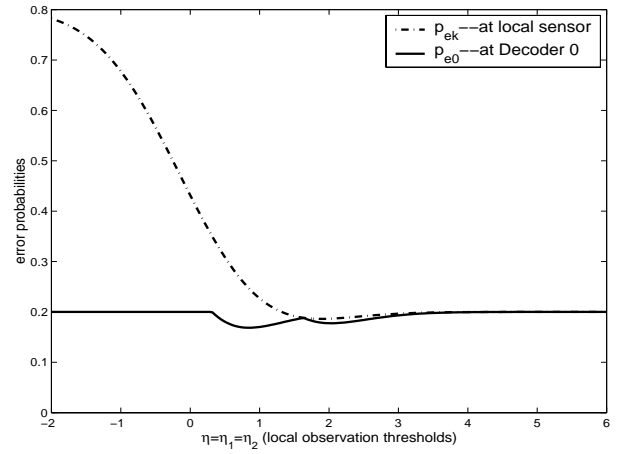
TABLE V

LOCAL MINIMA OBTAINED BY THE ERASURE CHANNEL MODEL  
APPROACH,  $\epsilon_k = 0.3$ ,  $\alpha_k = \lambda_k = 0.4023$

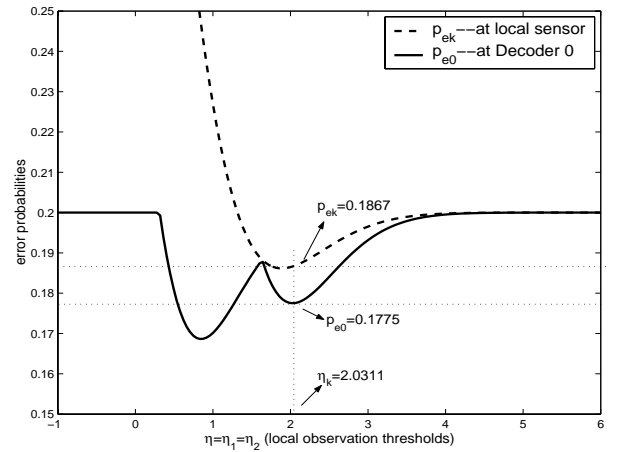
$\delta_k$	$\eta_k$	$P_{ek}$	$P_{e0}$	$Q$
0.2869	0.4784	0.3101	0.2645	0.514
0.2869	1.1812	0.3	0.2649	0.5063

missions are successful. From Table III and Fig. 4, for  $\pi_0 = 0.6$ , the minimum local sensor error probability is  $P_{e1} = P_{e2} = 0.2945$ . When both transmissions are successful, the fusion center will have an error probability  $P_{e0} = 0.2846$ , which is only marginally better than the individual sensor's performance. This improvement is much smaller than that achieved by the proposed constrained minimization approach.

- For the erasure channel model approach, as the erasure probability  $\delta_k$  approaches one, the obtained optimal local thresholds converge to that obtained using Approach 3 (minimizing the local error probabilities). This can be seen by comparing Tables II and III: the thresholds obtained using Approach 2 will approach that of Approach 3 as  $\delta_k$  increases. This is expected since large  $\delta_k$  implies that the channel is likely to break down, thus the local error probability will dominate the system performance.



(a)



(b)

Fig. 5. Analytically calculated error probability versus threshold plot for  $\pi_0 = 0.8$ ; (b) is a zoom-in of (a).

On the other hand, as the erasure probabilities approach zero, the obtained optimal local thresholds converge to those that minimize the error probability at Decoder 0 (corresponding to Approach 4). Intuitively, small  $\delta_k$  indicates a high probability of successful transmissions of both  $U_1$  and  $U_2$ . Thus, the error probability at Decoder 0 would largely determine the system performance. The same behavior can be observed from Fig. 6, plotted for  $\pi_0 = 0.6$ , by looking at the two extreme points corresponding to  $\delta_k = 0$  and  $\delta_k = 1$ . The associated error probabilities coincide with that of Approach 4 and 3 respectively.

- We have explored the intrinsic connections between Approach 1 and 2 in Section IV. Now we present numerical results to further elaborate the connections. Consider the case of  $\pi_0 = 0.6$ .
  - With  $\epsilon_k = 0.32$ , the corresponding  $\lambda_k = 0.1652$ . Set  $\alpha_k = 0.1652$ , we obtain two local minima that satisfy Eq. (17), as listed in Table IV. Since we want to choose the thresholds that minimize  $Q$ , it turns out that  $\eta_1 = \eta_2 = 1.237$  (with  $P_{e1} = P_{e2} = 0.3023$  and  $P_{e0} = 0.2636$ ) is the optimal solution for the erasure channel model approach. But the constrained

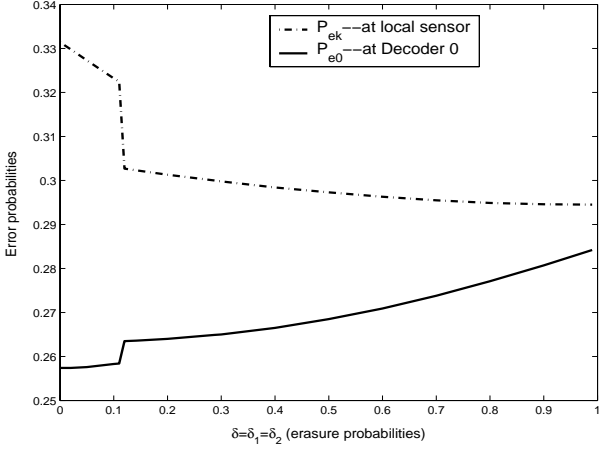


Fig. 6. Error probability versus erasure probability plot for  $\pi_0 = 0.6$  obtained using the channel-aware quantization for the erasure channel model.

minimization approach results in the thresholds  $\eta_1 = \eta_2 = 0.3609$  (with  $P_{e1} = P_{e2} = 0.32$  and  $P_{e0} = 0.2519$ ). From Table IV, it is clear that Eq.(19) does not hold, i.e., the  $Q$  function corresponding to  $P_{ek} = 0.32$  is not the smallest among the two. Hence in this particular setup, these two approaches do not have the same optimal solution.

- Now we examine a case when the two formulations share the same solution. Consider  $\epsilon_k = 0.3$ , the corresponding  $\lambda_k = 0.4023$ . Set  $\alpha_k = 0.4023$ , again there are two local minima as listed in Table V obtained using the erasure channel model approach. We notice that  $\eta_1 = \eta_2 = 1.1812$  is the optimal solution for both approaches and it is easy to check that Eq.(19) is satisfied.
- In general, the rate of convergence of the proposed iterative algorithm depends on the initial values of local thresholds. Our simulations indicate that the proposed iterative algorithm converges very fast. For all the scenarios we have examined, convergence happens typically after several ( $< 10$ ) iterations. For instance, the results in Table I were obtained after about six iterations on the average.

## VI. CONCLUSIONS

In this paper, we developed robust signal processing techniques for distributed sensor networks applications. In particular, we presented a distributed multiple description quantization (DMDQ) framework for the design of sensor signaling in the presence of sensor failures/channel outages. Two approaches are proposed to address the DMDQ design using a two-sensor distributed detection problem. The first scheme is based on a constrained minimization approach; and a solution using Lagrangian multiplier is presented. The second imposes a discrete erasure channel model; we developed the channel-aware quantizer design that minimizes the average error probability. Iterative algorithms were constructed in search of the optimal thresholds. The intrinsic connections between the two approaches were explored. A design example was used to show how the DMDQ can be implemented in a real distributed

detection problem, and to demonstrate its robust performance compared with the classical distributed detection approach in the presence of possible transmission losses.

Our future work will address the application of the MD principle to sensor networks involving more than two sensors. The problem becomes conceivably much more complex as the number of objective functions grow exponentially as the number of sensors. Thus the constrained minimization approach may not be feasible. On the other hand, the erasure channel model essentially collapses the multi-objective functions into a single error probability, making it more appealing in dealing with large sensor networks. Thoroughly understanding the connection between the constrained minimization problem and the erasure channel model will provide valuable insight in how to choose the erasure channel model parameters.

## APPENDIX I PROOF OF THEOREM 1

Without loss of generality, we expand  $P_{e0}$  with respect to  $U_1$  and rewrite  $P_{e0}$  as the form in Eq. (21), where  $A_1$  and  $B_1$  are defined in Eqs. (12) and (13), and

$$C_1 = \pi_0 \int_{U_2} P(U_2|H_0)P(U_0 = 1|U_1 = 0, U_2) + \pi_1 \int_{U_2} P(U_2|H_1)P(U_0 = 0|U_1 = 0, U_2)$$

$C_2$  can be similarly defined by swapping the roles of  $U_1$  and  $U_2$ . Without loss of generality, we can rewrite  $P_{e0}$  as:

$$P_{e0} = \pi_0 P(U_k = 1|H_0)A_k - \pi_1 P(U_k = 1|H_1)B_k + C_k$$

for  $k = 1, 2$ .

From Eq. (1), the local error probabilities can be expressed as  $P_{ek} = \pi_0 P_{fk} + \pi_1 (1 - P_{dk})$ , where  $P_{fk} = P(U_k = 1|H_0)$  and  $P_{dk} = P(U_k = 1|H_1)$ . Thus the left-hand side of Eq. (3) becomes

$$\begin{aligned} \frac{\partial P_{e0}}{\partial \tau_k} + \sum_{i=1}^2 \lambda_i \frac{\partial (P_{ei} - \epsilon_i)}{\partial \tau_k} \\ = \pi_0 A_k \frac{\partial P_{fk}}{\partial \tau_k} - \pi_1 B_k \frac{\partial P_{dk}}{\partial \tau_k} + \lambda_k (\pi_0 \frac{\partial P_{fk}}{\partial \tau_k} - \pi_1 \frac{\partial P_{dk}}{\partial \tau_k}) \\ = \pi_0 A_k \frac{\partial P_{fk}}{\partial \tau_k} - \pi_1 B_k \tau_k \frac{\partial P_{fk}}{\partial \tau_k} + \lambda_k (\pi_0 \frac{\partial P_{fk}}{\partial \tau_k} - \pi_1 \tau_k \frac{\partial P_{fk}}{\partial \tau_k}) \end{aligned} \quad (22)$$

where we have used the fact that  $\frac{dP_{dk}}{dP_{fk}} = \tau_k$ , and  $\tau_k$  is the LR threshold for the  $k$ th sensor.<sup>2</sup>

Set (22) equal to zero, we have  $\tau_k = \frac{\pi_0 (A_k + \lambda_k)}{\pi_1 (B_k + \lambda_k)}$ . Eqs. (8-11) follow by directly applying the Kuhn-Tucker theorem for the two cases  $\lambda_k = 0$  and  $\lambda_k > 0$  separately. Thus, Theorem 1 is proved.

## APPENDIX II PROOF OF THEOREM 2

Similar to the proof in Appendix I,  $P_{e0}$  can be expanded with respect to the individual decision rules, and we get, for

<sup>2</sup>This is the property of the receiver operating characteristics (ROC) curve for a likelihood ratio test. The threshold corresponding to the  $(P_f, P_d)$  pair

$$\begin{aligned}
P_{e0} &= \pi_0 P(U_0 = 1|H_0) + \pi_1 P(U_0 = 0|H_1) \\
&= \pi_0 \int_{U_1, U_2} P(U_0 = 1|U_1, U_2) P(U_1, U_2|H_0) + \pi_1 \int_{U_1, U_2} P(U_0 = 0|U_1, U_2) P(U_1, U_2|H_1) \\
&= \pi_0 \int_{U_2} P(U_2|H_0) [P(U_0 = 1|U_1 = 1, U_2) P(U_1 = 1|H_0) + P(U_0 = 1|U_1 = 0, U_2) P(U_1 = 0|H_0)] \\
&\quad + \pi_1 \int_{U_2} P(U_2|H_1) [P(U_0 = 0|U_1 = 1, U_2) P(U_1 = 1|H_1) + P(U_0 = 0|U_1 = 0, U_2) P(U_1 = 0|H_1)] \\
&= \pi_0 P(U_1 = 1|H_0) A_1 - \pi_1 P(U_1 = 1|H_1) B_1 + C_1
\end{aligned} \tag{21}$$

$k = 1, 2,$

$$\begin{aligned}
P_{e0} &= \int_{X_k} [\pi_0 A_k P(X_k|H_0) - \pi_1 B_k P(X_k|H_k)] \\
&\quad P(U_k = 1|X_k) dX_k + C_k
\end{aligned} \tag{23}$$

where  $C_k$  has no effect on the decision rule at sensor  $k$ .

Similarly, the error probability at the  $k$ th sensor can be expanded as

$$\begin{aligned}
P_{ek} &= \pi_0 P(U_k = 1|H_0) + \pi_1 P(U_k = 0|H_1) \\
&= \int_{X_k} [\pi_0 P(X_k|H_0) - \pi_1 P(X_k|H_1)] \\
&\quad P(U_k = 1|X_k) dX_k + \pi_1
\end{aligned} \tag{24}$$

Thus, using sensor 1 as an illustration, the average error probability  $P_e$  can be written as the form in Eq. (25), from Eqs. (14), (23), and (24). As  $D_1$  is independent of the quantizer rule at sensor 1, we need only to minimize the first term in Eq. (25) with respect to the local decision rule for sensor 1. Thus, the optimum local decision rule for sensor 1 is as follows.

$$P(U_1 = 1|X_1) = \begin{cases} 1, & \text{if } F_1 \geq 0 \\ 0, & \text{otherwise} \end{cases} \tag{26}$$

This is equivalent to the decision rule specified by Eqs. (15-16) for  $k = 1$ . The optimum quantizer rule for sensor 2 can be similarly established. This completes the proof of Theorem 2.

## REFERENCES

- [1] V. Goyal, "Multiple description coding: Compression meets the network," *IEEE Signal Processing Mag.*, vol. 19, pp. 74-93, Sep. 2002.
- [2] L. Ozarow, "On a source-coding problem with two channels and three receivers," *Bell Syst. Tech. J.*, vol. 59, no. 10, pp. 1909-1921, 1980.
- [3] V. Vaishampayan, "Design of multiple description scalar quantizer," *IEEE Trans. Inform. Theory*, vol. 39, pp. 821-834, May 1993.
- [4] J. Tsitsiklis, "Decentralized detection," in *Advances in Statistical Signal Processing*, H. Poor and J. Thomas, eds. Greenwich, CT: JAI Press, 1993.
- [5] R. Viswanathan and P. Varshney, "Distributed detection with multiple sensors: Part II — Fundamentals," *Proceedings IEEE*, vol. 85, no. 1, pp. 54-63, Jan. 1997.
- [6] J. Tsitsiklis, "On threshold rules in decentralized detection," in *Proc. 25th IEEE Conf. Decision Control*, Dec. 1986, vol. 1, pp. 232-236.
- [7] B. Chen and P. Willett, "Channel optimized binary quantizers for distributed sensor networks," in *Proc. IEEE Intl. Conf. Acoust. Speech, Signal Processing*, May 2004, vol. 3, pp. iii-845-8.
- [8] —, "On the optimality of likelihood ratio test for local sensor decisions in the presence of non-ideal channels," *IEEE Trans. Inform. Theory*, vol. 51, pp. 693-699, Feb. 2005.
- [9] B. Liu and B. Chen, "Joint source-channel coding for distributed sensor networks," in *Proc. Asilomar Conf. Signals, Syst., Computers*, Nov. 2004, pp. 1397-1401.

- [10] M. Aoki, *Introduction to Optimization Techniques*. New York: Macmillan, 1971.
- [11] I. Hoballah and P. Varshney, "Distributed Bayesian signal detection," *IEEE Trans. Inform. Theory*, vol. 35, pp. 995-1000, Sep. 1989.
- [12] P. K. Varshney, *Distributed Detection and Data Fusion*. New York: Springer, 1997.
- [13] Y. Zhou and W.-Y. Chan, "Multiple description quantizer design using a channel optimized quantizer approach," in *Proc. CISS'2004*, March 2004, pp. 1425-1430.
- [14] B. Chen, "On the local sensor signaling for inference centered wireless sensor networks," in *2nd IEEE Upstate New York Workshop Sensor Networks*, Oct. 2003.



signal processing.

**Ying Lin** (S'05) received the B.S. and M.S. degrees in electrical engineering from Harbin Institute of Technology, Harbin, China, in 1995 and 1997, respectively. From 1997 to 2000, she was a software engineer with Centell telecommunication corporation (CTC), Beijing. Since 2000, she has been working toward her Ph.D degree in the Department of Electrical Engineering and Computer Science at Syracuse University, Syracuse, NY. Her current research interests are related to wireless sensor network, wireless communication, and statistical



**Biao Chen** (S'98-M'99-SM'07) received his B.E. and E.E. in Electrical Engineering from Tsinghua University, Beijing, China, in 1992 and 1994 respectively. After a short stint with AT&T (China) Inc., Beijing, China, he joined the University of Connecticut, Storrs, in 1995 where he received his M.S. in Statistics and Ph.D. in Electrical Engineering, in 1998 and 1999, respectively. From 1999 to 2000 he was with Cornell University as a Post-Doc research associate. Since 2000, he has been with Syracuse University, Syracuse, NY, where he is currently an associate professor with the Department of Electrical Engineering and Computer Science. He is an associate editor for *IEEE Communications Letters* and for the *EURASIP Journal on Wireless Communications and Networking* (JWCN). He was a guest editor for a special issue on Wireless Sensor Networks of *EURASIP JWCN*, and is a member of the IEEE Signal Processing Society Sensor Array and Multichannel (SAM) technical committee. In 2006, he was the recipient of a NSF CAREER Award. His area of interest mainly focuses on signal processing for wireless sensor and ad hoc networks and in multi-user MIMO systems.

$$\begin{aligned}
P_e &= (1 - \delta_1)(1 - \delta_2)P_{e0} + \delta_2(1 - \delta_1)P_{e1} + \delta_1(1 - \delta_2)P_{e2} + \min\{\pi_0, \pi_1\}\delta_1\delta_2 \\
&= (1 - \delta_1)(1 - \delta_2) \int_{X_1} P(U_1 = 1|X_1) [\pi_0 A_1 P(X_1|H_0) - \pi_1 B_1 P(X_1|H_1)] dX_1 \\
&\quad + \delta_2(1 - \delta_1) \int_{X_1} P(U_1 = 1|X_1) [\pi_0 P(X_1|H_0) - \pi_1 P(X_1|H_1)] dX_1 + D_1 \\
&= \int_{X_1} P(U_1 = 1|X_1) F_1 dX_1 + D_1 \tag{25} \\
D_1 &= C_1 + \delta_2(1 - \delta_1)\pi_1 + \delta_1(1 - \delta_2) \int_{X_2} P(U_2 = 1|X_2) [\pi_0 P(X_2|H_0) - \pi_1 P(X_2|H_1)] dX_2 + \pi_1 \\
F_1 &= (1 - \delta_1)(1 - \delta_2) [\pi_0 A_1 P(X_1|H_0) - \pi_1 B_1 P(X_1|H_1)] + \delta_2(1 - \delta_1) [\pi_0 P(X_1|H_0) - \pi_1 P(X_1|H_1)]
\end{aligned}$$



**Bruce Suter** (S'69-M'72-SM'92) received the B.S. and M.S. degrees in electrical engineering in 1972 and the Ph.D. degree in computer science in 1988, all from the University of South Florida, Tampa, FL.

Since 1998, he has been with the Information Directorate of the Air Force Research Laboratory, Rome, NY, where he is the Founding Director of the Center for Integrated Transmission and Exploitation. Dr. Suter has authored over a hundred publications and is the author of the book *Multirate and Wavelet*

*Signal Processing* (Academic Press, 1998). His research interests include

multiscale signal and image processing, cross layer optimization, networking of unmanned aerial systems, and wireless communications. His professional background includes industrial experience with Honeywell Inc., St. Petersburg, FL and with Litton Industries, Woodland Hills, CA, and academic experience at the University of Alabama, Birmingham, AL and at the Air Force Institute of Technology, Wright-Patterson AFB, OH. Dr. Suter's honors include Fellow of the Air Force Research Laboratory, the Arthur S. Flemming Award: Science Category, and the General Ronald W. Yates Award for Excellence in Technology Transfer. He served as an associate editor of the IEEE TRANSACTIONS ON SIGNAL PROCESSING. Dr. Suter is a member of Tau Beta Pi and Eta Kappa Nu.

# Minimum Error Probability Cooperative Relay Design

Bin Liu, *Member, IEEE*, Biao Chen, *Member, IEEE*, and Rick S. Blum, *Fellow, IEEE*

**Abstract**—In wireless networks, user cooperation has been proposed to mitigate the effect of multipath fading channels. Recognizing the connection between cooperative relay with finite alphabet sources and the distributed detection problem, we design relay signaling via channel aware distributed detection theory. Focusing on a wireless relay network composed of a single source–destination pair with  $L$  relay nodes, we derive the necessary conditions for optimal relay signaling that minimizes the error probability at the destination node. The derived conditions are person-by-person optimal: each local relay rule is optimized by assuming fixed relay rules at all other relay nodes and fixed decoding rule at the destination node. An iterative algorithm is proposed for finding a set of relay signaling approaches that are simultaneously person-by-person optimal. Numerical examples indicate that the proposed scheme provides performance improvement over the two existing cooperative relay strategies, namely amplify-forward and decode-forward.

**Index Terms**—Cooperative relay, decentralized detection, finite alphabet, wireless relay network.

## I. INTRODUCTION

IN wireless networks, a severe limiting factor is multipath-induced channel fading. One of the most effective methods in mitigating fading is to exploit diversity. Examples include spatial diversity when multiple antennas are used at the transceivers, multipath diversity in frequency-selective channels, and temporal diversity in time-selective fading channels through the use of coding/interleaving. More recently, a new diversity resource has attracted considerable attention, especially in the context of wireless *ad hoc* networks [1]–[3]. There, multiple nodes collaborate in transmitting their information, thus providing diversity by exploiting the independence of the fading channels of different users. This is generally referred to as the *cooperative diversity*, and the collection of cooperating

nodes, including the source and the destination nodes, are referred to as a *relay network*.

Historically, study of relay networks has focused on the capacity issue, e.g., achievable rates. The classical three-node relay network was first introduced by van der Meulen [4], and its capacity was extensively studied by Cover and El Gamal [5]. Gastpar and Vetterli [6] considered the capacity of wireless networks with multiple relay nodes and showed that the lower and upper bounds became the same asymptotically as the number of nodes in the network goes to infinity. Sendonaris *et al.* [1], [2] were the first to introduce the concept of *user cooperation diversity* where the mobile users shared their antennas and other resources to obtain diversity gain through distributed transmission. Focusing on a two-user case, it was shown that user cooperation results in an increase in capacity for both users. In addition, the achievable rates are less susceptible to channel variations, making the cooperative network a more robust system. Kramer *et al.* considered several coding strategies for various relay networks in [7] and showed that a strategy that mixes decode-forward and compress-forward achieves capacity if the terminals form two closely-spaced clusters.

The performance of wireless relay networks has also been evaluated by diversity gain and outage probability. By constraining the nodes to half-duplex mode, Laneman *et al.* [3] developed various cooperative transmission protocols and showed that most of the protocols achieve full diversity order (equal to the number of cooperative nodes). Space–time code-based cooperative transmission protocols were developed in [8] and were also shown to achieve full diversity. In [9] and [10], symbol error probabilities were derived in the high signal-to-noise ratio (SNR) regime for the general multihop, multibranch wireless relay model using the amplify-forward (AF) scheme; the result provides insight on the optimum placement of relay nodes. Chen and Laneman [11] focused on the decode-forward (DF) scheme and developed a general framework for maximum-likelihood (ML) demodulation in cooperative wireless communication systems.

In this paper, we focus on a relay network consisting of a single source–destination pair and  $L$  relay nodes. As illustrated in Fig. 1, each relay node receives the signal from the source node and generates a processed signal based on its received signal. The processed signals from all the relay nodes are sent to the destination node using orthogonal channels. The destination node uses the relay signals along with the signal sent directly from the source node to determine the source signal. Novel in the current work is the attempt to find channel-aware processing that *minimizes the error probability at the destination node*. The proposed design approach exploits the finite-alphabet (FA) property of the source message, thereby enabling

Manuscript received March 29, 2005, revised April 3, 2006. The associate editor coordinating the review of this manuscript and approving it for publication was Dr. Sergio Barbarossa. This work was supported in part by the National Science Foundation under Grants ECS-0501534 and CCR-0112501, by the Air Force Office of Scientific Research under Grant FA9550-06-1-0051, and by the Air Force Research Laboratory under agreement No. F49620-03-1-0214 and FA8750-05-2-0120. This work was presented in part at the IEEE International Conference on Acoustics, Speech, and Signal Processing (ICASSP), Philadelphia, PA, March 2005.

B. Liu and B. Chen are with the Department of Electrical Engineering and Computer Science, Syracuse University, Syracuse, NY 13244 USA (e-mail: bilu{bichen}@ecs.syr.edu).

R. S. Blum is with the Department of Electrical and Computer Engineering, Lehigh University, Bethlehem, PA 18015 USA (e-mail: rblum@eecs.lehigh.edu).

Color versions of Figs. 2–10 are available online at <http://ieeexplore.ieee.org>. Digital Object Identifier 10.1109/TSP.2006.885778

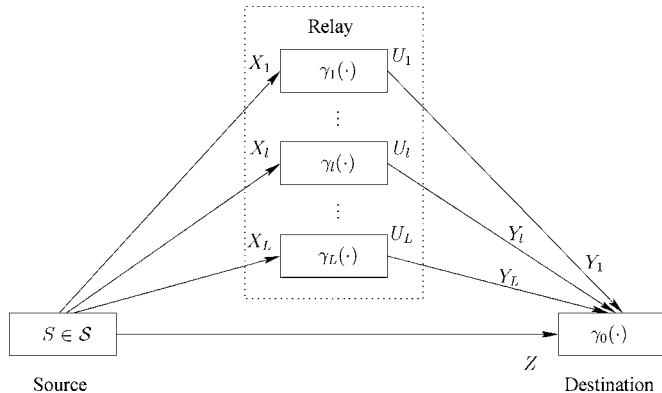


Fig. 1. Wireless relay network with  $L$  relay nodes and a direct link connecting the source and the destination nodes.

us to pose the cooperative relay design as a distributed multiple hypotheses testing problem. Notice that this FA property is ubiquitous in almost all wireless systems. A similar idea has been explored in [12] to study a diversity combining scheme using the quantized outputs from multiple antennas with independently faded binary frequency-shift keying (BFSK) signals. Distinctive in the current paper, in addition to considering a general FA source instead of BFSK, is that the relay outputs are assumed to also go through general non-ideal channels. Our approach is to generalize the channel aware distributed signaling design for binary hypothesis testing problem [13], [14] to this cooperative relay problem and derive a numerical procedure to compute the optimal local relay rules for minimum error probability at the fusion center.

While DF also utilizes the FA property, the proposed approach is based optimum detection theory and thus provides superior error probability performance. To motivate our proposed idea, we consider a simple relay network with one source–destination pair and two relay nodes. We also assume a parallel relay scheme where there is no direct transmission between the source node and the destination node. The source is binary with repetition coding, i.e., one transmits “+1 + 1 + 1 + 1” or “−1 − 1 − 1 − 1”, where the redundancy is used to combat channel impairment. We also restrict each relay node to send a four-bit sequence to the destination node. If we adopt a DF idea, each relay node attempts to recover the original binary source and resends it to the destination node. However, for this simple example, it will be seen that the optimum relay rule amounts to quantizing the local likelihood ratio; and better performance may result if one uses all possible output alphabet at the relay for the quantization. Contrasting this to the DF approach, one can consider our approach as using “soft” information from the relays as opposed to hard decisions for DF. As such, applying the distributed detection theory allows us to fully exploit the redundancy in the FA sources for improved detection performance.

Even without the redundancy in the FA sources, jointly designing the relay and destination signaling can still result in improved performance compared with DF. Consider, for example, a simple case in which the source signals are either “+1” or “−1”. The relay nodes are also restricted to transmit a binary (“+1” or “−1”) signal to the destination node. Assume that the

channels between the source and the two relay nodes have identical channel SNRs, while the SNRs of the channels between the two relays and the destination differ significantly from each other. One natural question is: How do we jointly determine the relay and destination processing/signaling that may minimize the error probability at the destination node? Clearly, if one resorts to the DF idea, each relay will try to recover the original signal and retransmit it to the destination node. As such, one can immediately conclude that this idea leads to identical relay rules at the two relay nodes. On the other hand, as the channels between the relays and the destination have different SNRs, should one design the processing/signaling differently for better performance? As demonstrated in Section IV, the optimum relaying for minimum error probability indeed uses different signaling at the two relays. Our goal is to come up with a mechanism to find out the optimal relay signaling.

The proposed cooperative relay signaling design assumes a clairvoyant case, i.e., the designer knows the global channel state information (CSI). While this is unrealistic, it provides important benchmark performance and reveals a significant gap in terms of error probability performance between what is achievable with the existing schemes and what is achievable theoretically. More important, the insight one draws from this clairvoyant case study may prove critical in devising cooperative signaling scheme under a more realistic setting with only distributed CSI knowledge (i.e., each relay node knows only its own CSI).

The rest of the paper is organized as follows: Section II describes the system model and the problem formulation. The problem setting allows us to derive, in Section III, the necessary conditions for optimal cooperative relay strategies at relay nodes to minimize the error probability at the destination node. In the same section, we also consider several special models and including the three-node relay network, the parallel relay model, and the singular relay network. Numerical examples are presented in Section IV to show the substantial performance gain of our approach over two existing relay strategies. We conclude in Section V.

## II. STATEMENT OF THE PROBLEM

Consider a wireless relay network which includes one source node,  $L$  relay nodes, and one destination node (Fig. 1). The data transmission is divided into two steps. In the first step, the source node broadcasts a signal  $S$  to all the relay nodes as well as the destination node. In the second step, the relay nodes then transmit the relay signals to the destination node in orthogonal channels. We assume that  $S$  is drawn from an FA set  $\mathcal{S} = \{s_0, \dots, s_{M-1}\}$  with prior probabilities  $\{\pi_0, \dots, \pi_{M-1}\}$ . Further, the received signals  $X_1, \dots, X_L$  at the relays and the received signal  $Z$  at the destination, which describe the broadcast channel during the first step, are characterized by

$$p(X_1, \dots, X_L, Z|S) = p(Z|S) \prod_{l=1}^L p(X_l|S) \quad (1)$$

i.e.,  $X_l$  and  $Z$  are conditionally independent given  $S$ . Here, the transmitted signal  $S$  can be a vector, and the received signal  $X_l$  and  $Z$  would have a similar structure. The  $l$ th relay node sends

a relay signal  $U_l$  to the destination node based on its received signal  $X_l$

$$U_l = \gamma_l(X_l), \quad l = 1, \dots, L. \quad (2)$$

We assume that, without loss of generality,  $U_l$  belongs to a FA set  $\mathcal{T} = \{u_0, u_1, \dots, u_{N-1}\}$ . While it may appear natural to require  $N = M$ , as in the case of DF, we can accommodate  $N \neq M$  in the proposed scheme. Indeed, as to be seen later, allowing  $N \neq M$  is advantageous as it provides flexibility in the relay signaling design. We note here that the condition  $N \neq M$  need not necessarily mean that the source sequence and the relay message have different lengths. Redundancy is typically built into the source sequence (e.g., channel coding), while the relay node may exploit all possible alphabets, as illustrated in the example in Section I. The relay outputs  $U_1, \dots, U_L$  are also sent through parallel transmission channels characterized by

$$p(Y_1, \dots, Y_L | U_1, \dots, U_L) = \prod_{l=1}^L p(Y_l | U_l). \quad (3)$$

Note that all the signals, including  $S$ ,  $Z$ ,  $X_l$ ,  $Y_l$ , and  $U_l$ , are assumed to be vectors.

Upon collecting the channel outputs from the relay nodes,  $\mathbf{y} = \{Y_1, \dots, Y_L\}$ , and from the source node  $Z$ , the destination node makes a final decision

$$U_0 = \gamma_0(\mathbf{y}, Z) \quad (4)$$

where  $U_0 \in \{s_0, \dots, s_{M-1}\}$  indicates which signal was sent from the source node.

An error happens if  $U_0 \neq S$ . The goal is, therefore, to jointly design the local relay schemes  $\gamma_l(\cdot)$ ,  $l = 1, \dots, L$  and the decoding rule  $\gamma_0(\cdot)$  such that the overall error probability at the destination node  $P(U_0 \neq S)$  is minimized. From the distributed detection point of view, this relay system can be regarded as an  $M$ -ary hypotheses testing system with each hypothesis corresponding to one of the input alphabet symbols, i.e.,  $H_i : S = s_i$ . Given independence among the transmission channels, the signals received at relay nodes are independent conditioned on the input source, or equivalently, a given hypothesis. Thus, the joint probability density function (pdf) of the signals received at the relays becomes

$$p(X_1, \dots, X_L | H_i) = \prod_{l=1}^L p(X_l | H_i), \quad i = 0, \dots, M-1. \quad (5)$$

Similarly, for the signals received at the destination node, the joint pdf conditioned on the decision made at the relays is

$$p(Y_1, \dots, Y_L, Z | U_1, \dots, U_L, H_i) = p(Z | H_i) \prod_{l=1}^L p(Y_l | U_l), \quad i = 0, \dots, M-1. \quad (6)$$

We point out here that integrating the transmission channels into the decoding rule design has been investigated before in the context of decision fusion in fading channels for wireless sensor networks (WSNs) [15]–[17]. The optimal decoding rule

in the Bayesian sense amounts to the maximum *a posteriori* probability (MAP) decision, i.e.,

$$U_0 = \gamma_0(\mathbf{y}, Z) = \arg \max_{s_i: i \in \{0, 1, \dots, M-1\}} \pi_i p(\mathbf{y}, Z | H_i). \quad (7)$$

Given a specified set of local relay strategies and the channel characteristics, this MAP decision rule can be obtained in a straightforward manner. As such, in the next section, we will focus on the local relay signaling design.

We close this section with a summary of the cooperative relay design problem.

1) *Problem Statement:* In a wireless relay network as described in Fig. 1, given the following:

- a FA source  $\mathcal{S} = \{s_0, \dots, s_{M-1}\}$  with prior probabilities  $\{\pi_0, \dots, \pi_{M-1}\}$ ;
  - the channels from the source to relay nodes described by  $p(X_l | S)$  for  $l = 1, \dots, L$ ;
  - the channels from the relay nodes to the destination node described by  $p(Y_l | U_l)$  for  $l = 1, \dots, L$ ;
  - the channel from the source to destination node described by  $p(Z | S)$ ;
  - and a decoding rule  $\gamma_0(\cdot)$  at the destination node;
- design the local relay rules  $\gamma_l(\cdot)$  for  $l = 1, \dots, L$  that minimize the overall error probability at the destination node  $\Pr(U_0 \neq S)$ .

### III. OPTIMAL LOCAL RELAY STRATEGIES

This is a joint optimization problem. In order to obtain a globally optimal scheme, we should simultaneously optimize the local relay schemes at all the relay nodes. This joint optimization, however, is not feasible due to the distributed nature of the problem [18]. In this paper, we adopt a person-by-person optimal (PBPO) approach, i.e., we optimize the local relay rule  $\gamma_l(\cdot)$  for the  $l$ th relay node given fixed relay rules at all other relay nodes and a fixed decoding rule  $\gamma_0(\cdot)$  at the destination node. As such, the conditions obtained are necessary, but not sufficient, for optimality. This PBPO approach has been widely adopted in various distributed inference problems (see, e.g., [19] and [20]).

Define

$$\mathbf{u} = [U_1, U_2, \dots, U_L], \quad \mathbf{x} = [X_1, X_2, \dots, X_L]$$

so that the error probability at the destination node can be written as

$$P_e \triangleq 1 - P_D = 1 - \int_{X_l} \sum_{j=0}^{N-1} P(U_l = u_j | X_l) D_{l_j} dX_l \quad (8)$$

where, for  $l = 1, \dots, L$ ,  $j = 0, \dots, N-1$

$$D_{l_j} = \sum_{i=0}^{M-1} \pi_i P(U_0 = s_i | U_l = u_j, H_i) p(X_l | H_i) \quad (9)$$

and

$$P(U_0 = s_i | U_l = u_j, H_i) = \int_Z \int_{\mathbf{y}} P(U_0 = s_i | \mathbf{y}, Z) p(Z | H_i) p(\mathbf{y} | U_l = u_j, H_i) d\mathbf{y} dZ. \quad (10)$$

Equations (8)–(10) can be obtained by expanding the error probability with respect to the  $l^{\text{th}}$  relay rule  $\gamma_l(\cdot)$ . The derivation is straightforward and follows the same spirit as that in [13]; hence, we skip the details.

Thus, to minimize  $P_e$ , or equivalently maximize  $P_D$ , we set  $P(U_l = u_{j^*} | X_l) = 1$ , where  $j^*$  is the index that maximizes  $D_{l_j}(X_l)$ . Hence, we have Theorem 1.

*Theorem 1:* The optimal relay rule for the  $l^{\text{th}}$  relay node must satisfy

$$U_l = \gamma_l(X_l) = \arg \max_{u_j: j \in \{0, 1, \dots, N-1\}} D_{l_j}(X_l) \quad (11)$$

for  $D_{l_j}(\cdot)$  defined in (9).

The major issue of Theorem 1 is to evaluate  $D_{l_j}(\cdot)$ . While it is possible to evaluate it analytically for some special cases, in general it requires numerical evaluation which is fairly straightforward.

As expressed in (9) and (10), given the fixed local relay rules of the other relay nodes  $p(\mathbf{y} | U_l = u_j, H_i)$ , and the decoding rule at the destination node  $P(U_0 = s_i | \mathbf{y}, Z)$ ,  $D_{l_j}(\cdot)$  only depends on the local observations at the  $l^{\text{th}}$  relay node and is a linear combination of the likelihood function of the local observations. Following the definition of likelihood ratio quantizer (LRQ) for multiple hypotheses testing [21], the optimal local relay rule as described in Theorem 1 is an LRQ.

An important distinction between the current work and that of [22] is that we are considering an  $M$ -ary hypotheses testing problem with general input (e.g., vector input such as a packet). As such, one does not have the luxury of equating the local relay rule to a scalar quantization problem; instead, one needs to quantize a  $(M - 1)$ -dimensional sufficient statistic [23]. Thus, convergence checking by comparing relay rules is generally not viable.

The fact that we use the PBPO criterion implies that the derived conditions are only necessary but not sufficient conditions for optimality. Recognizing that the necessary conditions for the relay function  $\gamma_l(\cdot)$  is coupled with the decoding rule, we propose the following iterative algorithm to find the relay and decoding rules that are at least locally optimum.

---

#### Iterative algorithm

---

- 1) Initialize the local relay strategies for each relay node  $\gamma_l^{(0)}$ ,  $l = 1, \dots, L$  and set the iteration index  $r = 1$ .
  - 2) Obtain the optimal decoding rule  $\gamma_0^{(r)}$  using (7) for fixed local relay rules  $\gamma_l^{(r-1)}$ ,  $l = 1, \dots, L$ .
  - 3) For each  $l$ , obtain the PBPO local relay rule  $\gamma_l^{(r)}$  of  $l^{\text{th}}$  relay node using (11) given the fixed local relay rules for the other relay nodes and fixed decoding rule.
  - 4) Evaluate the error probability  $P_e^{(r)}$  at the destination node given the relay rules  $\boldsymbol{\gamma}^{(r)} = \{\gamma_1^{(r)}, \dots, \gamma_L^{(r)}\}$  and decoding rule  $\gamma_0^{(r)}$ , and compare it with  $P_e^{(r-1)}$ . If the difference is less than a prescribed value, stop. Otherwise, set  $r = r + 1$  and go to Step 2).
- 

For each iteration, we optimize one rule given that the other rules are fixed. Therefore, the error probability is guaranteed to

be non-increasing after each step. Thus, the algorithm always converges as the error probability is lower bounded by zero.

#### A. Special Cases

The relay network described in Fig. 1 is rather general; it encompasses many special cases. For example, setting  $L = 1$  reduces it to the classical three-node relay network; and the corresponding optimum decoding rule and optimal local relay rule can be obtained by letting  $L = 1$  in (7) and (11). While this three-node network is not materially different from the general case, it does significantly reduce the computational complexity. Since there is a single relay node, there is no iteration among the relay rules. Instead, one only needs to iterate between the decoding rule and the relay rule.

Another interesting case is the parallel relay network where there is no direct transmission from the source node to the destination node. Following the same spirit of the derivation in Section III, we can easily get the optimal decoding rule and optimal relay rule which are similar to (7) and (11) except that  $Z$  is omitted from the expression.

We now consider the simplest possible relay system: there is only a single ( $L = 1$ ) relay node and there is no direct link between the source and the destination node. Notice that this simple model can be considered as a special case of either the three-node relay model or the parallel network. We term this as a *singular relay network*. In the context of channel optimized quantizer design for WSN, we have shown in [14] and [22] that for  $M = 2$  (i.e., a binary source), the optimum relay rule for a singular relay network is channel-blind; i.e., the local relay rule will remain unchanged when the relay-destination channel characteristics change. For this special case, the local relay rule is the same as that in the case with ideal relay-destination channel as this ideal channel can be treated as a limiting case of the fading channel. We show in the following that it is not true for the general case of  $M > 2$ ; that is, for a singular relay network with a general FA source, the relay signaling should always be channel aware.

By setting  $L = 1$  in (7) and (11) and omitting  $Z$ , we can easily obtain the decoding rule

$$U_0 = \gamma_0(Y) = \arg \max_{s_i: i \in \{0, 1, \dots, M-1\}} \pi_i p(Y | H_i) \quad (12)$$

and local relay rule

$$u = \gamma(X) = \arg \max_{u_j: j \in \{0, 1, \dots, N-1\}} D_j(X) \quad (13)$$

where

$$D_j(X) = \sum_{i=0}^{M-1} \pi_i P(U_0 = s_i | U = u_j) p(X | H_i). \quad (14)$$

Define

$$Z_{jl}(X) = \{X : D_j(X) < D_l(X)\}$$

which specifies a set such that a lower probability of error will result when the members of the set are assigned to index  $j$  instead of  $l$ . Define

$$P_{ijl} = P(U_0 = s_i | U = u_j) - P(U_0 = s_i | U = u_l) \quad (15)$$

and

$$L_i(X) = \frac{p(X|H_i)}{p(X|H_0)}.$$

Since

$$\sum_{i=0}^{M-1} P_{ijl} = 0$$

we have

$$\begin{aligned} D_j - D_l &= \sum_{i=0}^{M-1} \pi_i p(X|H_i) P_{ijl} \\ &= \sum_{i=1}^{M-1} \pi_i p(X|H_i) P_{ijl} - \sum_{i=1}^{M-1} \pi_0 p(X|H_0) P_{ijl} \\ &= \sum_{i=1}^{M-1} \pi_i p(X|H_0) P_{ijl} \left( L_i(X) - \frac{\pi_0}{\pi_i} \right). \end{aligned}$$

From (15), the change of channel characteristics may alter the value of  $P_{ijl}$ , which will result in a different region for deciding index  $j$  instead of  $l$ . In other words, the optimum relay rule for the singular relay network needs to be channel aware when  $M > 2$ .

#### IV. PERFORMANCE EVALUATION

In this section, through a number of numerical examples, we demonstrate the performance advantage of our approach over some existing relay strategies, namely DF and AF, for the relay network defined in Fig. 1. For DF, each relay node makes its own decision using an MAP rule, as follows:

$$U_l = \arg \max_{s_i: i \in \{0, \dots, M-1\}} \pi_i p(X_l | H_i), \quad l = 1, \dots, L \quad (16)$$

and re-encodes it and sends it to the destination node. This is different from the relay signaling specified in Theorem 1, i.e., (11) and (9), where all the relay rules are coupled with each other. We remark here that the DF approach considered in this paper is the vanilla version discussed in [8] and [11]. We assume that the relay node always forwards its best estimate to a destination node.

For AF, the output of the relay node is simply a scaled version of the received signal, i.e.,

$$U_l = c_l X_l, \quad l = 1, \dots, L$$

where the scaling factor  $c_l$  is determined so that all schemes have the same average power constraint. For fading channels, we have

$$c_l^2 = \frac{P_s}{P_s |\alpha_{1l}|^2 + \sigma_{1l}^2}$$

where  $P_s$  is the power constraint which is assumed to be the same for all the relay nodes as well as the source node,  $\alpha_{1l}$  is the channel coefficient and  $\sigma_{1l}^2$  is the variance of channel noise. At the destination node, all the schemes implement the MAP rule to obtain the final decision.

Throughout our simulations, we assume that the channels between the source and the relay nodes are identically and independently distributed (i.i.d.) Rayleigh-fading channels with average SNR denoted by  $\text{SNR}_{\text{sr}}$ . Similarly, the channels between the relay and destination node are also assumed to be i.i.d. Rayleigh fading channels with average SNR denoted by  $\text{SNR}_{\text{rd}}$  (except for the first example where both relay nodes experience different  $\text{SNR}_{\text{rd}}$ ). Notice that this is a somewhat simplifying assumption: In a homogeneous environment where the path loss exponent is a constant, the above assumption amounts to requiring that the relay nodes are equidistant to the source node as well as to the destination node. We will vary one of these two SNR with the other fixed; this captures the change in the placement of the relay nodes in terms of their distances to the source and to the destination nodes. The SNR for the direct link between the source and the destination node is denoted as  $\text{SNR}_{\text{sd}}$ . Further, all the channels are assumed to be slow fading channels so that the channel coefficients remain unchanged during the transmission of one symbol or a packet.

The signal sent from the source node is assumed to be a  $K$ -bit codeword drawn from a  $M$ -ary codebook with equal probability. Hence,  $M \leq 2^K$ . Each bit is assumed to use BPSK modulation. We also assume that the local decision at each relay node is  $K$  bits; thus, the relay output has a maximum alphabet size of  $N = 2^K$ .

#### A. Parallel Relay Network

We first consider an example that we discussed in Section I, the parallel relay network with  $K = 1$ ,  $M = N = 2$  and  $L = 2$ , i.e., a single BPSK symbol is sent from the source and is to be relayed to the destination node using two relay nodes. We assume that the BPSK signal has equal prior probability, i.e.,

$$P(S = -1) = P(S = +1) = 0.5.$$

We also assume that  $\text{SNR}_{\text{sr}}$  is identical for both relay nodes but  $\text{SNR}_{\text{rd}}$  may be different. In this case, the relay rule used by DF for the  $l$ th relay node can be easily obtained from (16),

$$\text{SST} \triangleq \text{Re}\{\alpha_l^* X\} \underset{-1}{\overset{+1}{\geq}} 0$$

where  $\alpha_l$  is the channel coefficient for the channel between the source node and the  $l$ th relay node and  $\text{Re}\{\cdot\}$  means real part. Application of Theorem 1 and our iterative algorithm show that our approach also compares SST to a threshold, but our threshold is obtained by jointly designing the relay rules and the decoding rule, which leads to performance gains. In Table I, with identical  $\text{SNR}_{\text{sr}}$  for both relay nodes and different  $\text{SNR}_{\text{rd}}$  for each relay node, we compare the thresholds of SST and overall error probability between DF and the proposed approach. As one can see, the proposed approach has better

TABLE I  
COMPARISON OF THRESHOLDS OF SST AND ERROR PROBABILITY BETWEEN DF AND PROPOSED APPROACH ( $\text{SNR}_{\text{sr}} = 5 \text{ dB}$ ).

$\text{SNR}_{r_d}$ for the first relay node	$\text{SNR}_{r_d}$ for the second relay node	Relay scheme	threshold at the first relay node	threshold at the second relay node	$P_e$
5dB	0dB	DF	0	0	0.0080
		Proposed approach	0.0005	-0.0063	0.0073
5dB	5dB	DF	0	0	0.0063
		Proposed approach	-0.0599	-0.0599	0.0045
5dB	10dB	DF	0	0	0.0060
		Proposed approach	-0.0786	-0.0512	0.0038

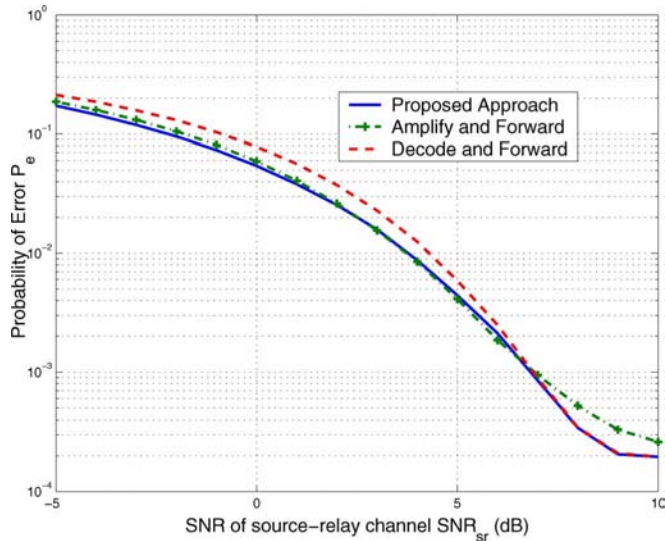


Fig. 2. Error probability versus SNR of source-relay channel for  $L = 2$ ,  $M = 2$ , and  $K = 1$  ( $\text{SNR}_{r_d} = 5 \text{ dB}$ ).

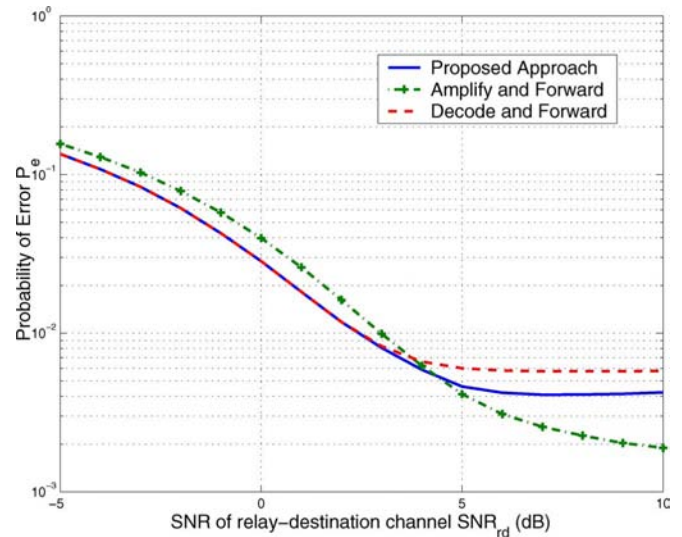


Fig. 3. Error probability versus SNR of relay-destination channel for  $L = 2$ ,  $M = 2$ , and  $K = 1$  ( $\text{SNR}_{\text{sr}} = 5 \text{ dB}$ ).

performance than DF and the thresholds of SST are different for the different relays for our approach.

We then consider a little different case where  $\text{SNR}_{r_d}$  is identical for both relay nodes. Figs. 2 and 3 plot the error probability at the destination node as a function of  $\text{SNR}_{\text{sr}}$  and  $\text{SNR}_{r_d}$ , respectively. From Fig. 2, where  $\text{SNR}_{r_d}$  is fixed at 5 dB, the proposed approach provides the best performance among all three relay schemes. In Fig. 3 where  $\text{SNR}_{\text{sr}}$  is fixed at 5 dB, the AF outperforms the proposed method at high  $\text{SNR}_{r_d}$  values. This is not surprising since the optimum performance is achieved with centralized processing, i.e., when all local observations are accessible by the decoder. With high  $\text{SNR}_{r_d}$ , the analog signal can be received at the destination almost noiselessly, hence it amounts to the centralized processing. The proposed scheme attempts to find the optimum relay scheme among all possible  $K$ -bit quantizers to minimize the error probability at the destination node. The AF apparently does not belong to the class of the  $K$ -bit quantizers.

We next consider a special case that we also discussed in Section I, the repetition coded binary source. This is equivalent to a binary hypotheses testing with soft (multibit) output. To alleviate the computational burden, one can approximate the

fading channel using a binary symmetric channel (BSC) where the crossover probability can be properly calculated using the channel SNR. The BSC provides a reasonable, *albeit* coarse, approximation of the fading channel; moreover, one can apply directly the distributed detection algorithm developed in [22] to find the optimal relay rules. We thus compare the BSC approximation with our approach using the actual fading channel model and the two existing relay strategies (i.e., AF and DF). Consider the system with  $L = 2$  relay nodes and  $K = 4$  bit source input. We generate the error probability plots as a function of  $\text{SNR}_{\text{sr}}$  and  $\text{SNR}_{r_d}$ , respectively. From Fig. 4 where we vary  $\text{SNR}_{\text{sr}}$  but fix  $\text{SNR}_{r_d} = 0 \text{ dB}$ , one can see that the proposed approach provides uniformly better performance compared with the other alternatives. Notice that all the error probabilities level off as  $\text{SNR}_{\text{sr}}$  increase. This is not unexpected: with large  $\text{SNR}_{\text{sr}}$ , the channels between the source and the relay nodes can be considered as ideal. Thus, the error probability performance is limited by the finite and fixed  $\text{SNR}_{r_d}$ . We also notice that the BSC approximation provides a reasonable performance compared with the proposed approach.

Fig. 5 is the error probability plot as a function of  $\text{SNR}_{r_d}$  with fixed  $\text{SNR}_{\text{sr}} = 0 \text{ dB}$ . Again, one observes error probability

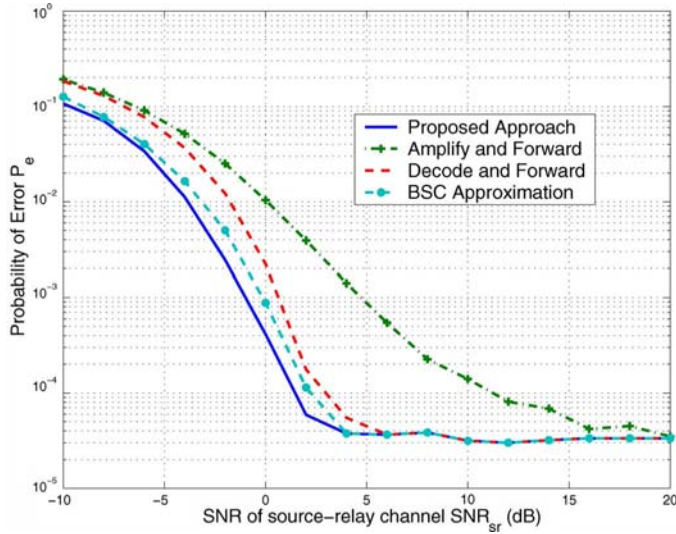


Fig. 4. Error probability versus SNR of source-relay channel for  $L = 2$ ,  $M = 2$ , and  $K = 4$  ( $\text{SNR}_{rd} = 0$  dB).

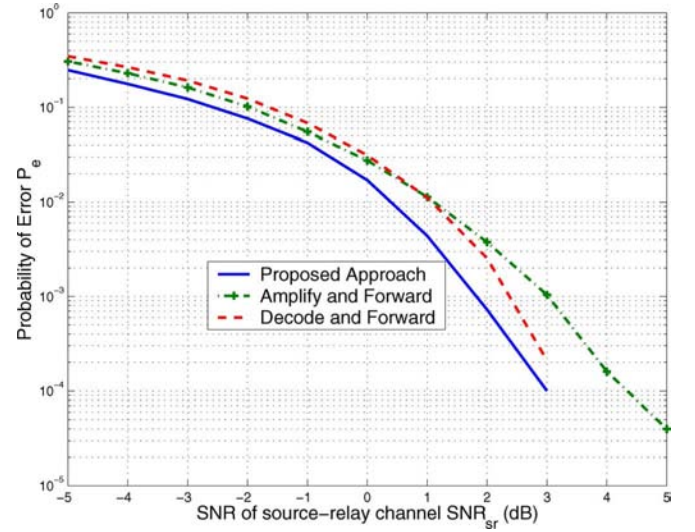


Fig. 6. Error probability versus SNR of source-relay channel for the case using  $L = 2$  and  $(7, 4)$  code as source input ( $\text{SNR}_{rd} = 5$  dB).

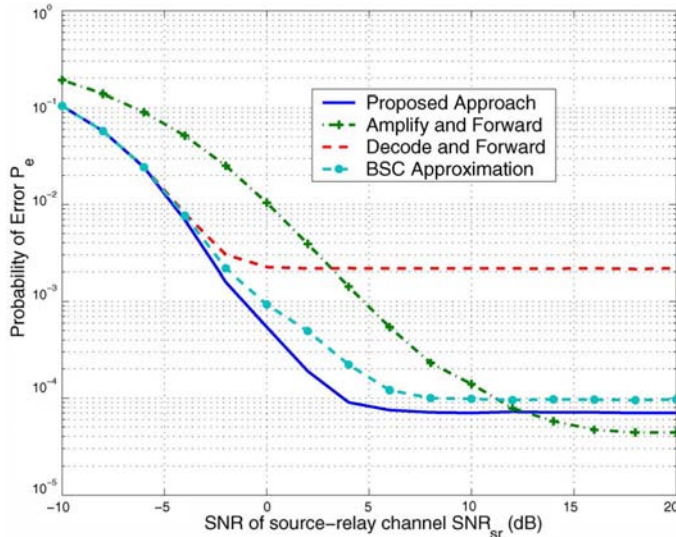


Fig. 5. Error probability versus SNR of relay-destination channel for  $L = 2$ ,  $M = 2$ , and  $K = 4$  ( $\text{SNR}_{sr} = 0$  dB).

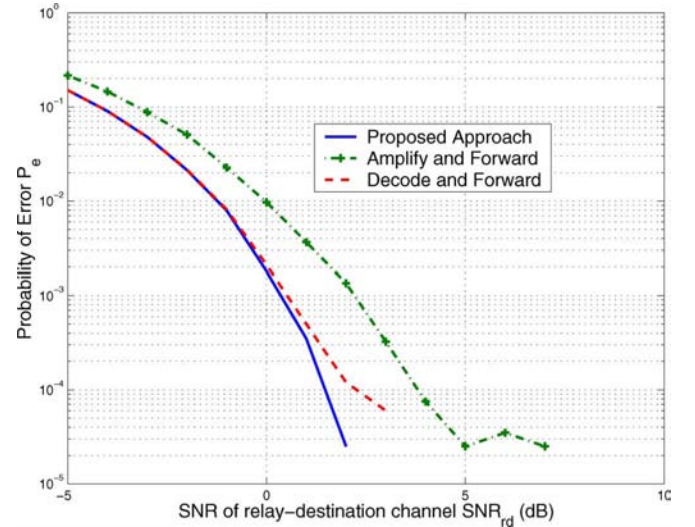


Fig. 7. Error probability versus SNR of relay-destination channel for the case using  $L = 2$  and  $(7, 4)$  code as source input ( $\text{SNR}_{sr} = 5$  dB).

floor as  $\text{SNR}_{rd}$  increases due to the fact that  $\text{SNR}_{sr}$  is fixed. Furthermore, the AF eventually outperforms all other schemes as  $\text{SNR}_{rd}$  gets large – this is again because at very high channel SNR between the relays and the destination, AF essentially amounts to a centralized processing. On the other hand, the DF is the first to level off in the error probability performance. This is because the DF uses a hard decision relaying—this is clearly not optimal at high SNR for the channel between the relays and the destination.

We also consider a more practical scenario where the packet is coded with a  $(7, 4)$  Hamming code [24] with  $L = 2$  relay nodes, and the generator matrix we use is

$$G = \begin{bmatrix} 1 & 0 & 0 & 0 & 1 & 0 & 1 \\ 0 & 1 & 0 & 0 & 1 & 1 & 1 \\ 0 & 0 & 1 & 0 & 1 & 1 & 0 \\ 0 & 0 & 0 & 1 & 0 & 1 & 1 \end{bmatrix}.$$

As shown in Figs. 6 and 7, the proposed approach again has the best performance.

### B. Three-Node Relay Network

We compare the performance of the proposed scheme with two existing relay schemes for the classical three-node model. In generating the error probability plots, we vary one channel SNR and fix the other two. As shown in Figs. 8–10, the proposed approach still has the best performance. When we vary  $\text{SNR}_{sr}$  or  $\text{SNR}_{rd}$ , the plots we obtain are similar to previous examples: the proposed scheme is uniformly better than others for varying  $\text{SNR}_{sr}$  and the advantage of the proposed scheme over DF diminishes at low SNR for varying  $\text{SNR}_{rd}$ . Since we have a direct transmission from source to destination node, when we vary  $\text{SNR}_{sd}$  and fix the other two, the performance gain of the proposed scheme diminishes to zero at high SNR, as shown in Fig. 10.

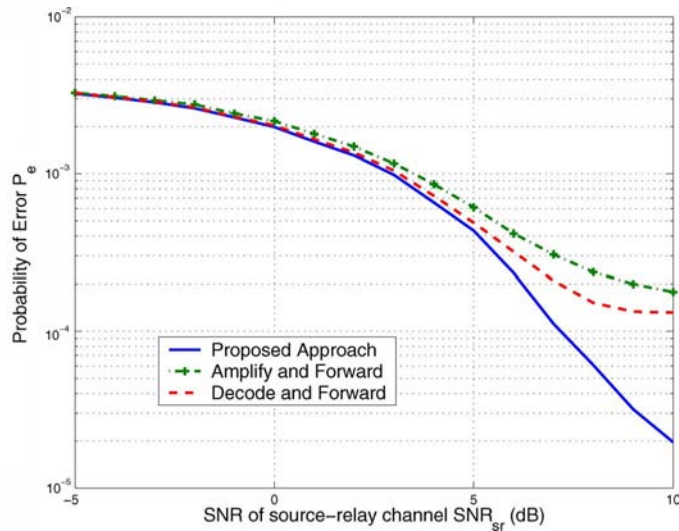


Fig. 8. Error probability versus SNR of source-relay channel for classical model with  $M = 3$  and  $K = 3$  ( $\text{SNR}_{rd} = 5$  dB,  $\text{SNR}_{sd} = 5$  dB).

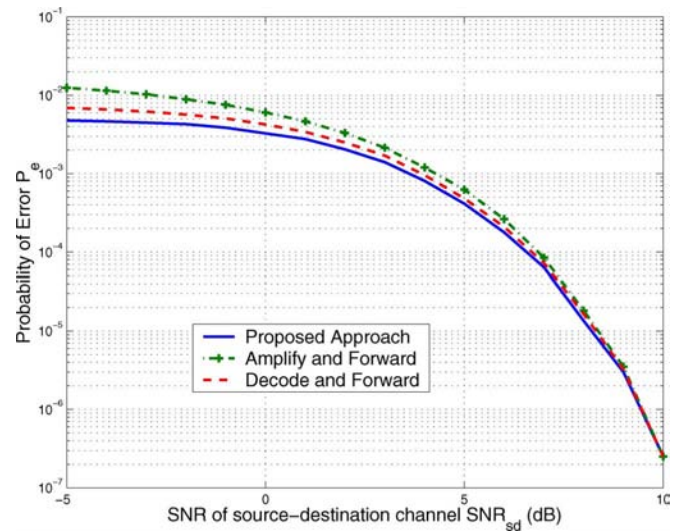


Fig. 10. Error probability versus SNR of source-destination channel for classical model with  $M = 3$  and  $K = 3$  ( $\text{SNR}_{sr} = 5$  dB,  $\text{SNR}_{rd} = 5$  dB).

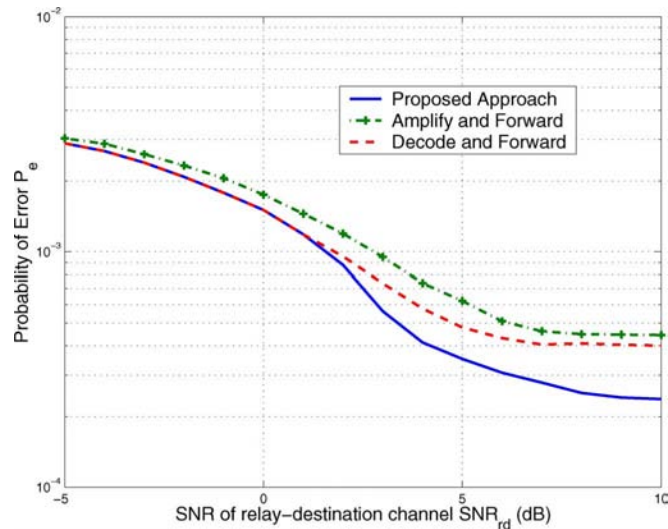


Fig. 9. Error probability versus SNR of relay-destination channel for classical model with  $M = 3$  and  $K = 3$  ( $\text{SNR}_{sr} = 5$  dB,  $\text{SNR}_{sd} = 5$  dB).

## V. CONCLUSION

In this paper, a novel cooperative relay signaling that applies channel aware decentralized detection theory was proposed to fully exploit the FA property of the source message. Aimed at minimizing the error probability at the destination node, we derived the necessary conditions for an optimal distributed signaling scheme for a FA source. An iterative algorithm was presented to find distributed relay schemes that are at least locally optimum. We further examined some special cases, including the classical three-node relay network and the parallel relay network. For the special case of a single relay node with no direct link between the source and the destination node, i.e., the singular relay network, we pointed out the significant difference between a binary source and a general  $M$ -ary source ( $M > 2$ ), that is, while the optimal relay rule is channel blind for the singular relay network with a binary source, it is channel aware when  $M > 2$ . Performance comparison with two existing relay

strategies, namely AF and DF, was conducted numerically. In almost all cases of practical interest, the proposed approach exhibits notable advantages over existing relay schemes that do not exploit the redundancy in FA sources.

One drawback of the proposed scheme is that the optimal signaling design requires global channel information. Distributed signaling design that only uses local channel information is more practical and will be investigated in the future. Similar work has been carried in the context of distributed detection for sensor networks [25] and can be extended to the cooperative relay signaling design. Another drawback is that the relay rule design of all relay nodes are *coupled* in the proposed design approach. This significantly increases the complexity of the design algorithm which typically scales exponentially in the number of nodes. One remedy is to resort to the large system regime to optimize the error exponent instead of the error probability, thereby circumventing the iterative algorithm that is needed to achieve the person-by-person optimality in error probability performance.

## REFERENCES

- [1] A. Sendonaris, E. Erkip, and B. Aazhang, "User cooperation diversity: Part I system description," *IEEE Trans. Commun.*, vol. 51, pp. 1927–1938, Nov. 2003.
- [2] —, "User cooperation diversity: Part I implementation aspects and performance analysis," *IEEE Trans. Commun.*, vol. 51, pp. 1939–1948, Nov. 2003.
- [3] J. N. Laneman, D. N. C. Tse, and G. W. Wornell, "Cooperative diversity in wireless networks: Efficient protocols and outage behavior," *IEEE Trans. Inf. Theory*, vol. 50, pp. 3062–3080, Dec. 2004.
- [4] E. C. van der Meulen, "A survey of multi-way channels in inf. Theory: 1961–1977," *IEEE Trans. Inf. Theory*, vol. 23, pp. 1–37, Jan. 1977.
- [5] T. M. Cover and A. El Gamal, "Capacity theorems for the relay channel," *IEEE Trans. Inf. Theory*, vol. 25, pp. 572–584, 1979.
- [6] M. Gastpar and M. Vetterli, "On the capacity of wireless networks: The relay case," in *Proc. IEEE INFOCOM 2002*, New York, NY, Jun. 2002, pp. 1577–1586.
- [7] G. Kramer, M. Gastpar, and P. Gupta, "Cooperative strategies and capacity theorems for relay networks," *IEEE Trans. Inf. Theory*, vol. 51, pp. 3037–3063, Sep. 2005.
- [8] J. N. Laneman and G. W. Wornell, "Distributed space-time-coded protocols for exploiting cooperative diversity in wireless networks," *IEEE Trans. Inf. Theory*, vol. 49, pp. 2415–2425, 2003.

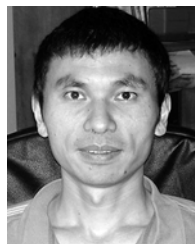
- [9] A. Ribeiro, X. Cai, and G. B. Giannakis, "Symbol error probabilities for general cooperative link," *IEEE Trans. Wireless Commun.*, vol. 4, pp. 1264–1273, May 2005.
- [10] W. Mo and Z. Wang, "Average symbol error probability and outage probability analysis for general cooperative diversity system at high signal to noise ratio," in *Proc. Conf. Information Sciences and Systems*, Princeton, NJ, Mar. 2004.
- [11] D. Chen and J. N. Laneman, "Modulation and demodulation for cooperative diversity in wireless systems," *IEEE Trans. Wireless Comm.*, vol. 5, pp. 1785–1794, Jul. 2006.
- [12] R. S. Blum, "Distributed detection for diversity reception of fading signals in noise," *IEEE Trans. Inf. Theory*, vol. 45, pp. 158–164, Jan. 1999.
- [13] B. Chen and P. K. Willett, "On the optimality of likelihood ratio test for local sensor decisions in the presence of non-ideal channels," *IEEE Trans. Inf. Theory*, vol. 51, pp. 693–699, Feb. 2005.
- [14] B. Liu and B. Chen, "Channel-optimized quantizers for decentralized detection in sensor networks," *IEEE Trans. Inf. Theory*, vol. 52, no. 7, pp. 3349–3358, Jul. 2006.
- [15] B. Chen, R. Jiang, T. Kasetkasem, and P. K. Varshney, "Fusion of decisions transmitted over fading channels in wireless sensor networks," in *Proc. 36th Asilomar Conf. Signals, Systems, Computers*, Pacific Grove, CA, Nov. 2002, pp. 1184–1188.
- [16] R. Niu, B. Chen, and P. K. Varshney, "Decision fusion rules in wireless sensor networks using fading statistics," presented at the Proc. 37th Annu. Conf. Information Sciences Systems, Baltimore, MD, Mar. 2003.
- [17] B. Chen, R. Jiang, T. Kasetkasem, and P. K. Varshney, "Channel aware decision fusion in wireless sensor networks," *IEEE Trans. Signal Process.*, vol. 52, no. 12, pp. 3454–3458, Dec. 2004.
- [18] R. Radner, "Team decision problems," *Ann. Math. Stat.*, vol. 33, pp. 857–881, 1962.
- [19] I. Y. Hoballah and P. K. Varshney, "Distributed Bayesian signal detection," *IEEE Trans. Inf. Theory*, vol. 35, pp. 995–1000, Sep. 1989.
- [20] Z.-B. Tang, K. R. Pattipati, and D. L. Kleinman, "A distributed M-ary hypothesis testing problem with correlated observations," *IEEE Trans. Autom. Control*, vol. 37, pp. 1042–1046, Jul. 1992.
- [21] J. N. Tsitsiklis, "Extremal properties of likelihood-ratio quantizers," *IEEE Trans. Commun.*, vol. 41, pp. 550–558, 1993.
- [22] B. Liu and B. Chen, "Joint source-channel coding for distributed sensor networks," presented at the 2004 Annu. Asilomar Conf. Signals, Systems, Computers, Pacific Grove, CA, Nov. 2004.
- [23] J. N. Tsitsiklis, "Decentralized detection," in *Advances in Statistical Signal Processing*, H. V. Poor and J. B. Thomas, Eds. Greenwich, CT: JAI Press, 1993.
- [24] J. Proakis, *Digital Communications*. New York: McGraw-Hill, 1995.
- [25] B. Liu and B. Chen, "Distributed detection in sensor networks with channel fading statistics," presented at the 2006 Int. Conf. Acoustic Speech, Signal Processing (ICASSP), Toulouse, France, May 2006.



**Bin Liu** (M'06) received the B.S. and M.S. degrees, both in electrical engineering, from University of Science and Technology of China, Hefei, Anhui, China, in 1998 and 2001, respectively. He has been working towards the Ph.D. degree with the Department of Electrical Engineering and Computer Science, Syracuse University, Syracuse, NY, since August 2001.

His current research interests are statistical signal processing with applications in wireless communications and distributed sensor networks.

Mr. Liu is the recipient of a Student Paper Contest Award of the IEEE International Conference on Acoustic, Speech, and Signal Processing (ICASSP), Philadelphia, PA, March 2005.



**Biao Chen** (S'96–M'00) received the B.E. and E.E. degrees, both in electrical engineering, from Tsinghua University, Beijing, China, in 1992 and 1994, respectively, and the M.S. degree in statistics and the Ph.D. degree in electrical engineering from the University of Connecticut, Storrs, in 1998 and 1999, respectively.

From 1994 to 1995, he worked at AT&T (China), Inc., Beijing, China. From 1999 to 2000, he was with Cornell University, Ithaca, NY, as a postdoctoral Research Associate. Since 2000, he has been an Assistant Professor with the Department of Electrical Engineering and Computer Science, Syracuse University, Syracuse, NY. His area of research interest mainly focuses on signal processing for wireless sensor and ad hoc networks and in multiuser MIMO systems.

Dr. Chen is an Associate Editor for the IEEE COMMUNICATIONS LETTERS and for the *EURASIP Journal on Wireless Communications and Networking* (JWCN). He has served as a Guest Editor for a Special Issue on Wireless Sensor Networks of EURASIP JWCN. He is the recipient of a National Science Foundation CAREER Award in 2006.



**Rick S. Blum** (S'83–M'84–SM'94–F'05) received the B.S. degree in electrical engineering from the Pennsylvania State University, University Park, in 1984 and the M.S. and Ph.D. degrees in electrical engineering from the University of Pennsylvania, Philadelphia, in 1987 and 1991.

From 1984 to 1991, he was a member of technical staff at General Electric Aerospace, Valley Forge, PA, and he graduated from GE's Advanced Course in Engineering. Since 1991, he has been with the Electrical and Computer Engineering Department at Lehigh University, Bethlehem, PA, where he is currently a Professor and holds the Robert W. Wieseman Chair Professorship in Electrical Engineering. He holds several patents. His research interests include communications, sensor networking, sensor processing, and related topics in the areas of signal processing and communications.

Dr. Blum is currently an Associate Editor for the IEEE COMMUNICATIONS LETTERS, and he is on editorial board for the *Journal of Advances in Information Fusion* of the International Society of Information Fusion. He was an Associate Editor for IEEE TRANSACTIONS ON SIGNAL PROCESSING and edited special issues for this journal and for the IEEE JOURNAL OF SELECTED AREAS IN COMMUNICATIONS (JSAC). He was a member of the Signal Processing for Communications Technical Committee of the IEEE Signal Processing Society and is a member of the Communications Theory Technical Committee of the IEEE Communication Society. He is also on the awards Committee of the IEEE Communication Society. He is an IEEE Third Millennium Medal winner and a member of Eta Kappa Nu and Sigma Xi. He was awarded an ONR Young Investigator Award in 1997 and an NSF Research Initiation Award in 1992. His IEEE Fellow citation "for scientific contributions to detection, data fusion and signal processing with multiple sensors" acknowledges some early contributions to the field of sensor networking.

# Sum Capacity Optimality of Orthogonal Transmissions in Vector Gaussian Multiple Access Channels

Xiaohu Shang, *Student Member, IEEE*, Biao Chen, *Senior Member, IEEE*, and John Matyjas, *Member, IEEE*

**Abstract**—We study in this paper the sum capacity achievability of orthogonal transmissions in vector Gaussian multiple access channels (MAC). Specifically, we derive sufficient and necessary conditions, in terms of channel matrices and transmitter power constraints, for orthogonal transmissions to achieve the sum capacity of a vector Gaussian MAC. The obtained conditions provide a unified framework that helps explain many intuitive and known results as well as explore cases that have not been addressed. In the cases when these conditions are violated, our results enable us to quantify the suboptimality of orthogonal transmission when the sum capacity can only be achieved by overlay transmission.

**Index Terms**—Sum capacity, vector Gaussian multiple access channel, frequency division multiple access.

## I. INTRODUCTION

**I**N A MULTIPLE access channel (MAC), multiple transmitters communicate with a single receiver. The capacity region of a two-user MAC is the closure of all  $(R_1, R_2)$  pairs satisfying

$$\begin{aligned} R_1 &< I(X_1; Y|X_2), \\ R_2 &< I(X_2; Y|X_1), \\ R_1 + R_2 &< I(X_1, X_2; Y), \end{aligned}$$

for some product distribution  $p_1(x_1)p_2(x_2)$  [1], [2], where  $\mathcal{X}_1, \mathcal{X}_2, \mathcal{Y}$  are respectively transmit and receive alphabets. For a two-user scalar Gaussian MAC, the capacity region is specified by

$$\begin{aligned} R_1 &< \frac{1}{2} \log \left( 1 + \frac{P_1}{N} \right), \\ R_2 &< \frac{1}{2} \log \left( 1 + \frac{P_2}{N} \right), \\ R_1 + R_2 &< \frac{1}{2} \log \left( 1 + \frac{P_1 + P_2}{N} \right), \end{aligned}$$

where  $P_1$  and  $P_2$  are respectively the average power constraint of the two transmitters, and  $N$  is the noise variance at the

Manuscript received May 25, 2007; revised November 2, 2007; accepted January 8, 2008. The associate editor coordinating the review of this paper and approving it for publication was N. Arumugam. This work was supported in part by AFOSR under Grant FA9550-06-1-0051, by AFRL under Agreement FA8750-05-2-0120, and by NSF under Grant CCF-0546491. This work was presented in part at IEEE International Conference on Acoustics, Speech, and Signal Processing, Honolulu, Hawaii, April, 2007.

X. Shang and B. Chen are with Syracuse University, Department of EECS, 335 Link Hall, Syracuse, NY 13244 (e-mail: xshang@syr.edu, bichen@ecs.syr.edu).

J. Matyjas is with AFRL, 525 Brooks Rd., Rome, NY 13442-4505 (e-mail: matyjasj@rl.af.mil).

Digital Object Identifier 10.1109/T-WC.2008.070560

receiver. While it is shown that the capacity region is achievable using overlay transmission, it is also well known that, for a scalar Gaussian MAC, orthogonal transmissions, e.g., frequency division multiple access (FDMA) or time division multiple access (TDMA) under an *average* power constraint, can achieve *the sum capacity* [2]. As such, although FDMA and TDMA is suboptimal in terms of the entire capacity region [3], if only the system throughput is of concern, orthogonal transmissions are sufficient, resulting in a much simplified transceiver structure, i.e., no successive interference cancellation is needed. Similar result holds for a scalar Gaussian MAC with more than two users.

With vector Gaussian MAC, the above claim - that orthogonal transmissions achieve the sum capacity - is not necessarily true. Indeed, it is observed that in most cases orthogonal transmissions fall well short of achieving the sum capacity of a vector Gaussian MAC [4]. The goal of this study is two-fold. First, we establish sufficient and necessary conditions for orthogonal transmissions to be optimal in achievable sum rate for a vector Gaussian MAC. The established conditions, in terms of singular values and singular vectors of the channel matrices as well as the power constraints, provide a unified framework behind many intuitive and well known results. In addition, it allows us to examine cases that have not been explored before in terms of the (sub)optimality of orthogonal transmissions for vector Gaussian MAC. We show that the channel must have proportional singular values, well aligned singular vectors and appropriate power constraints in order for FDMA/TDMA to achieve the sum capacity. Secondly, using the established conditions, we attempt to provide quantitative measure for the performance degradation of orthogonal transmission when they are suboptimal.

The paper is organized as follows. In Section II, we present the channel model and give the main results, namely the sufficient and necessary conditions in terms of channel matrices and power constraints, for FDMA to achieve the sum capacity. The equivalence of FDMA and TDMA in terms of achievable sum rate is also established in section II. In Section III, we examine several cases using the new framework to determine the (sub)optimality of FDMA. In the cases when FDMA becomes suboptimal, we propose a heuristic metric to quantify the degradation of sum capacity achievability of FDMA in section IV. We conclude in Section V.

The following notations will be used throughout the paper:  $\mathbf{A}^\dagger, |\mathbf{A}|, \text{tr}(\mathbf{A}), \text{rank}(\mathbf{A}), \|\mathbf{A}\|$  are respectively the Hermitian matrix, determinant, trace, rank, and 2-norm of matrix  $\mathbf{A}$ ;  $\bar{x} \triangleq$

$1 - \beta$ ;  $(x)^+ = \max\{x, 0\}$ ;  $\text{diag}(\sigma_1, \dots, \sigma_n)$  is a diagonal matrix with the diagonal entries  $\sigma_1, \dots, \sigma_n$ .

## II. MAIN RESULTS

Consider a vector Gaussian MAC

$$\mathbf{y} = \mathbf{H}_1 \mathbf{x}_1 + \mathbf{H}_2 \mathbf{x}_2 + \mathbf{z},$$

where  $\mathbf{H}_i$  is an  $n_r \times n_{t_i}$  full rank channel matrix,  $\mathbf{x}_i$  and  $\mathbf{y}$  are  $n_{t_i} \times 1$  transmit and  $n_r \times 1$  receive signal vectors respectively,  $\mathbf{z}$  is a  $n_r \times 1$  complex Gaussian noise vector, with  $E(\mathbf{z}) = \mathbf{0}$ ,  $E(\mathbf{z}\mathbf{z}^\dagger) = \mathbf{I}$ , where  $\mathbf{I}$  is the  $n_r \times n_r$  identity matrix.

The covariance matrix of  $\mathbf{x}_i$  is denoted by  $\mathbf{S}_i = E(\mathbf{x}_i \mathbf{x}_i^\dagger)$  with power constraint  $\text{tr}(\mathbf{S}_i) \leq P_i$ . Both the transmitters and receivers are assumed to have full channel state information. For simplicity, we use  $\text{MAC}(\mathbf{H}_1, \mathbf{H}_2, P_1, P_2)$  to denote this vector Gaussian MAC, of which, the sum capacity is

$$C = \max_{\text{tr}(\mathbf{S}_1) \leq P_1, \text{tr}(\mathbf{S}_2) \leq P_2} \log \left| \mathbf{H}_1 \mathbf{S}_1 \mathbf{H}_1^\dagger + \mathbf{H}_2 \mathbf{S}_2 \mathbf{H}_2^\dagger + \mathbf{I} \right|. \quad (1)$$

It was established in [5] that the sufficient and necessary condition to achieve the sum capacity is the mutually water-filling scheme, i.e., choose  $\mathbf{S}_i$  as single-user water-filling covariance matrix by treating other user's signals as channel noise. On the other hand, the maximum achievable sum rates by using FDMA and TDMA are respectively

$$C_F = \max_{0 \leq \alpha \leq 1} C_F(\alpha), \quad C_T = \max_{0 \leq \alpha \leq 1} C_T(\alpha),$$

where  $\alpha$  is the fraction of bandwidth or time allocated to the first user, by normalizing the bandwidth or the time, we obtain from [2, (15.150), (15.151)]

$$\begin{aligned} C_F(\alpha) &= \max_{\text{tr}(\mathbf{S}_1) \leq P_1, \text{tr}(\mathbf{S}_2) \leq P_2} \left\{ \alpha \log \left| \frac{1}{\alpha} \mathbf{H}_1 \mathbf{S}_1 \mathbf{H}_1^\dagger + \mathbf{I} \right| \right. \\ &\quad \left. + \bar{\alpha} \log \left| \frac{1}{\bar{\alpha}} \mathbf{H}_2 \mathbf{S}_2 \mathbf{H}_2^\dagger + \mathbf{I} \right| \right\}, \quad (2) \\ C_T(\alpha) &= \max_{\text{tr}(\mathbf{S}_1) = \frac{P_1}{\alpha}, \text{tr}(\mathbf{S}_2) = \frac{P_2}{\bar{\alpha}}} \left\{ \alpha \log \left| \mathbf{H}_1 \mathbf{S}_1 \mathbf{H}_1^\dagger + \mathbf{I} \right| \right. \\ &\quad \left. + \bar{\alpha} \log \left| \mathbf{H}_2 \mathbf{S}_2 \mathbf{H}_2^\dagger + \mathbf{I} \right| \right\}. \quad (3) \end{aligned}$$

Both  $C_F(\alpha)$  and  $C_T(\alpha)$  are obtained by two independent single user water-fillings in their respective channels. We will show later that  $C_F(\alpha) = C_T(\alpha)$  for all  $\alpha$  for a given MAC, therefore we can explore the achievability of sum capacity focusing only on FDMA. In addition, we have Proposition 1, whose proof is nearly identical to the proof of concavity of FDMA sum rate for the vector Gaussian interference channel [6, (14)], as the two sum rates bear exactly the same expression.

*Proposition 1:*  $C_F(\alpha)$  is a concave function of  $\alpha$ .

Proposition 1 guarantees convergence of simple gradient methods to the global maximum [7].

Before proceeding, we first show the following lemma.

*Lemma 1:* If  $\mathbf{S}_{opt} = \arg \max_{\text{tr}(\mathbf{S}) \leq P} \log \left| \frac{1}{\alpha} \mathbf{H} \mathbf{S} \mathbf{H}^\dagger + \mathbf{I} \right|$ , where  $\alpha > 0$  is a constant, then for any  $\beta \in (0, 1)$ , the two matrices  $\frac{\beta}{\alpha} \mathbf{H} \mathbf{S}_{opt} \mathbf{H}^\dagger$  and  $\frac{\beta}{\alpha} \mathbf{H} \mathbf{S}_{opt} \mathbf{H}^\dagger$  satisfy the mutually water-filling condition.

*Proof:* Consider a  $\text{MAC}(\frac{1}{\sqrt{\alpha}} \mathbf{H}, \frac{1}{\sqrt{\alpha}} \mathbf{H}, \beta P, \beta P)$ , the sum capacity is

$$\begin{aligned} C &= \max_{\text{tr}(\mathbf{S}_1) \leq \beta P, \text{tr}(\mathbf{S}_2) \leq \beta P} \log \left| \frac{1}{\alpha} \mathbf{H} \mathbf{S}_1 \mathbf{H}^\dagger + \frac{1}{\alpha} \mathbf{H} \mathbf{S}_2 \mathbf{H}^\dagger + \mathbf{I} \right| \\ &= \max_{\text{tr}(\mathbf{S}_1) \leq \beta P, \text{tr}(\mathbf{S}_2) \leq \beta P} \log \left| \frac{1}{\alpha} \mathbf{H} (\mathbf{S}_1 + \mathbf{S}_2) \mathbf{H}^\dagger + \mathbf{I} \right| \\ &\leq \max_{\text{tr}(\mathbf{S}) \leq P} \log \left| \frac{1}{\alpha} \mathbf{H} \mathbf{S} \mathbf{H}^\dagger + \mathbf{I} \right| \\ &= \log \left| \frac{1}{\alpha} \mathbf{H} \mathbf{S}_{opt} \mathbf{H}^\dagger + \mathbf{I} \right|. \end{aligned}$$

The above sum capacity is achieved by choosing  $\mathbf{S}_1 = \beta \mathbf{S}_{opt}$  and  $\mathbf{S}_2 = \beta \mathbf{S}_{opt}$ . According to Theorem 1 of [5], the two matrices  $\frac{\beta}{\alpha} \mathbf{H} \mathbf{S}_{opt} \mathbf{H}^\dagger$  and  $\frac{\beta}{\alpha} \mathbf{H} \mathbf{S}_{opt} \mathbf{H}^\dagger$  satisfy the mutually water-filling condition. ■

Our goal is to find the sufficient and necessary conditions such that  $C_F = C$ . Our main result is summarized below.

*Theorem 1:* For a  $\text{MAC}(\mathbf{H}_1, \mathbf{H}_2, P_1, P_2)$ , FDMA can achieve its sum capacity if and only if there exist  $0 < \alpha < 1$ ,  $\mathbf{S}_{1opt}$ , and  $\mathbf{S}_{2opt}$  that jointly satisfy

$$\frac{1}{\alpha} \mathbf{H}_1 \mathbf{S}_{1opt} \mathbf{H}_1^\dagger = \frac{1}{\alpha} \mathbf{H}_2 \mathbf{S}_{2opt} \mathbf{H}_2^\dagger, \quad (4)$$

$$\mathbf{S}_{1opt} = \arg \max_{\text{tr}(\mathbf{S}_1) \leq P_1} \log \left| \frac{1}{\alpha} \mathbf{H}_1 \mathbf{S}_1 \mathbf{H}_1^\dagger + \mathbf{I} \right|, \quad (5)$$

$$\mathbf{S}_{2opt} = \arg \max_{\text{tr}(\mathbf{S}_2) \leq P_2} \log \left| \frac{1}{\alpha} \mathbf{H}_2 \mathbf{S}_2 \mathbf{H}_2^\dagger + \mathbf{I} \right|. \quad (6)$$

*Proof: Sufficient condition* From (4)-(6), by choosing  $\mathbf{S}_1 = \mathbf{S}_{1opt}$  and  $\mathbf{S}_2 = \mathbf{S}_{2opt}$ , the achievable sum rate is

$$\begin{aligned} &\log \left| \mathbf{H}_1 \mathbf{S}_{1opt} \mathbf{H}_1^\dagger + \mathbf{H}_2 \mathbf{S}_{2opt} \mathbf{H}_2^\dagger + \mathbf{I} \right| \\ &= \log \left| \frac{1}{\alpha} \mathbf{H}_1 \mathbf{S}_{1opt} \mathbf{H}_1^\dagger + \mathbf{I} \right| \\ &= \max_{\text{tr}(\mathbf{S}_1) \leq P_1} \log \left| \frac{1}{\alpha} \mathbf{H}_1 \mathbf{S}_1 \mathbf{H}_1^\dagger + \mathbf{I} \right|. \end{aligned}$$

From Lemma 1,  $\mathbf{H}_1 \mathbf{S}_{1opt} \mathbf{H}_1^\dagger$  and  $\frac{\bar{\alpha}}{\alpha} \mathbf{H}_1 \mathbf{S}_{1opt} \mathbf{H}_1^\dagger$  (or  $\mathbf{H}_2 \mathbf{S}_{2opt} \mathbf{H}_2^\dagger$ ) satisfy the mutually water-filling condition. From Theorem 1 of [5], they achieve the sum capacity.

Apply FDMA to the same channel with  $\mathbf{S}_1 = \mathbf{S}_{1opt}$ ,  $\mathbf{S}_2 = \mathbf{S}_{2opt}$  and the bandwidth allocation factor  $\alpha$ , the sum rate is

$$\begin{aligned} C_F &= \alpha \log \left| \frac{\mathbf{H}_1 \mathbf{S}_{1opt} \mathbf{H}_1^\dagger}{\alpha} + \mathbf{I} \right| + \bar{\alpha} \log \left| \frac{\mathbf{H}_2 \mathbf{S}_{2opt} \mathbf{H}_2^\dagger}{\bar{\alpha}} + \mathbf{I} \right| \\ &= \alpha \log \left| \frac{\mathbf{H}_1 \mathbf{S}_{1opt} \mathbf{H}_1^\dagger}{\alpha} + \mathbf{I} \right| + \bar{\alpha} \log \left| \frac{\mathbf{H}_1 \mathbf{S}_{1opt} \mathbf{H}_1^\dagger}{\alpha} + \mathbf{I} \right| \\ &= \log \left| \frac{1}{\alpha} \mathbf{H}_1 \mathbf{S}_{1opt} \mathbf{H}_1^\dagger + \mathbf{I} \right| = C, \end{aligned}$$

i.e., it achieves the sum capacity.

*Necessary condition* Assume FDMA can achieve the sum capacity with  $\alpha, \mathbf{S}_{1opt}, \mathbf{S}_{2opt}$ . We only need to show that (4) must be satisfied since (5) and (6) must be true. From the

assumption, we have

$$\begin{aligned} C &= \alpha \log \frac{\mathbf{H}_1 \mathbf{S}_{1opt} \mathbf{H}_1^\dagger}{\alpha} + \mathbf{I} + \bar{\alpha} \log \frac{\mathbf{H}_2 \mathbf{S}_{2opt} \mathbf{H}_2^\dagger}{\bar{\alpha}} + \mathbf{I} \\ &\stackrel{(a)}{\leq} \log \alpha \left( \frac{\mathbf{H}_1 \mathbf{S}_{1opt} \mathbf{H}_1^\dagger}{\alpha} + \mathbf{I} \right) + \bar{\alpha} \left( \frac{\mathbf{H}_2 \mathbf{S}_{2opt} \mathbf{H}_2^\dagger}{\bar{\alpha}} + \mathbf{I} \right) \\ &\leq C, \end{aligned}$$

where (a) follows from the concavity of  $\log |\cdot|$  for positive semi-definite matrices [2], with equality if and only if (4) is true. Since equality must hold, (4) must be true. ■

Conditions (5) and (6) can be interpreted as that  $\mathbf{S}_{iopt}$  water-fills  $\mathbf{H}_i$  for the given  $\alpha$ . To be able to dissect more complicated cases, we next present Theorem 2, derived directly from Theorem 1. We assume that the channel matrices admit respective singular value decompositions  $\mathbf{H}_i = \mathbf{U}_i \Sigma_i \mathbf{V}_i^\dagger$ ,  $i = 1, 2$ . We denote by  $\sigma_{ij}$  and  $\mathbf{u}_{ij}$  the  $j^{th}$  singular value and left singular vector for  $\mathbf{H}_i$ . Without loss of generality, we assume  $\sigma_{i1} \geq \sigma_{i2} \geq \dots \geq \sigma_{i r_i}$ ,  $r_i = \text{rank}(\mathbf{H}_i)$ ,  $i = 1, 2$ .

**Theorem 2:** For a MAC( $\mathbf{H}_1, \mathbf{H}_2, P_1, P_2$ ), FDMA achieves the sum capacity if and only if there exists an integer  $1 \leq m \leq \min\{r_1, r_2\}$  that satisfies the following conditions.

Singular value conditions For some constant  $k$ ,

$$\frac{\sigma_{11}^2}{\sigma_{21}^2} = \dots = \frac{\sigma_{1m}^2}{\sigma_{2m}^2} = k. \quad (7)$$

Singular vector conditions For any  $\sigma_{1n_1-1} \neq \sigma_{1n_1} = \sigma_{1n_1+1} = \dots = \sigma_{1n_2} \neq \sigma_{1n_2+1}$  with  $1 \leq n_1 \leq n_2 \leq m$ ,

$$\mathcal{S}\{\mathbf{u}_{1n_1}, \dots, \mathbf{u}_{1n_2}\} = \mathcal{S}\{\mathbf{u}_{2n_1}, \dots, \mathbf{u}_{2n_2}\}, \quad (8)$$

where  $\mathcal{S}\{\mathbf{u}_1, \dots, \mathbf{u}_L\}$  denotes the subspace spanned by  $\mathbf{u}_1, \dots, \mathbf{u}_L$ . In the event that all singular values are distinct, we have  $\mathbf{u}_{1i} = \pm \mathbf{u}_{2i}$  for  $1 \leq i \leq m$ .

Power constraint conditions

$$v_1 P_2 = v_2 P_1, \quad (9)$$

where

$$\sum_{i=1}^{r_1} \left( v_1 - \frac{\alpha}{\sigma_{1i}^2} \right)^+ = \sum_{i=1}^m \left( v_1 - \frac{\alpha}{\sigma_{1i}^2} \right) = P_1, \quad (10)$$

$$\sum_{i=1}^{r_2} \left( v_2 - \frac{\bar{\alpha}}{\sigma_{2i}^2} \right)^+ = \sum_{i=1}^m \left( v_2 - \frac{\bar{\alpha}}{\sigma_{2i}^2} \right) = P_2, \quad (11)$$

$$\alpha = \frac{k P_1}{k P_1 + P_2}. \quad (12)$$

*Proof:* From (4) we have

$$\frac{1}{\alpha} \mathbf{U}_1 \Sigma_1 \tilde{\mathbf{S}}_1 \Sigma_1^\dagger \mathbf{U}_1^\dagger + \mathbf{I} = \frac{1}{\bar{\alpha}} \mathbf{U}_2 \Sigma_2 \tilde{\mathbf{S}}_2 \Sigma_2^\dagger \mathbf{U}_2^\dagger + \mathbf{I},$$

where  $\tilde{\mathbf{S}}_1 = \mathbf{V}_1^\dagger \mathbf{S}_{1opt} \mathbf{V}_1$  and  $\tilde{\mathbf{S}}_2 = \mathbf{V}_2^\dagger \mathbf{S}_{2opt} \mathbf{V}_2$ . With (5)-(6) we have

$$\begin{aligned} \mathbf{U}_1 \text{diag} \left( \frac{\sigma_{11}^2 v_1}{\alpha}, \dots, \frac{\sigma_{1m_1}^2 v_1}{\alpha}, 1, \dots, 1 \right) \mathbf{U}_1^\dagger \\ = \mathbf{U}_2 \text{diag} \left( \frac{\sigma_{21}^2 v_2}{\bar{\alpha}}, \dots, \frac{\sigma_{2m_2}^2 v_2}{\bar{\alpha}}, 1, \dots, 1 \right) \mathbf{U}_2^\dagger, \end{aligned} \quad (13)$$

where  $v_1$  and  $v_2$  are the water-filling level

$$\sum_{i=1}^{r_1} \left( v_1 - \frac{\alpha}{\sigma_{1i}^2} \right)^+ = P_1, \quad (14)$$

$$\sum_{i=1}^{r_2} \left( v_2 - \frac{\bar{\alpha}}{\sigma_{2i}^2} \right)^+ = P_2. \quad (15)$$

Assume the power is allocated until the  $m_1^{th}$  and  $m_2^{th}$  eigenmodes for user 1 and user 2 respectively. Then  $m_1 = m_2 \triangleq m$ , because  $\frac{\sigma_{1m_1}^2 v_1}{\alpha}$  and  $\frac{\sigma_{2m_2}^2 v_2}{\bar{\alpha}}$  are strictly greater than 1. Thus

$$v_1 = \frac{1}{m} \left( P_1 + \alpha \sum_{i=1}^m \frac{1}{\sigma_{1i}^2} \right), \quad (16)$$

$$v_2 = \frac{1}{m} \left( P_2 + \bar{\alpha} \sum_{i=1}^m \frac{1}{\sigma_{2i}^2} \right). \quad (17)$$

In (13), the two matrices on both sides must have the same eigenvalues and the same corresponding eigenvector subspaces, therefore,  $\mathbf{U}_i$  must satisfy the singular vector conditions (8) and singular value conditions

$$\frac{\sigma_{11}^2}{\sigma_{21}^2} = \dots = \frac{\sigma_{1m}^2}{\sigma_{2m}^2} = \frac{\alpha v_2}{\bar{\alpha} v_1} \triangleq k. \quad (18)$$

Substitute (17) into (18) we have (12) and (9). In order that power is allocated until the  $m^{th}$  element we must have  $\frac{\alpha}{\sigma_{1m}^2} < v_1 \leq \frac{\alpha}{\sigma_{1m+1}^2}$  and  $\frac{\bar{\alpha}}{\sigma_{2m}^2} < v_2 \leq \frac{\bar{\alpha}}{\sigma_{2m+1}^2}$ . ■

Equations (7) and (8) establish that the two channel matrices must have proportional singular values and perfectly aligned singular vectors, while the last condition dictates that the corresponding power constraints must be such that the respective water-filling uses the same number of eigenmodes for the two users in the FDMA transmission for the optimal  $\alpha$ .

For a MAC with  $\frac{\sigma_{1m}^2}{\sigma_{2m}^2} \neq \frac{\sigma_{1,m+1}^2}{\sigma_{2,m+1}^2}$ , even if the singular vector conditions in Theorem 2 are satisfied, if  $P_i > \frac{m}{\sigma_{1,m+1}^2} - \sum_{j=1}^m \frac{1}{\sigma_{1j}^2}$  for either  $i = 1$  or  $2$ , the power conditions are violated and FDMA is suboptimal due to the generous power constraint, which favors overlay transmission with successive interference cancellation. Proposition 2 shows the relation of power conditions and the achievability of sum capacity of FDMA.

**Proposition 2:** For a MAC( $\mathbf{H}_1, \mathbf{H}_2, P_1, P_2$ ) if  $k \triangleq \frac{\sigma_{11}^2}{\sigma_{21}^2} = \dots \neq \frac{\sigma_{1m}^2}{\sigma_{2m}^2} \neq \frac{\sigma_{1,m+1}^2}{\sigma_{2,m+1}^2}$ , and the singular vector conditions in Theorem 2 are satisfied, FDMA achieves the sum capacity if and only if the power constraint pair  $(P_1, P_2)$  belongs to  $\mathcal{P}$ , where

$$\mathcal{P} = \left\{ (P_1, P_2) \mid k P_1 + P_2 \leq m k \right. \\ \left. \cdot \left( \frac{1}{\max\{\sigma_{1,m+1}^2, k \sigma_{2,m+1}^2\}} - \frac{1}{\sigma_{1,m}^2} \right), P_1, P_2 > 0 \right\}, \quad (19)$$

where  $\widehat{\sigma}_{i,m}^2$  is the harmonic mean of  $\sigma_{i1}^2, \dots, \sigma_{im}^2$ , i.e.,

$$\frac{1}{\widehat{\sigma}_{i,m}^2} \triangleq \frac{1}{m} \sum_{i=1}^m \frac{1}{\sigma_{ii}^2}.$$

*Proof:* If the power is allocated up to the  $m^{\text{th}}$  eigenmode for both users, from Theorem 2 (10) and (11),  $C_F = C$  if

$$\frac{\alpha}{\sigma_{1,m}^2} < v_1 \leq \frac{\alpha}{\sigma_{1,m+1}^2}, \quad (20)$$

$$\frac{\bar{\alpha}}{\sigma_{2,m}^2} < v_2 \leq \frac{\bar{\alpha}}{\sigma_{2,m+1}^2}. \quad (21)$$

Substitute (10)-(12) to (20) and (21) we have

$$\begin{aligned} mk \frac{1}{\sigma_{1,m}^2} - \frac{1}{\sigma_{1,m}^2} &< kP_1 + P_2 \\ &\leq mk \frac{1}{\max(\sigma_{1,m+1}^2, k\sigma_{2,m+1}^2)} - \frac{1}{\sigma_{1,m}^2}. \end{aligned} \quad (22)$$

Therefore, for all the power constraint pairs  $(P_1, P_2)$  satisfying (22), FDMA achieves the sum capacity. Notice that it is not necessary that the power must be allocated up to the  $m^{\text{th}}$  eigenmode for FDMA to be optimal. If both users allocate the power to the  $t^{\text{th}} < m^{\text{th}}$  eigenmode and the power constraint conditions in Theorem 1 are also satisfied, FDMA can still achieve the sum capacity. Consider the same constraints in (20) and (21) with  $m$  replaced by  $t$ , we have (23), where  $t = 1, \dots, \not/m - 1$ . Denote the sets defined in (23) as  $\mathcal{P}_i, i = 1, \dots, \not/m - 1$  and the set in (22) as  $\mathcal{P}_m$ . For the MAC, if the power constraint pairs satisfy  $(P_1, P_2) \in \mathcal{P}$ , FDMA can achieve the sum capacity, where  $\mathcal{P} = \bigcup_{i=1}^m \mathcal{P}_i$ , which is the same as (19). In (19) we exclude the trivial cases that FDMA always achieves sum capacity if either  $P_1$  or  $P_2$  is zero, since it reduces to a single user channel. ■

In the following, we establish the equivalence of FDMA and TDMA in terms of achievable sum rate.

*Proposition 3:* For a MAC( $\mathbf{H}_1, \mathbf{H}_2, P_1, P_2$ ),  $C_F(\alpha) = C_T(\alpha)$  for all  $0 < \alpha < 1$ .

*Proof:* Define  $\hat{\mathbf{S}}_1 = \frac{\mathbf{S}_1}{\alpha}$  and  $\hat{\mathbf{S}}_2 = \frac{\mathbf{S}_2}{\bar{\alpha}}$ , and substitute them into (2), it can be shown that (3) and (2) are equivalent. ■

Therefore all the results of FDMA can be readily extended to TDMA.

Finally, we extend Theorem 1 to the multiple-user MAC. The proof follows exactly the same proof of Theorem 1, and is omitted because of the space limit.

*Theorem 3:* For a  $k$ -user MAC( $\mathbf{H}_1, \dots, \mathbf{H}_k, P_1, \dots, P_k$ ), FDMA achieves the sum capacity if and only if there exist  $0 < \alpha_i < 1, \prod_{i=1}^k \alpha_i = 1, \mathbf{S}_{iopt}, i = 1, \dots, k$  that jointly satisfy

$$\frac{1}{\alpha_1} \mathbf{H}_1 \mathbf{S}_{1opt} \mathbf{H}_1^\dagger = \dots = \frac{1}{\alpha_k} \mathbf{H}_k \mathbf{S}_{kopt} \mathbf{H}_k^\dagger \quad (24)$$

$$\mathbf{S}_{iopt} = \arg \max_{\text{tr}(\mathbf{S}_i) \leq P_i} \log \frac{1}{\alpha_i} \mathbf{H}_i \mathbf{S}_i \mathbf{H}_i^\dagger + \mathbf{I} \quad (25)$$

### III. CASES FOR FDMA BEING SUM-CAPACITY OPTIMAL

The sufficient and necessary conditions in Theorem 1 or 2 appear to be overly restrictive. Such conditions are rarely satisfied for the general vector Gaussian MAC. The results, however, provide a unified approach to determine the sum capacity optimality of orthogonal transmissions. More importantly, Theorem 2 also allows us to gain insight into how to quantify the suboptimality of orthogonal transmissions as demonstrated later in this section.

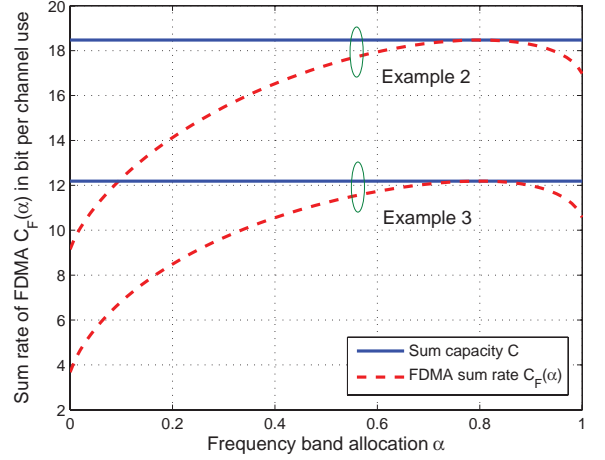


Fig. 1. Sum rate of FDMA versus frequency allocation factor, where, for Example 2  $n_r = n_{t1} = n_{t2} = 8, P_1 = P_2 = 1, \gamma = 2, \mathbf{H}$  and  $\mathbf{A}$  are randomly chosen; for Example 3,  $n_r = n_{t1} = 8, n_{t2} = 10, \sigma_1 = \sqrt{3}, \sigma_2 = \sqrt{12}, P_1 = P_2 = 1, \mathbf{U}_1, \mathbf{U}_2, \mathbf{V}_1$  and  $\mathbf{V}_2$  are randomly chosen.

In the following, we demonstrate the utility of the proposed sufficient and necessary conditions by reviewing some examples, in which FDMA is sum capacity optimal.

*Example 1:*  $n_r = 1, n_{t1}, n_{t2} \geq 1$ .

In this case, both channels have only one singular value  $\sigma_1 = \|\mathbf{H}_1\|, \sigma_2 = \|\mathbf{H}_2\|, m = 1, k = \frac{\|\mathbf{H}_1\|^2}{\|\mathbf{H}_2\|^2}$ , and  $\mathbf{U}_1 = \mathbf{U}_2 = 1$ . From (10) and (11) we obtain  $v_i = P_i \left(1 + \frac{1}{\|\mathbf{H}_1\|^2 P_1 + \|\mathbf{H}_2\|^2 P_2}\right), i = 1, 2$ . Therefore all the conditions in Theorem 2 hold and  $C_F = C$ .

*Example 2:*  $\mathbf{H}_1 = \gamma \mathbf{H}_2 \mathbf{A}, \gamma$  is a constant and  $\mathbf{A} \mathbf{A}^\dagger = \mathbf{I}$ .

Define  $n_t \triangleq n_{t1} = n_{t2}$  and  $r = r_1 = r_2$ , we have  $\mathbf{U}_1 = \mathbf{U}_2$  and  $k = \frac{\sigma_{1i}^2}{\sigma_{2i}^2}, i = 1, \dots, \not/r$ , with these and (10) and (11) we have

$$\begin{aligned} &\sum_{i=1}^r \left| \frac{v_1}{P_1} - \frac{\gamma^2}{\sigma_{1i} (\gamma^2 P_1 + P_2)} \right|^+ \\ &= \sum_{i=1}^r \left| \frac{v_2}{P_2} - \frac{\gamma^2}{\sigma_{1i} (\gamma^2 P_1 + P_2)} \right|^+ \\ &= 1. \end{aligned}$$

Then  $\frac{v_1}{P_1} = \frac{v_2}{P_2}$ . Depending on  $P_1, P_2, m$  can be any integer between 1 and  $r$ . Therefore, all the conditions of Theorem 2 are satisfied and  $C_F = C$ . Intuitively, as  $\mathbf{A}$  is a unitary matrix, one can apply capacity-preserving precoding  $\mathbf{A}$  to  $\mathbf{x}_2$ , resulting in

$$\mathbf{y} = \mathbf{H}_1 \mathbf{x}_1 + \mathbf{H}_2 \mathbf{A} \mathbf{x}_2 + \mathbf{z} = \mathbf{H}_2 \mathbf{A} (\gamma \mathbf{x}_1 + \mathbf{x}_2),$$

i.e., effectively reducing the MAC channel to a single user channel, where  $\mathbf{H}_2 \mathbf{A}$  is the channel matrix, and  $\gamma \mathbf{x}_1$  and  $\mathbf{x}_2$  are two independent signals transmitted by this single user. Therefore FDMA achieves the sum capacity.

*Example 3:*  $n_r \leq \min\{n_{t1}, n_{t2}\}, \mathbf{H}_1$  and  $\mathbf{H}_2$  have identical singular values  $\sigma_{ij} = \sigma_i, i = 1, 2; j = 1, 2, \dots, \not/n_r$ .

In this case,  $k = \frac{\sigma_1^2}{\sigma_2^2}, m = n_r$ , and  $\mathcal{S}\{\mathbf{u}_{11}, \dots, \not/\mathbf{u}_{1n_r}\} = \mathcal{S}\{\mathbf{u}_{21}, \dots, \not/\mathbf{u}_{2n_r}\} = \mathbb{R}^{n_r}$ , using the same argument in Example 2 one can show  $v_1 P_2 = v_2 P_1$ . Therefore all the conditions in Theorem 2 are satisfied and  $C_F = C$ .

Two special cases of Examples 2 and 3 are shown in Fig.1 with  $C_F = C$  when  $\alpha = 0.8$ . The example in [5, page 148]

$$kt \frac{1}{\sigma_{1,t}^2} - \frac{1}{\sigma_{1,t}^2} < kP_1 + P_2 \leq kt \frac{1}{\sigma_{1,t+1}^2} - \frac{1}{\sigma_{1,t}^2} \quad (23)$$

is also achievable by FDMA with  $\alpha = 0.5$ . In the above examples, the channel matrices make the power constraint automatically satisfied regardless of the values of  $P_1$  and  $P_2$ , i.e., the water-filling level  $v_i$  is always proportional to  $P_i$ . However, there are cases that, even if the channel matrices satisfy the singular value/vector constraints, one still need the right  $P_1$  and  $P_2$  as Proposition 2. Here is an example.

*Example 4:* For a MAC with  $\mathbf{H}_1 = \text{diag}\left(1, \frac{1}{\sqrt{3}}, \frac{1}{\sqrt{8}}\right)$  and  $\mathbf{H}_2 = \text{diag}\left(\frac{1}{\sqrt{2}}, \frac{1}{\sqrt{6}}, \frac{1}{\sqrt{10}}\right)$ , we show in Fig.2 the relation of  $\frac{C_F}{C}$  v.s.  $(P_1, P_2)$ . It can be shown from Proposition 2 that  $C_F = C$  when  $2P_1 + P_2 \leq 12$  and

$$\begin{aligned} \mathcal{P}_1 &= \{(P_1, P_2) | 2P_1 + P_2 \leq 12, P_1 > 0, P_2 > 0\} / \\ \mathcal{P}_2 &= \{(P_1, P_2) | 4 < 2P_1 + P_2 \leq 12, P_1 > 0, P_2 > 0\} / \end{aligned}$$

In Fig.2,  $\mathcal{P}_1$  denotes the area between the axis and the line segment  $EF$ , in which,  $C_F = C$  by allocating the power only to the first eigenmode, and  $\mathcal{P}_2$  denotes the area between the line segment  $EF$  and  $MN$ , in which,  $C_F = C$  by allocating the power up to the second eigenmode.

We will show in the following example that although FDMA is suboptimal in a fading MAC, the ergodic sum capacity can be asymptotically achieved when the number of antennas becomes large.

*Example 5:* The ergodic sum capacity of a fading MAC is

$$C_e = E \log \frac{P_1 \mathbf{H}_1 \mathbf{H}_1^\dagger + P_2 \mathbf{H}_2 \mathbf{H}_2^\dagger + \mathbf{I}}{n_{t_1} n_{t_2}}$$

where, all entries of  $\mathbf{H}_1$  and  $\mathbf{H}_2$  are assumed to be zero mean independent complex Gaussian with unit variance. From [8] and [9] the ergodic sum capacity can be achieved by choosing

$$\mathbf{S}_1 = \frac{P_1}{n_{t_1}} \mathbf{I}_{n_{t_1} \times n_{t_1}}; \quad \mathbf{S}_2 = \frac{P_2}{n_{t_2}} \mathbf{I}_{n_{t_2} \times n_{t_2}}.$$

For the same reason the ergodic maximum sum rate of FDMA is

$$\begin{aligned} C_{Fe} = \max_{0 < \alpha < 1} E \quad & \alpha \log \frac{P_1 \mathbf{H}_1 \mathbf{H}_1^\dagger + \mathbf{I}}{\alpha n_{t_1}} \\ & + \bar{\alpha} \log \frac{P_2 \mathbf{H}_2 \mathbf{H}_2^\dagger + \mathbf{I}}{\bar{\alpha} n_{t_2}}. \end{aligned}$$

For each realization of  $\mathbf{H}_1$  and  $\mathbf{H}_2$ , with probability 1, the condition of theorem 1 can not be satisfied. But when  $n_{t_1}$  and  $n_{t_2}$  increase while  $n_r$  is fixed, from Law of Large Number,

$$\frac{1}{n_{t_1}} \mathbf{H}_1 \mathbf{H}_1^\dagger \rightarrow \mathbf{I}; \quad \frac{1}{n_{t_2}} \mathbf{H}_2 \mathbf{H}_2^\dagger \rightarrow \mathbf{I}.$$

So we have

$$\begin{aligned} \lim_{n_{t_1}, n_{t_2} \rightarrow \infty} C_e &= n_r \log(P_1 + P_2 + 1), \\ \lim_{n_{t_1}, n_{t_2} \rightarrow \infty} C_{Fe} &= \max_{0 < \alpha < 1} n_r \alpha \log \left( \frac{P_1}{\alpha} + 1 \right) \\ &\quad + n_r \bar{\alpha} \log \left( \frac{P_2}{\bar{\alpha}} + 1 \right) \\ &= n_r \log(P_1 + P_2 + 1), \end{aligned}$$

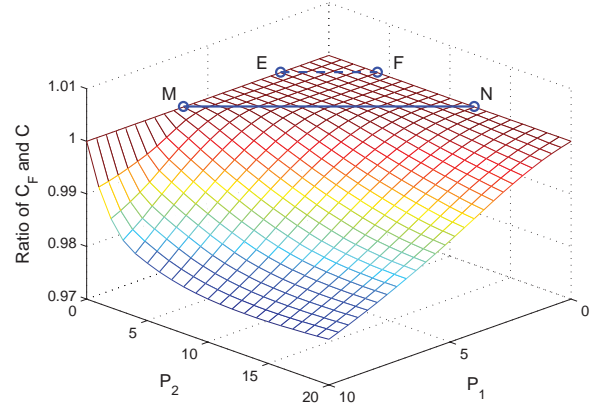


Fig. 2.  $\frac{C_F}{C}$  as a function of  $P_1, P_2$  for Example 4.

where the maximum is achieved when  $\alpha = \frac{P_1}{P_1 + P_2}$ .

Therefore, in fading MAC, with increasing number of transmit antennas, ergodic sum capacity can be asymptotically achieved by FDMA and the bandwidth allocation factor is proportional to the power of the corresponding user. This result can also be explained by Theorem 2. Example 5 can be considered as a counterpart of Example 3, since all the singular values of  $\mathbf{H}_1$  and  $\mathbf{H}_2$  asymptotically become identical respectively when  $n_{t_1}, n_{t_2}$  become large while  $n_r$  is fixed. In both the fading and non-fading cases, the optimal power allocation for FDMA is to evenly distribute the power among all transmit antennas. However,  $k$  is dropped in the expression of the optimal  $\alpha$  for the fading case because the singular values converge to  $\sqrt{n_{t_1}}$  and  $\sqrt{n_{t_2}}$  while the allocated power is  $\frac{P_1}{n_{t_1}}$  and  $\frac{P_2}{n_{t_2}}$ .

Intuitively, the asymptotic achievability of ergodic sum capacity by FDMA can be seen from the degrees of freedom's point of view. For a Gaussian vector MAC, the degrees of freedom is  $\min(n_{t_1} + n_{t_2}, n_r)$  if overlay transmission is used, and is  $\min(n_{t_1}, n_{t_2}, n_r)$  if FDMA is used. So when both  $n_{t_1} > n_r$  and  $n_{t_2} > n_r$ , the total degree of freedoms is not decreased by orthogonal transmission, which makes it feasible for FDMA to achieve the sum capacity.

In Figure 3, as  $n_t$  becomes large,  $C_{Fe}$  becomes close to  $C_e$ .

#### IV. QUANTIFICATION OF SUM-CAPACITY SUBOPTIMALITY OF FDMA

A simple example for FDMA to be suboptimal is  $\frac{\sigma_{11}}{\sigma_{21}} = \frac{\sigma_{12}}{\sigma_{22}}$  and  $\mathbf{u}_{11} = \pm \mathbf{u}_{21}$ . Next, we decouple the singular value and vector conditions, and use Theorem 2 to evaluate their individual impact on the sum capacity achievability of FDMA.

1) *Singular vector:* In this section the singular value conditions are assumed to be satisfied, but the subspaces spanned by the corresponding singular vectors are now different. In practice it applies to the low SNR case, in which the power for both users is allocated only to the largest eigenmode and

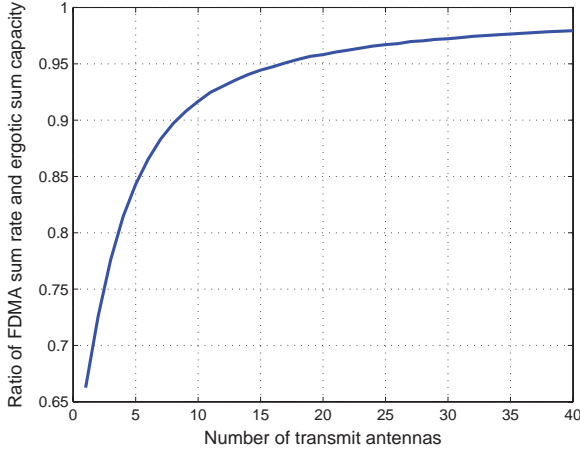


Fig. 3. Ratio of FDMA sum rate and ergodic sum capacity, where  $n_r = 8$ ,  $n_{t_1} = n_{t_2}$ ,  $P_1 = P_2 = 1$ .

$k = \frac{\sigma_{11}^2}{\sigma_{21}^2}$ . However, the singular vector conditions in Theorem 2, which require that the singular vectors of  $\mathbf{H}_1$  and  $\mathbf{H}_2$  expand the same subspace, are seldom satisfied in practice. If the singular vector subspaces associated to  $\sigma_{11}$  and  $\sigma_{21}$  are both rank 1, we can use the Euclidean inner product to measure the angle of these two subspaces. Otherwise, in order to evaluate the relation of singular vectors and  $\frac{C_F}{C}$ , we must have a mechanism that allows us to quantify the difference of two subspaces. We use the *distance* between two subspaces, defined in [10, page 76] as

$$\text{dist}(\mathcal{U}_1, \mathcal{U}_2) \triangleq \|\mathbf{Q}_1 - \mathbf{Q}_2\|_{\neq} \sigma_{\max}(\mathbf{Q}_1 - \mathbf{Q}_2), \quad (26)$$

where  $\mathcal{U}_i$ ,  $i = 1, 2$  are the subspaces,  $\mathbf{Q}_i$  is the orthogonal projection matrix for  $\mathcal{U}_i$ , i.e.,  $\mathbf{Q}_i = \mathbf{U}_i (\mathbf{U}_i^\dagger \mathbf{U}_i)^{-1} \mathbf{U}_i^\dagger$ , where the column vectors of matrix  $\mathbf{U}_i$  consist of the orthonormal basis of the subspace  $\mathcal{U}_i$ , and the 2-norm of  $\mathbf{Q}_1 - \mathbf{Q}_2$  is its largest singular value. In this definition  $\mathcal{U}_1$  and  $\mathcal{U}_2$  can have different ranks. When  $\mathcal{U}_1$  and  $\mathcal{U}_2$  have the same rank, we can use their largest principal angle  $\phi$  to quantify their distance, which is shown to be [10]

$$\phi = \sin^{-1}(\text{dist}(\mathcal{U}_1, \mathcal{U}_2)). \quad (27)$$

With (26) and (27) we can calculate  $\phi$  and  $\frac{C_F}{C}$  for a given MAC, if  $\mathbf{U}_1$  and  $\mathbf{U}_2$  are two  $n \times h$  real matrices. However, in order to have a complete picture of the relation between  $\phi$  and  $\frac{C_F}{C}$ , we must develop a mechanism to allow  $\phi$  to vary continuously from 0 to  $2\pi$  to access its effect on  $\frac{C_F}{C}$ . Toward this end, we introduce the idea of *rotation*. The unitary matrix  $\mathbf{U}_2$  can be obtained by rotating  $\mathbf{U}_1$  along an axis defined by the subspace  $\mathcal{A}$  of dimension  $n - 2$  and by an angle  $\theta$ ,

$$\mathbf{U}_2 = \text{rot}(\mathbf{U}_1, \mathcal{A}, \theta),$$

where  $\text{rot}(\cdot)$  is derived in the Appendix. In the rotation operation, each column vectors of  $\mathbf{U}_1$  has been rotated along  $\mathcal{A}$  by  $\theta$ , the principal angles of singular vector subspaces of  $\mathbf{U}_1$  and  $\mathbf{U}_2$  for each corresponding eigenmode can be different. The relation between  $\theta$  and  $\phi$  depends on the choice of  $\mathcal{A}$ . By choosing  $\mathcal{A}$  and let  $\theta$  vary in  $[0, 2\pi]$ , different  $\mathbf{U}_2$  is generated resulting in  $\phi \in [0, 2\pi]$ . This mechanism allows us to quantify the relation of  $\frac{C_F}{C}$  and  $\phi$ . Here is an example.

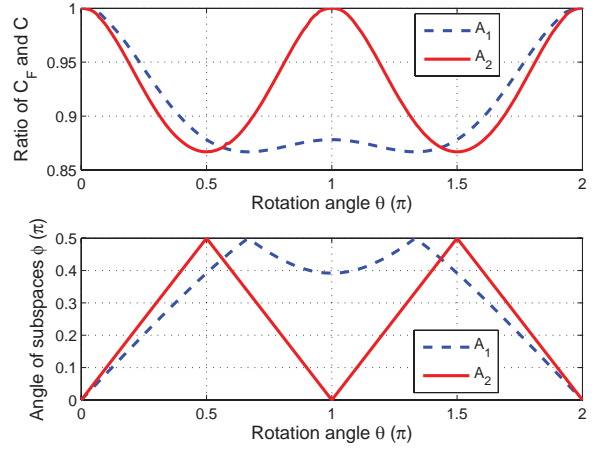


Fig. 4. Example 6. The top plot is the ratio of  $C_F$  and  $C$ , and the bottom plot is the angle of subspaces versus the rotation angle.

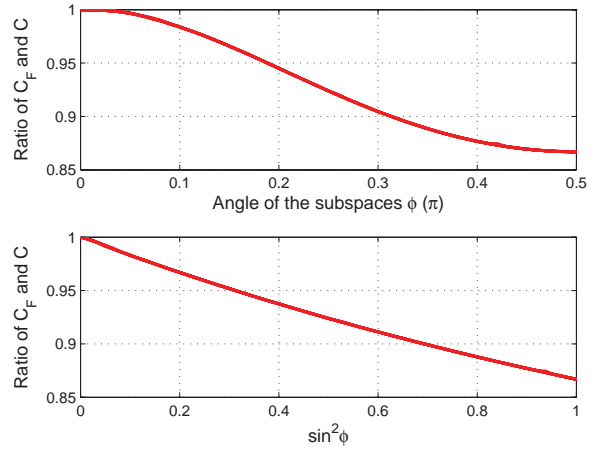


Fig. 5. The ratio of  $C_F$  and  $C$  versus  $\phi$ , the principal angle of the subspaces for Example 6.

*Example 6:*  $\mathbf{U}_1 = \mathbf{V}_1 = \mathbf{V}_2 = \mathbf{I}$ ,  $\Sigma_1 = \text{diag}(1, 1, \frac{1}{9}, \frac{1}{10})$ ,  $\Sigma_2 = \text{diag}(2, 2, \frac{1}{8}, \frac{1}{15})$ ,  $\mathcal{A}_1 = \begin{bmatrix} 1 & 0 & 0 & 0 \\ 0 & 1 & 1 & 1 \end{bmatrix}^T$ ,  $\mathcal{A}_2 = \begin{bmatrix} 1 & 1 & 0 & 0 \\ 0 & 0 & 1 & 1 \end{bmatrix}^T$ ,  $\mathbf{U}_2 = \text{rot}(\mathbf{I}, \mathcal{A}, \theta)$ ,  $\theta \in [0, 2\pi]$ ,  $P_1 = P_2 = 1$ .

The singular value conditions are satisfied and power is allocated to only the first two eigenmodes. Signals are transmitted in the subspaces  $\mathcal{U}_i$  spanned by  $[\mathbf{u}_{i1}, \mathbf{u}_{i2}]$ , where  $\mathbf{u}_{i1}$  and  $\mathbf{u}_{i2}$  are unitary and orthogonal vectors. The projection matrix for  $\mathcal{U}_i$  is,

$$\mathbf{Q}_i = [\mathbf{u}_{i1}, \mathbf{u}_{i2}][\mathbf{u}_{i1}, \mathbf{u}_{i2}]^T. \quad (28)$$

From (26)-(28), the angle of  $\mathcal{U}_1$  and  $\mathcal{U}_2$  is

$$\phi = \sin^{-1}(\sigma_{\max}(\mathbf{u}_{11}\mathbf{u}_{11}^T + \mathbf{u}_{12}\mathbf{u}_{12}^T - \mathbf{u}_{21}\mathbf{u}_{21}^T - \mathbf{u}_{22}\mathbf{u}_{22}^T)).$$

The results are shown in Figs. 4 and 5. While different choices of the rotation axes  $\mathcal{A}_1$  and  $\mathcal{A}_2$  result in different curves of  $\theta$  and  $\phi$ , the curves of  $\frac{C_F}{C}$  coincide and are monotonically decreasing with  $\phi$ . As shown in Fig.5,  $\frac{C_F}{C}$  is approximately linear with  $\sin^2 \phi$ . When  $\theta = 0, 2\pi$ , if  $\mathcal{A}_1$  is the rotation axis, or when  $\theta = 0, \pi, 2\pi$  if  $\mathcal{A}_2$  is the rotation axis,  $\phi = 0$ , consequently  $\mathcal{U}_1 = \mathcal{U}_2$ , the conditions of Theorem 2 are satisfied and  $\frac{C_F}{C} = 1$ . This is when the mutual interferences from the two users are the worst, and FDMA benefits the

TABLE I  
OVERLAY TRANSMISSION.

$\sigma$ (dB)	user 1	user 2	$C$ (bit/Hz/s)
$< 0$	(0, 1)	(1, 0)	2
$= 0$	( $a, 1-a$ )	( $1-a, a$ )	2
$> 0$	(1, 0)	(0, 1)	$1 + \log(1 + \sigma^2)$

TABLE II  
FDMA TRANSMISSION.

$\sigma$ (dB)	user 1	user 2	$C$ (bit/Hz/s)
$\leq -4.8$	( $\frac{1}{2}, \frac{1}{2}$ )	(1, 0)	1.79
$> -4.8$	( $\frac{1}{2}, \frac{1}{2}$ )	( $\frac{\alpha_o}{2} + \frac{1-\alpha_o}{2\sigma^2}, 1 - \frac{\alpha_o}{2} - \frac{1-\alpha_o}{2\sigma^2}$ )	$\max C_F(\alpha)$

most via orthogonalization. Notice that in this case, generally it is not necessary for the corresponding subspaces of all the eigenmode to coincide, but only the subspace of the active eigenmodes effective. When  $\theta = 0.66\pi, 1.33\pi$  for  $\mathcal{A}_1$ , and  $\theta = \frac{\pi}{2}, \frac{3\pi}{2}$  for  $\mathcal{A}_2$ ,  $\phi = 0.5\pi$ ,  $\mathcal{U}_1 \perp \mathcal{U}_2$  and  $\frac{C_F}{C}$  becomes the minimum. This agrees with intuition: the orthogonality of the subspaces allows both users to communicate simultaneously at maximum rate without interfering each other. Therefore overlay transmission outperforms FDMA since the latter unnecessarily orthogonalizes transmission while the effective channels  $[\mathbf{u}_{11}, \mathbf{u}_{12}]$  and  $[\mathbf{u}_{21}, \mathbf{u}_{22}]$  are already orthogonal.

2) *Singular value*: We still assume  $\mathbf{H}_1$  and  $\mathbf{H}_2$  are  $n \times n$  real matrices. The singular vector conditions are satisfied, but the singular value conditions are not. Since there are no general matrices to represent this case and the involvement of power conditions as in Proposition 2, there is no uniform way to show the individual effect of singular value conditions in FDMA sum capacity achievability. Hence, we use the following example and, without loss of generality, we assume  $\mathbf{U}_1 = \mathbf{U}_2 = \mathbf{V}_1 = \mathbf{V}_2 = \mathbf{I}$ .

*Example 7*:  $\mathbf{H}_1 = \begin{bmatrix} 1 & 0 \\ 0 & 1 \end{bmatrix}$ ,  $\mathbf{H}_2 = \begin{bmatrix} 1 & 0 \\ 0 & \sigma \end{bmatrix}$ ,  $-20\text{dB} \leq \sigma \leq 20\text{dB}$ ,  $P_1 = P_2 = 1$ .

The results are shown in Fig. 6, the sum rate and optimal power allocation for overlay and FDMA are shown in Table I and II. For overlay transmission, the second user always puts all the power to the eigenmode of the largest eigenvalue, while the first user adaptively puts all the power to the orthogonal direction. For FDMA, the optimal frequency allocation is  $\alpha_o = 0.48$  when  $\sigma \leq \left(1 + \frac{P_2}{1-\alpha_1}\right)^{-\frac{1}{2}} = -4.8\text{dB}$ , and  $\alpha_o = \arg \max_{\alpha \in [0,1]} C_F(\alpha)$  when  $\sigma > -4.8\text{dB}$ , where

$$C_F(\alpha) = \left\{ \alpha \log \left( \frac{P_1}{2\alpha} + 1 \right) + \bar{\alpha} \log \left( \frac{\sigma P_2}{2\bar{\alpha}} + \frac{1 + \sigma^2}{2\sigma} \right) \right\}.$$

So when  $\sigma = 0\text{dB}$ ,  $\mathbf{S}_{f_2} = 0.5\mathbf{I}$ ,  $\alpha_o = 0.5$ ,  $C_F = C = 2\text{bit}$ . In the neighborhood of  $0\text{dB}$ ,  $\frac{C_F}{C}$  decreases as  $\sigma$  moves away

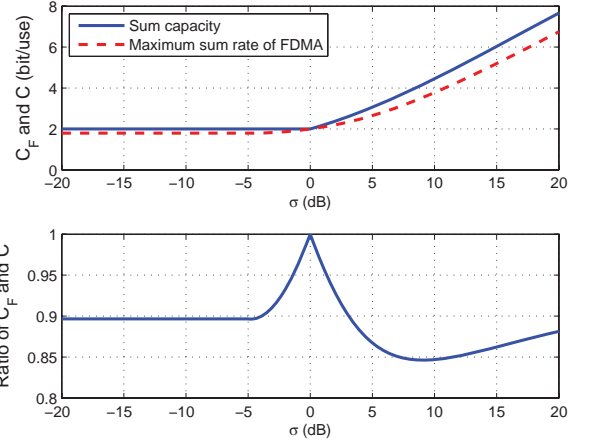


Fig. 6.  $C$ ,  $C_F$  and their ratio versus  $\sigma$  for Example 7.

from  $0\text{dB}$ . When  $\sigma \rightarrow \infty$ ,  $\alpha_o \rightarrow 0$  and

$$\begin{aligned} & \lim_{\sigma \rightarrow \infty} (C - C_F) \\ &= \lim_{\sigma \rightarrow \infty} \left\{ 1 + \log(1 + \sigma^2) - \log \left( \frac{\sigma}{2} + \frac{\sigma}{2} \left( 1 + \frac{1}{\sigma^2} \right) \right)^2 \right\} \\ &= \lim_{\sigma \rightarrow \infty} \left\{ 1 + \log \sigma^2 - \log \left( \frac{\sigma}{2} + \frac{\sigma}{2} \right)^2 \right\} \\ &= 1. \end{aligned}$$

One user's rate becomes dominant, thus FDMA asymptotically achieves the sum capacity with bandwidth allocation increasingly favoring the dominant user. The difference between  $C$  and  $C_F$  approaches to  $1\text{bit/Hz/s}$ . However,  $\frac{C_F}{C}$  is not monotone in  $\sigma$ .

## V. CONCLUSION AND EXTENSION

Orthogonal transmission in vector Gaussian MAC was studied in this paper. We derived sufficient and necessary conditions for FDMA to achieve the sum capacity. The sum rate degradation of orthogonal transmission was quantified by the distance of singular vector subspaces and disproportional singular values. Parallel results for Gaussian vector MAC with more than two users can also be similarly obtained.

### APPENDIX A ROTATION OF SUBSPACE

We use Fig.7 as an example to derive  $\text{rot}(\mathbf{U}_1, \mathcal{A}, \theta)$ .  $\mathcal{A}$  is a rank  $n-2$  subspace in  $R^n$ , and is the rotation axis depicted as a line in Fig.7.  $\mathbf{A}_\perp$  is a  $n \times (n-2)$  matrix, whose column vectors consist of the orthonormal basis of the subspace  $\mathcal{A}$ . Vector  $\overline{OB}$  is the  $i^{\text{th}}$  column vector of  $\mathbf{U}_1$  and is denoted as  $\mathbf{u}_i$ . Then from the definition of  $\overline{OM}$  and  $\overline{ME}$  we have

$$\mathbf{u}'_i \triangleq \overline{OB'} = \overline{OM} + \overline{ME} + \overline{EB'}. \quad (29)$$

Define  $\mathbf{Q}$  as the projection matrix of the subspace  $\mathcal{A}$ , then  $\mathbf{Q} = \mathbf{A}_\perp \cdot \mathbf{A}_\perp^\dagger$ . With this we have

$$\overline{OM} = \mathbf{Q}\mathbf{u}_i, \quad (30)$$

$$\begin{aligned} \overline{ME} &= (\overline{OB} - \overline{OM}) \cos \theta \\ &= (\mathbf{u}_i - \mathbf{Q}\mathbf{u}_i) \cos \theta. \end{aligned} \quad (31)$$

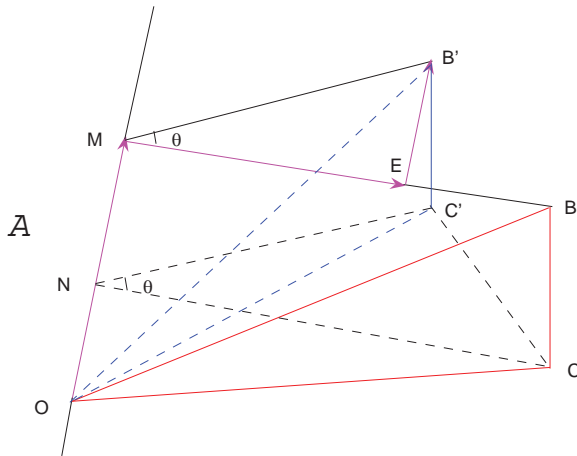


Fig. 7. Rotation of the subspace  $\mathcal{U}_1$  in  $R^n$  by the angle  $\theta$  along the axis  $\mathcal{A}$ , where  $\mathcal{A}$  can be any subspaces of dimension  $n-2$  and  $\mathcal{U}_1$  can be any subspaces formed by some column vectors of matrix  $\mathbf{U}_1$ .  $O$  is the origin of the space, vectors  $\overline{OM}$  and  $\overline{ON}$  are in  $\mathcal{A}$ ,  $\overline{OB}$  and  $\overline{OC}$  are two linearly independent vectors of  $\mathcal{U}_1$  and are rotated to vector  $\overline{OB'}$  and  $\overline{OC'}$  respectively. The projections of  $\overline{OB}$  and  $\overline{OC}$  in  $\mathcal{A}$  are  $\overline{OM}$  and  $\overline{ON}$  respectively.  $\theta = \angle CNC' = \angle BMB'$  is the rotation angle.  $\overline{ME}$  is the projection of  $\overline{MB'}$  on  $\overline{MB}$ .

Since  $S/\overline{MB}, \overline{MB'} \perp \mathcal{A}$ , then  $\overline{EB'} \perp S/\overline{MB}, \mathcal{A}$ . Define a  $n \times n$  matrix

$$\mathbf{W} = \begin{bmatrix} \mathbf{1}^T \\ (\mathbf{u}_i - \mathbf{Q}\mathbf{u}_i)^T \cos \theta \\ \mathbf{A}_\perp^T \end{bmatrix}, \quad (32)$$

where  $\mathbf{1}^T$  is a  $1 \times n$  row vector with all elements equal to 1. Define the adjugate of  $\mathbf{W}$  as  $\mathbf{W}^*$  and the first column vector of  $\mathbf{W}^*$  as  $\mathbf{w}_1$ , then  $\mathbf{w}_1 \perp \overline{MB}$  and  $\mathbf{w}_1 \perp \mathcal{A}$  since  $\mathbf{W}\mathbf{W}^* = |\mathbf{W}|\mathbf{I}$ . With this, we have

$$\begin{aligned} \overline{EB'} &= \overline{EB'} \cdot \frac{\overline{EB'}}{\overline{EB'}} \\ &= \|\mathbf{u}_i - \mathbf{Q}\mathbf{u}_i\| \sin \theta \cdot \frac{\mathbf{w}_1}{\|\mathbf{w}_1\|}. \end{aligned} \quad (33)$$

From (29)-(33) we have

$$\begin{aligned} \mathbf{u}'_i &= \mathbf{P}\mathbf{u}_i + (\mathbf{u}_i - \mathbf{Q}\mathbf{u}_i) \cos \theta \\ &\quad + \|\mathbf{u}_i - \mathbf{P}\mathbf{u}_i\| \sin \theta \cdot \frac{\mathbf{w}_1}{\|\mathbf{w}_1\|} \end{aligned} \quad (34)$$

Then we have  $\mathbf{U}_2 = \text{rot}\{\mathbf{U}_1, \mathcal{A}, \theta\} = [\mathbf{u}'_1, \dots, \mathbf{u}'_n]$ , as  $\mathbf{u}'_i, i = 1, \dots, n$  defined in (34).

In Fig.7, although the rotation angle is  $\theta$ , depending on the choice of  $\mathcal{A}$ , the angle of the two vectors  $\overline{OB}$  and  $\overline{OB'}$  and the principle angle  $\phi$  of the two subspaces  $S/\overline{OB}, \overline{OC}$  and  $S/\overline{OB'}, \overline{OC'}$  can be different from  $\theta$ .

## REFERENCES

- [1] H. Liao, "Multiple access channels," Ph.D. thesis, University of Hawaii, Honolulu, 1972.
- [2] T. M. Cover and J. A. Thomas, *Elements of Information Theory*. New York: Wiley, 2nd edition, 2006.
- [3] G. Caire, D. Tuninetti, and S. Verdú, "Suboptimality of TDMA in the low-power regime," *IEEE Trans. Inform. Theory*, vol. 50, pp. 608–620, Apr. 2004.
- [4] D. Tse and P. Viswanath, *Fundamentals of Wireless Communications*. Cambridge, UK: Cambridge University Press, 2005.

- [5] W. Yu, W. Rhee, S. Boyd, and J. M. Cioffi, "Iterative water filling for Gaussian vector multiple-access channels," *IEEE Trans. Inform. Theory*, vol. 50, no. 1, pp. 145–152, Jan. 2004.
- [6] X. Shang, B. Chen, and M. J. Gans, "On achievable sum rate for MIMO interference channels," *IEEE Trans. Inform. Theory*, vol. 52, no. 9, pp. 4313–4320, Sept. 2006.
- [7] D.P. Bertsekas, *Nonlinear Programming*. Athena Scientific, Belmont, MA, 2003.
- [8] E. Telatar, "Capacity of multi-antenna Gaussian channels," *European Trans. Telecomm.*, vol. 10, pp. 585–595, Nov./Dec. 1999.
- [9] W. Rhee and J. M. Cioffi, "On the capacity of multiuser wireless channels with multiple antennas," *IEEE Trans. Inform. Theory*, vol. 49, pp. 2580–2595, Oct. 2003.
- [10] G. H. Golub and C. F. Van Loan, *Matrix Computations*. Baltimore, MD: The Johns Hopkins University Press, 1990.



**Xiaohu Shang** (S'07) received the B.S. and M.S. degrees in Electronics and Information Engineering from Huazhong University of Science and Technology, Wuhan, China, in 1999 and 2002, respectively. From 2002 to 2003, he worked at Guoxin Lucent Technologies Network Technologies Co., Ltd., Shanghai, China. Since 2003, he has been with the Department of Electrical Engineering and Computer Science, Syracuse University, Syracuse, NY, where he is pursuing the Ph.D. degree in Electrical Engineering. In 2007, he worked as a summer intern

student at Communications and Statistical Sciences Research Department of Bell-Labs, Alcatel-Lucent, Murray Hill, NJ. His area of interest mainly focuses on multi-user information theory and MIMO systems.



**Biao Chen** (S'96-M'99-SM'07) received the B.E. and E.E. degrees in electrical engineering from Tsinghua University, Beijing, China, in 1992 and 1994, respectively. From 1994 to 1995, he worked at AT&T (China) Inc., Beijing, China. He joined the University of Connecticut, Storrs, in 1995, where he received the M.S. degree in statistics and the Ph.D. degree in electrical engineering, in 1998 and 1999, respectively. From 1999 to 2000, he was with Cornell University, Ithaca, NY, as a Postdoctoral Research Associate. Since 2000, he has been with

Syracuse University, Syracuse, NY, where he is currently an Associate Professor in the Department of Electrical Engineering and Computer Science. He is an associate editor for the EURASIP JOURNAL ON WIRELESS COMMUNICATIONS AND NETWORKING (JWCN) and IEEE COMMUNICATIONS LETTERS. His area of interest mainly focuses on signal processing for wireless sensor and ad hoc networks and in multiuser MIMO systems. Dr. Chen is the recipient of an NSF CAREER Award in 2006.



**John D. Matyjas** John D. Matyjas received the A.S. degree in pre-engineering from Niagara University, Lewiston, NY, in 1996 and the B.S., M.S., and Ph.D. degrees in electrical engineering from the State University of New York at Buffalo in 1998, 2000, and 2004, respectively. From 1998 to 2002, he was a Teaching Assistant with the Department of Electrical Engineering, State University of New York at Buffalo. He also served as a Research Assistant with the Communications and Signals Laboratory, Department of Electrical Engineering,

State University of New York at Buffalo from 1998 through 2004. Currently, he is employed by the Air Force Research Laboratory in Rome, NY, performing research and development in the information connectivity branch. His research interests are in the areas of wireless multiple-access communications and networking, statistical signal processing and optimization, and neural networks. Additionally, he serves as an adjunct faculty in the Department of Electrical Engineering at the State University of New York Institute of Technology at Utica/Rome.

Dr. Matyjas is the recipient of the State University of New York at Buffalo Presidential Fellowship and the SUNY Excellence in Teaching Award for Graduate Assistants. He is a member of the IEEE Communications, Information Theory, Computational Intelligence, and Signal Processing Societies; secretary of the IEEE Mohawk Valley Chapter Signal Processing Society; and a member of the Tau Beta Pi and Eta Kappa Nu engineering honor societies.